①

THE EFFECTS OF EXPLOSIVE SHOCK WAVE PROPAGATION
THROUGH A SOLID STATE MOLECULAR STRUCTURE

N00228-85-G-3359

AD-A197 029

DTIC
ELECTE
S   D
JUL 1 2 1988
  H

APPROVED:

Robert E. Wyatt

Robert E. Wyatt

Richard A. Friesner

Richard A. Friesner

James E. Boggs

James E. Boggs

88

THE EFFECTS OF EXPLOSIVE SHOCK WAVE PROPAGATION
THROUGH A SOLID STATE MOLECULAR STRUCTURE

by

David Edwin Clark, B.S.

THESIS

Presented to the Faculty of the Graduate School of

The University of Texas at Austin

in Partial Fulfillment

of the Requirements

for the Degree of

MASTER OF ARTS

THE UNIVERSITY OF TEXAS AT AUSTIN

August 1988

TABLE OF CONTENTS

DTIC
COPY
INSPECTED
6

iii

LIST OF FIGURES

I. Introduction

Shock waves have been studied in the past in order to provide insight to the energy released during an external shock to a system and the resultant physical and chemical reactions which occur. A detonation may be defined as a supersonic wave which propagates throughout a crystal lattice structure, and whose energy is released during an exothermic chemical reaction.[1] It is convenient to classify a detonation into two categories, the first category being defined as the shock front which is characterized by a sharp rise in energy and agitation over time occuring on the order of picoseconds. As the shock front passes through a lattice, an almost instantaneous change in atom position and momentum may be observed. The second category is the shock wave which is usually characterized by the slowly decaying nature of the wave until thermal equilibrium has been established.[2] The shock wave transfers energy through the lattice in a much slower fashion. Time delays are experienced with respect to atom displacement as well as energy transfer. Shock waves propagate through most materials on the order of 2500 meters per second (5.49×10^{-2} a_0/ps).[1] There has been considerable attention in the past devoted to the examination of shock waves and whether they may be classified into two seperate categories (first and second sound). This idea has been disputed in the literature for several years.[3-8]

Shock waves produce a variety of anomolous optical and electrical properties as well as nonthermal chemistry, and they are capable of producing bond dissociation, phase changes, and a redistribution of vibrational, electronic and rotational energy within a lattice. Shock waves are also unique in that energy may be deposited to vibrational modes of a molecule under nonequilibrium conditions.[2]

1

Early studies concerning simulations of shock waves propagating within crystal lattices were restricted to classical dynamics with finite dimensions, consisting of non-oscillatory atoms prior to the introduction of a shock wave.[3-4] These studies were primarily aimed at understanding the shock wave, and its velocity and kinetic energy effects upon a crystal lattice. Later studies[5-8] devoted considerable attention to the characteristics of the shock wave and the various phases of velocity transformations. Classical studies have been completed on systems which were initially at a nonzero temperature (zero temperature being defined as no oscilatory motion),[9-10] and on models which incorporated deformations within the crystal lattice.[11-14] These studies were concerned with affects of free radicals, mass defects which were randomly dispersed, and mass defects of heavy and light impurities on shock wave propagation throughout the lattice.

There have been few quantum mechanical studies concerning shock waves. Dancz and Rice derived expressions for the quantum mechanical equations of motion for coupled anharmonic oscillators.[15] There have been other studies which were also devoted to deriving equations of motion for quantum systems by the introduction of raising and lowering operators for interacting Morse potentials.[16] Other studies examined the probability of occupation of excited states and the state to state energy flow in which energy became trapped in excited states.[17]

Experimental work using picosecond lasers has also been done in order to understand shock wave propagation through lattices.[2] In this experiment, a picosecond laser (capable of 10^{12} Watts/cm^2) imposed a shock upon a sample of water which was analyzed using Raman Spectroscopy. This was the first experiment

in which energy transfer from a macroscopic shock to intermolecular states has been observed.

Most of the previous studies have been devoted extensively to the classical study of shock waves, and the subsequent interface with a lattice model using classical mechanics. Much work has been devoted to examining the shock wave and the resultant energy transfer associated with it. Recent studies [Wyatt and Marston] have been devoted to describing a shock wave effect quantum mechanically in a one dimensional crystal lattice. This work was primarily devoted towards a high energy shock wave and its effect upon a completely harmonic system. A classical linear model of twenty diatoms was formulated and perturbed via a ballistic particle of equivalent mass. The inner two diatom pairs were chosen for the classical study in order to restrict center of mass movement within the lattice and to represent inner lattice substituents. These inner atoms were perturbed by direct interactions of their neighbor atoms (entering and absorbing driving atoms). Wyatt and Marston used the action of these atoms to establish a time-dependent driving potential for two diatoms. The entering atom ($q_<$) provided the initial interaction from the shock to the cluster; whereas, the absorbing atom ($q_>$) acted as a resevoir for the energy to be released from the cluster. The dynamical data from the classical results of $q_<$ and $q_>$ was used directly to formulate an interaction potential for a quantum mechanical model of two diatoms; thus, the classical and quantum model experienced similar potentials. The quantum model was represented by four normal modes, upon perturbation yielded quantum dynamical data for comparison to the classical system. Wyatt and Marston showed that a high energy shock imposed upon a harmonic quantum system converges, as expected, to the classical results.

This work is devoted to the replacement of harmonic oscillators with cubic anharmonic oscillators and in making comparisons to classical dynamics. A similar anharmonic classical model is established in order to provide for a driving potential in our quantum system. In the quantum system the cubic anharmonicities provide various mode couplings; thus, our Hamiltonian may be not separated exclusively into the four modes as in Marston's; however, it will be represented by all four modes. This fact will restrict our quantum basis size.

The remainder of this thesis is organized in the following fashion. Section II develops the model for both classical and quantum systems. The classical equations of motion are derived showing how we obtained dynamical data for comparison and for the quantum potential. The quantum coupled anharmonic Hamiltonian is derived using the normal modes representation and the time dependent system is developed by approximately solving the Schrödinger time dependent equation. Quantum formulation for position expectation values, normal mode energies, and bond energies is presented in this section.

Section III presents results of quantum harmonic and anharmonic calculations of several basis sizes and compares these results to classical dynamical data. Section IV draws conclusions based upon thse results and also provides commentary based upon different formulations of the problem.

II. Method

Model

A one-dimensional twenty-diatom classical model was established in order to study the effects of the propagation of a shock wave through a crystal lattice. All of the atoms in the chain are of equal mass (mass of fluorine atom); the intermolecular distances represent the intermolecular separations of diatomic fluorine. Each diatom was connected with a force constant $K_>$ and equilibrium separation ρ_0. The equilibrium separation between diatoms was R_0 with a connecting force constant $K_<$ (see Figure 1 and Table 1). A ballistic particle of equal mass will impose a shock wave upon the chain of atoms. In order to compare a classical model with a quantum model, the central pair of diatoms in the classical one dimensional chain will be isolated. This pair of diatoms is far enough from the ballistic particle to reduce any sporadic results from the strong potential and a smaller system of two diatoms was chosen for comparison to an equivalent quantum model based on the fact that a twenty diatom cluster is numerically intractable to handle quantum mechanically. Classically, the central diatom pair will be perturbed via interaction with the nearest atoms in the chain. The entering atom $(q_<)$ provides the initial interaction from the shock to the cluster; whereas, the absorbing atom $(q_>)$ acts as a reservoir for the energy to be released from the cluster. The dynamical data from the classical results of $q_<(t)$ and $q_>(t)$ will be used directly to formulate an interaction potential for a quantum mechanical model of two diatoms; thus, the classical and quantum models will be experiencing similar potentials, thus allowing for direct comparisons.

Classically, these atoms may be thought of as forty harmonic or anharmonic oscillators. At time $t=0$, atom positions were arbitrarily set at their equilibrium values,

5

and atom number one in the chain was originally chosen to have zero momentum.

Atom momenta are easily obtainable through the following relationships:[18]

$$\frac{(p_2 - p_1)^2}{2\mu} + \frac{1}{2} K_> (q_2 - q_1 - \rho_o)^2 + \gamma (q_2 - q_1 - \rho_o)^3 = E_T \qquad (1)$$

p_1 = momentum of atom number one = 0

ρ_o = equilibrium separation (Table 1)

$(q_2 - q_1) = \rho_o$; since at equilibrium

E_T = Total energy (sum of potential, and kinetic terms)

μ = reduced mass (Table 1)

γ = degree of anharmonicity (Table 1)

$K_>$ = Force constant between atoms (Table 1)

The total energy (E_T) between any two atoms was calculated from the ground state energy of a diatom pair ($E_T = \frac{1}{2} h\omega$ where $\omega = \sqrt{K/\mu}$). Equation (1) readily reduces to $\frac{(p_2^2)}{2\mu} = E_T$, since the potential energy term and the anharmonic term consistently drop out of the initial equations because all interatomic distances are at their equilibrium separation. From this equation, the momentum of atom number two can be calculated, thus allowing all other momenta to be calculated for their initial values via:

$$\frac{(p_{n+1} - p_n)^2}{2\mu} = E_{KE}$$

In order to initiate a shock wave into the forty diatom chain, a ballistic particle (impact atom) with equal mass of a flourine atom imparts a potential upon the system. The interaction potential of the impact atom and with atom number one is given by the following equation:

$$V_{int} = Ae^{-\alpha(q_1 - q_o)}$$

$A = 0.0029$ Hartree

$\alpha = 1.0(\text{Bohr}^{-1})$

q_1 = position of chain atom number one

q_0 = position of impact atom

The quantity A was chosen as twice the ground state energy value of a diatom pair, and α was chosen as 1.0 Bohr $^{-1}$ to optimize the trajectory of the impact atom in order to produce a movement of the atoms at a speed greater than 2500 m/sec (speed of a shock wave). The entire classical potential of the chain may now be written as a combination of the interaction potential from the ballistic particle, the sum of harmonic potential interaction of the particles and an anharmonic term:

$$V = Ae^{-\alpha(q_1 - q_0)} + \sum_{n=1,3,5...}^{40} \frac{1}{2} K_< (q_{n+1} - q_n - \rho_0)^2 + \sum_{n=2,4,6...}^{40} \frac{1}{2} K_> (q_{n+1} - q_n - R_0)^2$$
$$+ \sum_{n=1,3,5...}^{40} \gamma (q_{n+1} - q_n - \rho_0)^3 + \sum_{n=2,4,6...}^{40} \gamma (q_{n+1} - q_n - R_0)^3$$

where

q_n = position of atom n

ρ_0 = intramolecular equilibrium distance (Table 1)

R_0 = intermolecular equilibrium distance (Table 1)

As the ballistic particle moves toward atom one with twice the initial momentum of atom number two, the repulsive potential becomes more significant, thus creating transverse motion within the chain. These atoms move according to Hamilton's equations of motion:

$$\dot{q}_i = \frac{p_i}{m}, \quad \dot{p}_i = -\frac{\partial V}{\partial q_i}, \quad i = 0, 1 \dots n.$$

Upon numerical integration, these coupled differential equations yield atom momenta and positions as a function of time. The Adams-Moulton integrator was used in this study with the following parameters:

Order = 6

DT = 1 atomic time unit (2.5×10^{-5} ps)

EPS = 10^{-3}, maximum relative degree of iteration

N = 60,000 = numbers of time step iterations

Results produce classical trajectory values for the one dimensional system. As stated previously, the two diatoms located at the center of the cluster are of main interest for this classical problem and for comparison to the quantum mechanical problem.

In the quantum mechanical system, the four atoms are initially all located at their average equilibrium value corresponding to their counterparts in the classical system. These four atoms are connected to driving atoms ($q_<$ entering atom; $q_>$ absorbing atom) as formulated in the classical problem, and the motion of these driving atoms in the classical system is converted into the driving potential for the quantum system. This potential creates a perturbation within the quanutm model causing atom displacement. Since the one dimensional quantum mechanical system may be thought of as four harmonic or anharmonic coupled oscillators, motion in the system is described by four normal modes. The positions in the system may be expressed as a sum of initial cartesian position plus a time dependent displacement δ:

$$q_1 = q_1^o + \delta_1 \tag{2a}$$

$$q_2 = q_2^o + \delta_2 \tag{2b}$$

$$q_3 = q_3^o + \delta_3 \tag{2c}$$

$$q_4 = q_4^o + \delta_4 \tag{2d}$$

From these relationships, calculations of transverse atom movement are performed.

Formulation of the Hamiltonian for the Cluster

For a set of atoms which are interconnected via sets of anharmonic springs, there are many types of internal motions, vibrations, which are dependent upon the initial displacements of the atoms. The Hamiltonian for the anharmonic system may be expressed as the sum of a harmonic part (H^o), anharmonic part (V_a), and time dependent part ($V(t)$).

$$H_T = H^o + V_a + V(t)$$

Formulation of Harmonic Hamiltonian

The harmonic Hamiltonian for this one dimensional two diatom case is expressed as the sum of the potential and kinetic operators[19]

$$H^o = \sum_{i=1}^{4} \frac{p^2}{2m_i} + \frac{K_<}{2}[(q_1 - q_<(t) - R_o)^2 + (q_>(t) - q_4 - R_o)^2]$$

$$+ \frac{K_>}{2}[(q_2 - q_1 - \rho_o)^2 + (q_4 - q_3 - \rho_o)^2] + \frac{K_<}{2}(q_3 - q_2 - R_o)^2$$

where

$p_i = m_i \dot{q}_i$ = momentum of atom i

m_i = mass of atom i

q_i = position of atom i

ρ_o = equilibrium intramolecular distance

R_0 = equilibrium intermolecular distance

$K_<$ = Force constant of intermolecular bond

$K_>$ = Force constant of intramolecular bond

As stated previously, the positions of the four atoms as a function of time may be described as the sum of an initial position and a displacement position (δ). The positions of the impact and absorbing atoms ($q_<$ and $q_>$) may also be expressed as an initial position plus a displacement:

$$q_<(t) = q_<^o + \delta_<(t) \tag{3a}$$

$$q_>(t) = q_>^o + \delta_>(t) \tag{3b}$$

The harmonic Hamiltonian is time independent, thus $\delta_<(t)$ and $\delta_>(t)$ are equal to zero until a perturbation is introduced. Utilizing the previous relations of initial positions of atoms, it is clear that:

$$q_2^o - q_1^o = \rho_o$$

$$q_4^o - q_3^o = \rho_o$$

$$q_3^o - q_2^o = R_o$$

$$q_>^o - q_4^o = R_o$$

$$q_1^o - q_<^o = R_o$$

This enables simplification of the harmonic Hamiltonian:

$$H^o = \sum_{i=1}^{4} \frac{p_i^2}{2m_i} + \frac{K_<}{2}(\delta_1^2 + \delta_4^2) + \frac{K_>}{2}[(\delta_2 - \delta_1)^2 + (\delta_4 - \delta_3)^2] + \frac{K_>}{2}(\delta_3 - \delta_2)^2 \qquad (4)$$

Formulation of Harmonic Time Independent Hamiltonian Matrix

If an atom has an original position q^o and throughout time moves to a different position $q(t)$ the resulting vector describes the displacement (δ) from its equilibrium value . This may be represented in mass scaled displacement coordinates (η_i).

$$\eta_i = (m_i)^{1/2}\delta_i$$

In matrix notation, η and δ are defined as a row vector, and $M^{1/2}$ is a square matrix with the root values of atom masses on the diagonal.

$$\eta = \delta M^{1/2}$$

The kinetic energy may now be represented as

$$T = \frac{1}{2}\sum_{i}^{N} m_i \dot{\delta}_i^2 = \frac{1}{2}\sum_{i}^{N}\dot{\eta}_i^2$$

or in matrix notation

$$T = \frac{1}{2}\dot{\eta}\,\dot{\eta}^t$$

where $\dot{\eta}^t$ is the transpose of the row vector $\dot{\eta}$.

The potential energy of the system may also be represented in the same manner. We expand V in a Taylor series in the mass scaled displacements:

$$V = V_o + \sum_{j=1}^{n} \eta_j \left(\frac{\partial V}{\partial \eta}\right) + \frac{1}{2} \sum_i \sum_j \eta_i \eta_j \left(\frac{\partial^2 V}{\partial \eta_i \partial \eta_j}\right) + \ldots$$

where

V = potential energy

$V_o = V(\delta=0) = 0$

$$\sum_{j=1}^{n} \eta_j \left(\frac{\partial V}{\partial \eta_j}\right) = 0 \quad (\text{Expanded about } \delta=0, \text{ the minimun of V})$$

Thus, the harmonic potential energy may be expressed as

$$V = \frac{1}{2} \sum_i \sum_j \eta_i \eta_j \left(\frac{\partial^2 V}{\partial \eta_i \partial \eta_j}\right) = \frac{1}{2} \eta K \eta^t$$

where η is the mass scaled coordinate row vector, η^t is its transpose (a column vector), and K = force constant matrix which may be represented as follows:

$$K = \begin{bmatrix} K & -K_> & 0 & 0 \\ -K_> & K & -K_< & 0 \\ 0 & -K_< & K & -K_> \\ 0 & 0 & -K_> & K \end{bmatrix}$$

$K_<$ is the weak intramolecular force constant

$K_>$ is the strong intermolecular force constant

$K = K_> + K_<$

In order to analyze the system, an orthogonal transformation is required such that $A^t = A^{-1}$. Define $\zeta = \eta A$ and $\zeta^t = A^t \eta^t$ where ζ is the normal coordinate row vector. The kinetic and potential matrices may now be rewritten with this substitution.

$$T = \tfrac{1}{2}(\dot{\zeta}(A^t))((A)\dot{\zeta}^t) = \tfrac{1}{2}\ddot{\zeta}\zeta^t$$

$$\zeta = \delta M^{1/2}A \qquad \delta = \zeta A^t M^{-1/2}$$

$$V = (\tfrac{1}{2})\zeta(A^t X A)\zeta^t = (\tfrac{1}{2})\eta A(A^t X A)A^t \eta^t$$

The $A^t X A$ matrix may be redefined as the diagonal normal mode frequency square matrix (Ω^2). The potential energy is then

$$V = \tfrac{1}{2}\zeta\Omega^2\zeta^t$$

From these relations the normal mode frequencies have been established (Table 2). The displacements of the atoms from their respective equilibrium positions may be represented as linear combinations of the normal modes

$$\delta = \zeta A^t M^{-1/2}$$

where a representation of the A matrix follows:

$$A = \begin{bmatrix} -0.5 & -0.5 & 0.5 & -0.5 \\ -0.5 & -0.5 & -0.5 & 0.5 \\ -0.5 & 0.5 & -0.5 & -0.5 \\ -0.5 & 0.5 & 0.5 & 0.5 \end{bmatrix}$$

During the analysis of the two diatom case the values of the A matrix were all approximately +0.5 or -0.5. This enabled the ζ operators to be presented as simplified combinations of the displacements of atoms from their respective equilibrium positions. (See Fig. 2 for description of modes.)

$$\zeta_1 = -0.5\sqrt{m}(\delta_1 + \delta_2 + \delta_3 + \delta_4) \tag{5a}$$

$$\zeta_2 = +0.5\sqrt{m}(-\delta_1 - \delta_2 + \delta_3 + \delta_4) \tag{5b}$$

$$\zeta_3 = +0.5\sqrt{m}(\delta_1 - \delta_2 - \delta_3 + \delta_4) \tag{5c}$$

$$\zeta_4 = +0.5\sqrt{m}(-\delta_1 + \delta_2 - \delta_3 + \delta_4) \tag{5d}$$

Formulation of Anharmonic Time Independent Hamiltonian

If one considers an arbitrary potential $V(q)$ between atoms n and n+1 which has a minimum at $q=q_o$, the potential function $V(q)$ may be expanded in a Taylor series about q_o:[20]

$$V(q) = \alpha + \beta(q_{n+1} - q_n - q_o)^2 + \gamma(q_{n+1} - q_n - q_o)^3$$

Gamma (γ) represents the physical size of the anharmonicity (deviation from harmonic potential well) and is negative. If one were to make the assumption that the $(q_{n+1} - q_n - q_o)^3$ term is sufficiently small compared to the first terms of the expansion, a harmonic oscillator would define the system. The $(q_{n+1} - q_n - q_o)^3$ interaction of the potential function cannot be ignored in real systems; thus, this term has been added to the total Hamiltonian for the model. In order to generate actual physical models, these cubic anharmonicities between the two diatoms and interconnecting sets of atoms were

introduced. The anharmonicities for the two molecules in the cluster are $\gamma(\delta_4 - \delta_3)^3$ and $\gamma(\delta_2 - \delta_1)^3$. We are assuming that anharmonicities exist only between diatom pairs, and that only the cubic anharmonicity is significant.

From equations (5), the following normal mode operator equations were derived:

$$\gamma(\delta_4 - \delta_3)^3 = \gamma m^{-3/2}(\zeta_4 - \zeta_3)^3$$
$$\gamma(\delta_2 - \delta_1)^3 = \gamma m^{-3/2}(\zeta_4 + \zeta_3)^3$$

Anharmonicities within the intramolecular bonds couple only modes three and four. If the intermolecular bond is anharmonic, all four modes would couple. Expansion of these terms resulted in the following anharmonic potential operator:

$$V_a = \gamma m^{-3/2}(2\zeta_4^3 + 6\zeta_3^2 \zeta_4) \tag{6}$$

Formulation of Time Dependent Hamiltonian (V(t))

In the time independent Hamiltonian, the impact and absorbing atoms were stationary; thus, the $\delta_<(t)$ and $\delta_>(t)$ were equal to zero. Now movement of these atoms must take place in order to propagate a shock through the cluster. The terms two of the harmonic Hamiltonian containing these groups were as follows:

$$\frac{K_<}{2}(q_1^o - q_>^o + \delta_1 - \delta_<(t) - R_o)^2 = \frac{K_<}{2}(\delta_1 - \delta_<(t))^2$$

$$\frac{K_<}{2}(q_>^o - q_4^o - \delta_4 + \delta_>(t) - R_o)^2 = \frac{K_<}{2}(\delta_>(t) - \delta_4)^2$$

Expansion of these term yields:

$$\frac{K_<}{2} [\delta_1{}^2 - 2\delta_1 \delta_<(t) + \delta_<{}^2(t) + \delta_>(t)^2 - 2\delta_>(t)\delta_4 + \delta_4{}^2] \tag{7}$$

The time independent terms, $(\delta_1{}^2, \delta_4{}^2)$, are formulated in the time independent Harmonic Hamiltonian Eq. (4), thus equation (7) may be seperated into time dependent and time independent terms. The time dependent terms will produce our driving potential for the atoms in the cluster. Expansio⟨ of δ_1 and δ_4 in terms of normal mode operators (eqns 5) ζ's yields:

$$\frac{K_<}{2} [\delta_<(t) \, m^{-1/2} (\zeta_1 + \zeta_2 - \zeta_3 + \zeta_4) + \delta_>(t) \, m^{-1/2} (\zeta_1 - \zeta_2 - \zeta_3 - \zeta_4) + \delta_>(t)^2 + \delta_<{}^2(t)]$$

Movement of the impact and absorbing atoms therefore generates a change in position which results in a potential being developed.

Definition of Raising and Lowering Operators

The operators which correspond to momentum and coordinates must satisfy the commutation relation. In matrix mechanics, the one dimensional harmonic oscillator Hamiltonian is as follows:

$$H = \frac{p_\zeta{}^2}{2} + \frac{1}{2}\Omega^2\zeta^2$$

In order to procced with normal mode analysis, the following raising ($a^\dagger$) and lowering operators (a) are introduced.[19]

$$a = \alpha p_\zeta + \beta \zeta$$

$$a^\dagger = \alpha^* p_\zeta + \beta^* \zeta$$

$\alpha^*\beta$ is chosen as a purely imaginary value such that $\alpha\beta^* = -\alpha^*\beta$

$$\alpha = \frac{i}{\sqrt{2}}$$

$$\beta = \frac{\Omega}{\sqrt{2}}$$

Substitution of these values yields the following:

$$a^\dagger a = \tfrac{1}{2}[p_\zeta^2 + \Omega^2 \zeta^2] + \frac{\hbar\Omega}{2}$$

$$a^\dagger a = H - \frac{\hbar\Omega}{2}$$

$$a = \frac{1}{\sqrt{2}}(+ip_\zeta + \Omega\zeta) \tag{8a}$$

$$a^\dagger = \frac{1}{\sqrt{2}}(-ip_\zeta + \Omega\zeta) \tag{8b}$$

So the Hamiltonian of the system may be described as

$$H = a^\dagger a + \frac{\hbar\Omega}{2}$$

The Hamiltonian may now be applied to the Schrödinger equation in order to evaluate the eigenstates.

$$H \,|E> = E\,|E>$$

$$(a^{\dagger}a + \frac{\hbar\Omega}{2}) \,|\, E\rangle = E \,|\, E\rangle$$

$$a^{\dagger}a \,|\, E\rangle = (E - \frac{\hbar\Omega}{2}) \,|\, E\rangle$$

such that

$$\langle E \,|\, a^{\dagger}a \,|\, E\rangle = (E - \frac{\hbar\Omega}{2})\langle E \,|\, E\rangle$$

$$\langle E \,|\, E\rangle = 1$$

$$\langle E \,|\, a^{\dagger}a \,|\, E\rangle = (E - \frac{\hbar\Omega}{2})$$

This will provide a harmonic basis for the problem. The states may be labeled as numbers with corresponding energies evaluated from the numbered states.

The raising and lowering operators may now be defined through their action upon the eigenstates.

$$a \,|\, n\rangle = \sqrt{n\hbar\Omega} \,|\, n\text{-}1\rangle \tag{9a}$$

$$a^{\dagger} \,|\, n\rangle = \sqrt{(n+1)\hbar\Omega} \,|\, n+1\rangle \tag{9a}$$

In the model problem, the normal mode operators were defined from equations (8):

$$\zeta = (\tfrac{1}{\sqrt{2\Omega}}) \, (a + a^{\dagger}) \tag{10a}$$

$$p_{\zeta} = (\tfrac{1}{i\sqrt{2}}) \, (a - a^{\dagger}) \tag{10a}$$

Using the above relations for a and $a^{\dagger}$ the cubic anharmonic operators may now be evaluated

$$\zeta_i \,|\, n_i\rangle = (\frac{\hbar}{2m_i\Omega_i})^{1/2} [(n_i)^{1/2} \,|\, n_i - 1\rangle + (n_i + 1)^{1/2} \,|\, n_i + 1\rangle]$$

$$\zeta_i^2 |n_i\rangle = (\frac{\hbar}{2m_i \Omega_i}) [(n_i)^{1/2}(n_i - 1)^{1/2} |n_i - 2\rangle + (n_i) |n_i\rangle + (n_i + 1) |n_i\rangle$$

$$+ (n_i + 1)^{1/2}(n_i + 2)^{1/2} |n_i + 2\rangle]$$

$$\zeta_i^3 |n_i\rangle = (\frac{\hbar}{2m_i \Omega_i})^{3/2} [(n_i)^{1/2}(n_i - 1)^{1/2}(n_i - 2)^{1/2} |n_i - 3\rangle + ((n_i)^{1/2}(n_i - 1) + (n_i)^{1/2}(n_i + 1)$$

$$+ (n_i)^{3/2} + (n_i + 1)^{3/2}) |n_i - 1\rangle + ((n_i)(n_i + 1)^{1/2} + (n_i + 1)^{1/2}(n_i + 2)) |n_i + 1\rangle$$

$$+ (n_i + 1)^{1/2}(n_i + 2)^{1/2}(n_i + 3)^{1/2} |n_i + 3\rangle]$$

The original basis set chosen for the problem consisted of the product of four normal modes ($|n_1\rangle |n_2\rangle |n_3\rangle |n_4\rangle$). The normal mode operator acts only upon its corresponding basis state (i.e. ζ_4^3 operated only upon $|n_4\rangle$). The normal mode operators were used to formulate the anharmonic and time dependent Hamiltonian matrix elements. In the total Hamiltonian matrix, the harmonic terms correspond to the diagonal elements and the anharmonic terms correspond to the symmetric off-diagonal elements.

$$\langle n_i' | \zeta_i | n_i\rangle = (\frac{\hbar}{2m_i \Omega_i})^{1/2} [(n_i)^{1/2}\delta_{n_i' n_{i-1}} + (n_i + 1)^{1/2}\delta_{n_i' n_{i+1}}]$$

The anharmonic Hamiltonian matrix was generated and diagonalized to obtain the appropriate eigenvalues and eigenstates (Table 3).

$$Z^t H Z = \Xi$$

where Z = eigenvector matrix

Z^t = transpose of eigenvector matrix

Ξ = diagonal eigenvalue matrix

Propagation of Time Dependent Hamiltonian

The following passages formulate the time dependent perturbation introduced

into the one-dimensional system.[21] The basic solution to the time dependent

Schrödinger equation is as follows:

$$H\psi = (ih) \left(\frac{d\psi}{dt}\right)$$

where H is a function of position and time in a Cartesian coordinate system. This is

extremely difficult to solve; therefore, the Hamiltonian is divided into a time-

independent and time dependent part:

$$H = H_{TI} + V(t)$$

H_{TI} = time independent term of Hamiltonian

$V(t)$ = time dependent term of Hamiltonian

$$\Psi = \psi(t)e^{-i(E/\hbar)t}$$

The spatial equation to solve is

$$H_{TI}\psi = E\psi$$

E = separation constant

It has well behaved solutions when E is equal to E_n

$$H_{TI}\psi_n{}^o = E_n\psi_n{}^o$$

Assume the $\Psi(q,t)$ can be written as a linear combination of orthogonal functions:

$$\Psi(q,t) = \sum_n a_n(t)\ \psi_n{}^o(q,t)$$

$$\Psi_n{}^o = \Psi_n{}^o e^{-iE_n t/\hbar}$$

The quantity Ψ_n^o is described by the eigenfunctions of a harmonic oscillator and the quantities $a_n(t)$ are defined as the occupation coefficients. Since the wave function is normalized,

$$\sum_n a_n(t)^* a_n(t) = 1$$

the series expansion for $\Psi(q,t)$ may now be substituted into the Schrödinger wave equation yielding:

$$\frac{d}{dt} a_m(t) = -\frac{h}{i} \sum_{n=1}^{\infty} a_n(t) \int \psi_m^{o*} V(t) \psi_n^o \, dq$$

where $m = 1, 2, 3, \ldots$

This yields the rate of change (with respect to time) of the mth component of the basis. A_m (rate of amplitude change) depends upon all basis amplitudes. The following equations are shown to exemplify the above differential equation.

$$-\frac{h}{i}\frac{da_1}{dt} = a_1 \int \psi_1^{o*} V(t) \psi_1^o \, dt + a_2 \int \psi_1^{o*} V(t) \psi_2^o \, dt + \ldots + a_K \int \psi_1^{o*} V(t) \psi_K^o \, dt + \ldots$$

$$-\frac{\hbar}{i}\frac{da_2}{dt} = a_1 \int \psi_2^{o*} V(t) \psi_1^o \, dt + a_2 \int \psi_2^{o*} V(t) \psi_2^o \, dt + \ldots + a_K \int \psi_2^{o*} V(t) \psi_K^o \, dt + \ldots$$

Utilizing these coupled first order differential equations, numerical analysis using the Adams Moulton integrator provided the coefficients for the various states of the model.

Calculation of Quantum Position of Atoms

In order to calculate positions of atoms, computations of expectation values of displacements from equilibrium were performed. The matrix elements of operators δ_i were evaluated in the normal mode basis, and then transformed into the harmonic representation using the eigenvector matrices , as follows:

$$Z^t D_i Z = D'_i$$

where

Z^t = transpose of eigenvector matrix

Z = eigenvector matrix

D_i = displacement matrix

D'_i = transformed displacement matrix

Upon transformation, D'_i was then summed over each state with its corresponding energy and probability:

$$P^t(t) D'_i P(t)$$

where

$$[P(t)]_i = c_i(t) \exp[-iE_i t/\hbar]$$

where P is a column vector based on probablity and eigenvalues, and P^t is a row vector. This summation yields the displacement of atom i from its equilibrium position.

Calculation of Quantum Bond Energies

The total energy of a particular bond is expressed as the summation of the bond's potential and kinetic energy. The potential energy for the quantum system is calculated from the expectation values of position for the corresponding atoms.

$$\text{Potential energy} = (1/2)(K_{bond})(\delta_j - \delta_i)^2$$

From equations (5) the potential energy can be represented in terms of normal modes:

$$PE_{12} = (\tfrac{1}{2})\,(K_>)\,(\delta_2 - \delta_1)^2 = (\tfrac{1}{m})\,(K_>)\,(\zeta_4 - \zeta_3)^2$$

$$PE_{23} = (\tfrac{1}{2})\,(K_<)\,(\delta_3 - \delta_2)^2 = (\tfrac{1}{m})\,(K_<)\,(\zeta_2 - \zeta_4)^2$$

$$PE_{34} = (\tfrac{1}{2})\,(K_>)\,(\delta_4 - \delta_3)^2 = (\tfrac{1}{m})\,(K_>)\,(\zeta_4 + \zeta_3)^2$$

These operators will act upon our normal mode basis set in order to establish potential energy matrices. Upon transformation of the potential energy matrix with the eigenvector matrix, summation over all states at a particular time yields the potential energy of a bond.

$$Z^t\,PE_{ij}\,Z = PE_{ij}$$

$$P^t(t)\,PE_{ij}\,P(t) = \text{potential energy of bond ij}$$

As stated previously the kinetic energy is calculated by:

$$T = \tfrac{1}{2}\dot{\eta}\,\dot{\eta}^t$$

$$\dot{\zeta}^t = \dot{\eta}^t A^t$$

$$T = \tfrac{1}{2}\dot{\zeta}\dot{\zeta}^t$$

where $\dot{\zeta}^t$ is a column vector and is normal mode momentum. As mentioned with respect to position, normal mode momentum ($p_{\zeta i}$) may be expressed as a summation of corresponding atom momentum (p_i)

$$p_{\zeta 1} = -0.5\sqrt{m}\,(p_1 + p_2 + p_3 + p_4) = (1/(i\sqrt{2}))\,(a_1 - a_1)$$

$$p_{\zeta 2} = +0.5\sqrt{m}\,(-p_1 - p_2 + p_3 + p_4) = (\,1/(i\sqrt{2}))\,(a_2 - a_2)$$

$$p_{\zeta 3} = +0.5\sqrt{m}\ (p_1 - p_2 - p_3 + p_4) = (1/(i\sqrt{2}))\ (a_3\text{-}\dot{a_3})$$

$$p_{\zeta 4} = +0.5\sqrt{m}\ (-p_1 + p_2 - p_3 + p_4) = (1/(i\sqrt{2}))\ (a_4\text{-}\dot{a_4})$$

The kinetic energy of the i-j bond is expressed as:

$$T_{ij} = \frac{(p_j - p_i)^2}{2\mu}$$

which is expressed by normal momentum operators as:

$$T_{12} = \frac{(p_{\zeta 4} - p_{\zeta 3})^2}{2\mu} = \text{kinetic energy operator for bond } R_{12}$$

$$T_{23} = \frac{(p_{\zeta 2} - p_{\zeta 4})^2}{2\mu} = \text{kinetic energy operator for bond } R_{23}$$

$$T_{34} = \frac{(p_{\zeta 4} + p_{\zeta 3})^2}{2\mu} = \text{kinetic energy operator for bond } R_{34}$$

Each kinetic energy operator established a kinetic energy matrix which is transformed to the harmonic representation via the eigenvector matrix $\mathbb{Z}$.

$$\mathbb{Z}^t\,\mathbb{K}\,\Xi_{ij}\,\mathbb{Z} = \mathbb{K}\,\Xi_{ij}'$$

Upon transformation we sum over all states:

$$\mathbb{P}^t(t)\,\mathbb{K}\,\Xi_{ij}'\,\mathbb{P}(t)$$

Calculation of Classical Bond Energies

Classical potential and kinetic bond energies are calculated directly from atom position.

$$\text{Potential energy} = (\tfrac{1}{2})(K_{bond})(q_{n+1} - q_n - \rho_o)^2$$

$$\text{Kinetic energy} = (\tfrac{1}{2\mu})(p_{n+1} - p)^2$$

Calculation of Atomic Period

The atomic period for this model was based upon the stonger force constant.

$$\omega = (K_> / \mu)^{1/2}$$

$$T = 2\pi / \omega = 2.1 \times 10^3 \text{ atu}$$

Energy Evaluations of the Two Diatom Model

In order to evaluate the normal mode energies, the original Hamiltonian matrix was separated into four normal modes, a time-independent anharmonic term, and the time-dependent potential term.

$$H_T = H_1^o + H_2^o + H_3^o + H_4^o + V_a + V(t)$$

Each matrix was initially transformed into the harmonic basis by multiplication with the eigenvector and transpose eigenvector matrix (Z = eigenvector matrix).

$$Z^t H_i Z = H_i'$$

Upon transformation, each term was summed over all possible states to provide the energies of the particular parts.

$$P^t(t) H_i' P(t)$$

III.   Discussion of Results

A.   Classical Trajectories

When the ballistic particle imposes a shock, it adds .005884 Hartrees of energy to the chain of atoms. The shock wave propagates through the classical chain at approximately 6.5×10^{-2} a_0/ps, causing displacement of atoms (Figures 3,4). The classical system responds as expected with respect to atom position and bond energies. Atom position is directly related to the neighbor atoms, and atoms tend to oscillate in diatom pairs. The impact atom provides a disturbance within the lattice which is not felt by the central atom pairs for approximately eight periods (Figs. 5). The transverse displacement of the entering atom (q_0) imparts energy to the first atom in the lattice which causes the transverse movement of this atom and so forth; thus, resulting in the propagation of the disturbance throughout the lattice. Since this shock wave is a comparatively low energy disturbance with respect to previous calculations [Wyatt,Marston], atoms are not significantly displaced and atom separation is fairly constant. The atoms connected by a strong bond tend to move as a pair, with most of the lattice deformation occuring within the intermolecular bond.

Bond energies indicate that energy is transferred between kinetic and potential energy . As the energy from the shock wave is transferred to the bonds, nonuniformities in the oscillator behavior are observed. The strong bonds exhibit a tendency to remain relatively constant, while most of the energy from the shock is transferred to the intermolecular bond (Figures 6-11).

26

B. Convergence of the Quantum Model

The time dependent coefficients for the quantum states $a_i(t)$ will help us in examining the convergence of the results of our system, the nature of occupation of various quantum states, and the conservation of probability. Quantum eigenvalues of a sixteen state model are listed in Table 3. In the present model, the classical positions of $q_<$ and $q_>$ are used in calculating a driving potential. The classical system was initialized with all atoms in the chain located at their respective eqilibrium values. Initial momenta were calculated for these atoms, and Hamilton's equations of motion were solved for position and momentum. Upon solving the equations of motion, the atoms were no longer located at equilibrium displacements. This has been defined as $t = 0$ for the system. Since $q_<$ and $q_>$ were displaced from equilibria, a small driving potential for the system was established causing population of excited states in the quantum model. The model may now be thought of as being non-zero temperature. (atoms are oscillatory).

When a shock wave is introduced to the quantum model, energy is transferred into the crystal lattice resulting in excitation and population of higher energy states. This corresponding population of states may be represented as $a_i{}^*a_i$ where a_i is the coefficient of occupation of state i (.04% deviation in the 16 state model, .008% deviation in the 100 state model). Plots of a 16 state basis illustrate a periodic transfer of energy from state to state and a tendency to retain most of the energy within the lower mode states (Figures 12-27). Harmonic and anharmonic 16 state bases exhibit similar tendencies. Examination of a larger basis (100 states) shows a larger retention of energy in lower mode states. Since there is a ratio of 5:5:2:2 (n_1:n_2:n_3:n_4) in the 100 state system compared to a 2:2:2:2 ratio in our lower (16 state) model, the energy

distributes itself differently; thus, allowing for even less population of higher energy levels (Figures 28-33).

C. Comparison of Position Trajectories

Comparison of expectation values for the positions of atoms for several bases indicates fairly good convergence of the system. (Figures 34-41) We have learned from [Wyatt and Marston] that quantum harmonic atom positions at high energy converges towards the classical results. Although there are deviations from this expected result one can see that the larger harmonic basis sets move toward convergence to classical results. (Figures 42-45) This is also the case with convergence of the anharmonic system.

Anharmonicities produce deviations in energy level spacing as compared with a purely harmonic system. The deviations in energy spacing produces a variance in energy state occupation; thus, there will be variances in position plots of harmonic and anharmonic models. Since there are only two states in the higher frequency modes, the 100 state system does not fully describe the cubic anharmonicity making differences between the harmonic and anharmonic models small. (Figures 46-49) Atom motion in the anharmonic model deviates slightly in frequency and amplitude as compared to the harmonic model.

In comparison to classical harmonic trajectories, the quantum harmonic model does not converge exactly to the classical harmonic trajectory, as expected [Wyatt, Marston]. The initial oscillatory motion of the quantum model prior to a shock is deviates slightly coupled with small deviations of average position away from average equilibrium values. This result is most likely caused by the low number of energy

states in the quantum model. If one were to examine the frequencies of the four modes (Table 2), one can see that they are in a ratio of 11.5:6.6:1:1 ($\Omega_1:\Omega_2:\Omega_3:\Omega_4$).

The quantum model currently has a 5:5:2:2 basis ratio. Movement in each system should be characterized by oscillations of diatom pairs. For instance, normal oscillations of atoms one and two should be directly out of phase as observed in the classical system; however, careful observation of quantum diatom pairs yields small phase dissimilarities which may be caused by the population of various energy states. Since we have a low number of internal mode states (modes one and two), the higher modes are increasingly populated. If one were to examine the modes (Figure 2), one can see that linear combinations of the modes describe the normal oscillator motion of the atoms. Since the higher energy modes are more populated, we observe phase dissimilarities within diatom pairs. Classical anharmonic results versus quantum anharmonic results correspond in a similar fashion.

The quantum harmonic model of [Wyatt, Marston] was easily separated into four independent modes. This allowed for vast numbers of low frequency mode states as compared to the higher energy modes (500:200:100:100) ($n_1:n_2:n_3:n_4$) giving a total basis size of 10^9. The low frequncy modes were now capable of describing center of mass and oscillatory motion. Addition of this number of states to the present model makes the problem numerically intractible.

It is also interesting to note the dependence of the present model upon $q_>$. The absence of the potential created by $q_>$ causes great phase dissimilarities with respect to diatom oscillations, and it also inhibits proper atom atom displacements with respect to a shock induced lattice. Several cases have been examined (Figures 50-59) in order to show these effects. Since the $q_>$ potential is no longer present prior to a shock (ramp

shock) or not present at all, this causes the excited state population to vary significantly; thus, atom energy and displacement become less uniform. The potential caused by $q_>$ has a significant affect upon lattice dynamics.

Another interesting point to note is the dependence of this model on the size of the anharmonicity. The degree of anharmonicity was increased 10 fold as a trial experiment. Small deviations in position are observed as well as small frequency shifts in oscillations Fig. (60-61). In the present model, we are limited to a ground state and first excited state in modes three and four. This limitation in basis size effectively reduced the survival terms of the anharmonic operators; thus, allowing for small deviations in frequency and amplitude of atom positions.

D. Quantum Mode Energy Comparisons

A slightly larger difference between our quanutm harmonic and anharmonic models is observed in mode energies. (Figures 62-65). Energy level spacing in the harmonic model is different as compared with the anharmonic model in which energy level spacing decreases towards higher levels. This spacing difference exhibits variances in mode energies prior to and after shock wave introduction. If both models were initially stationary states, one would observe that mode energies would start at 0.5 quanta. As stated earlier, t =0 corresponds to a time in which atom positions are displaced from their equilibrium values causing a driving potential to be created by $q_<$ and $q_>$. This deviation in $q_<$ and $q_>$ is fed into our quantum system providing for population of some excited states. Since the excited states became populated, initial values of mode energies increased above 0.5 quanta. Initially, the harmonic model distributes energy to its excited states in a different fashion as compared with the

anharmonic model. The anharmonic model slowly distributes its energy to higher states then reaches a steady value prior to the shock wave. Energy transitions are much smoother in the anharmonic model because energy levels have been lowered.

As shock energy is introduced to both systems, the anharmonic model reacts more quickly and distributes energy to higher states. This is evidenced by the fact that the higher modes reach a steady state at slightly higher values as compared to the harmonic model, and the lower mode energies in the anharmonic case achieve smaller energies as compared to the lower modes. In each case, the upper modes pick up approximately 0.2 quanta of energy as compared with approximately 0.6 quanta for the lower modes. A ratio of this (0.6:0.2) corresponds quite well with a ratio of states (5:2).

Addition of states to the lower frequency modes in these models will definitely improve the energy transfer prior to and during the shock wave. Energy will be distribute differently among the lower states allowing for the system to stabilize.

E. Comparison of Bond Energies

The classical models react as expected with respect to bond energies. Diatom pairs are oscillating in a uniform fashion prior to a shock wave resulting in kinetic and potential energy to be directly out of phase and total energy to remain constant. As the system is perturbed, oscillations and dispacements vary; thus, variances in potential, kinetic and total energy may be observed. The strong bonds have an inherent tendency to resist change with respect to a low energy shock. (Figures 6-11)

Prior to a shock in the quantum models, energy within the bonds is dependent upon the coupling of various modes. Since the system is non-stationary, population of various energy levels vary with time. This causes individual bond energies to fluctuate transferring energy between bonds. As the shock wave is introduced to the system, bonds exchange energy slightly faster and the overall energy within the bonds is higher (Figures 70-79). There are few differences between the harmonic and anharmonic quantum models; however total bond energy is slightly lower in the anharmonic system. Careful examination of the potential versus kinetic energy plots of bond energy in both quantum systems shows that potential and kinetic energies are in phase. Part of this is due to the sharing of energy between bonds; however, some is caused by an small number of low frequency mode states (modes one and two). Excessive energy is placed into the higher mode states; thus causing an imbalance in the system. This was not as evident in positions as it is in bond energies.

IV. Conclusions

Examination of a crystal lattice using a coupled mode basis yielded a great deal of information concerning both harmonic and anharmonic models. The following conclusions may be drawn from these results:

(1) The deviations in energy spacing from the anharmonicities cause transitions to occur more easily as compared with the harmonic model

(2) Addition of states to the quantum model allowed for convergence toward classical results.

(3) The anharmonicities produce slight deviations in frequency of oscillation and displacement because of energy spacing differences.

(4) The quantum model is not only dependent on the potential created by $q_<$: the potential created by $q_>$ is necessary to allow the atoms to act as a cluster. Any deviations in the potential created by $q_>$ causes the model to change significantly.

(5) Energy spacing differences allowed for deviations in mode energies.

(6) Bond energies within the classical models correspond directly to atom positions. There are instances in time in which potential energy is at a maximum (corresponding to maximum deviation of atom position from equilibria) and minimum kinetic energy. Total energy is constant prior to a shock. Most of the energy is transferred to the intermolecular bond.

(7) Bond energies within both quantum models are not constant prior to a shock. Since energies are dependent upon mode population, total energy within a bond may oscillate. Energy may be transfered from bond to bond. The total energy of all bonds prior to a shock should be constant.

33

(8)   Deviations from the expected results of [Wyatt, Marston] in a harmonic model were caused primarily by the absence of states which resulted in normal oscillator motion of the atoms and center of mass motion to be inconsistent. Careful examination of the mode frequencies yielded information concerning the proper number of states one must have in order to describe atom motions properly. Lack of a substantial number of states also restricted the amount of energy transferred into the lattice.

Upon re-examination of the problem, one sees that the total quantum Hamiltonian was written as follows:

$$H_T = H^o + V_a + V(t)$$

The anharmonic substituent (V_a) of the Hamiltonian was formulated using a coupled normal mode operator:

$$V_a = \gamma(m)^{-3/2} (2\zeta_4^3 + 6\zeta_3^2 \zeta_4)$$

Instead of using a Hamiltonian which had all four modes coupled, we should have formulated the problem using a harmonic uncoupled Hamiltonian for modes one and two, and a coupled anharmonic Hamiltonian for modes three and four.

$$H_T = H_1^o + H_2^o + H_{34}^o + V_{34}^a + V_1(t) + V_2(t) + V_{34}(t)$$

where

H_T = total Hamiltonian

H_i^o = Harmonic Hamiltonian for mode i

H_{34}^o = Harmonic Hamiltonian of coupled modes three and four

V_{34}^a = Anharmonic Hamiltonian of coupled modes three and four

$V_i(t)$ = Potential for mode i

$V_{34}(t)$ = Potential for coupled modes three and four

This would have allowed for an increased number of low frequency mode state (modes one and two), thus, placing the energy levels of all the modes in proper ratios.

In conclusion, an entirely coupled Hamiltonian severely restricted proper formulation of this problem; however, reformulation using uncoupled modes should prove beneficial. Since desired results were not obtained using the harmonic model, deviations are most likely present in our anharmonic model. Once the Hamiltonian is uncoupled, an extremely large number of states may be added, and it will afford extremely large additions of energy to the crystal lattice.

Table 1

Equilibrium values for position, atom separations, mass, and force constants

$q_<^o = -6.9316\ a_o$　　　　　　$q_>^o = +6.9316\ a_o$

$q_1^o = -3.4658\ a_o$　　　　　　$q_3^o = +1.7329\ a_o$

$q_2^o = -1.7329\ a_o$　　　　　　$q_4^o = +3.4658\ a_o$

$\rho_o = +1.7329\ a_o$　　　　　　$R_o = +3.4658\ a_o$

$m_1 = m_3 = 34629\ amu$　　　　$K_< = 0.00468\ Hartree/Bohr^2$

$m_2 = m_4 = 34629\ amu$　　　　$K_> = 0.14985\ Hartree/Bohr^2$

$\mu = 17314.5\ amu$

$\lambda = -3.0 \times 10^{-4}\ Hartree/Bohr^3$

Table 2

Frequencies and energy spacings for the normal modes.

Normal Mode Frequencies (a.u.)	Energy Spacing ($h\Omega$)(eV)
$\Omega_1 = 0.000256$	6.966×10^{-3}
$\Omega_2 = 0.000445$	12.108×10^{-3}
$\Omega_3 = 0.002927$	79.644×10^{-3}
$\Omega_4 = 0.002949$	80.243×10^{-3}

Table 3

Eigenvalues for the anharmonic and harmonic quantum 16 state system.

State (n_4 n_3 n_2 n_1)	Anharmonic Energy (a.u.)	Harmonic Energy (a.u.)
0000	0.003284	0.003290
0001	0.003540	0.003546
0010	0.003722	0.003735
0011	0.003989	0.003992
0100	0.006163	0.006217
1000	0.006235	0.006239
0101	0.006435	0.006473
1001	0.006594	0.006496
0110	0.006634	0.006662
1010	0.006684	0.006685
0111	0.006896	0.006919
1011	0.006942	0.006942
1100	0.009165	0.009166
1101	0.009421	0.009423
1110	0.009610	0.009612
1111	0.009859	0.009869

Figure Captions

Figure 1   Representation of the four atom cluster , with $q_<$ and $q_>$.
$q_<$ = initial cartisian coordinate position of entering qroup atom
q_1 = initial cartesian coordinate position of atom one
q_2 = initial cartesian coordinate position of atom two
q_3 = initial cartesian coordinate position of atom three
q_4 = initial cartesian coordinate position of atom four
$q_>$ = initial cartesian coordinate position of the absorbing atom
$K_>$ = force constant utilized between diatom pairs
$K_<$ = force constant utilized for entering, absorbing, and coupling of diatoms
R_0 = cartesian distance utilized for entering, leaving, and coupling of diatoms

ρ_0 = cartesian distance utilized for coupling of diatom pairs

Figure 2   Pictoral representation of the four normal modes.
Normal mode one represents center of mass motion of the four atoms.
Normal mode two represents paired diatom stretching about the central bond between atoms two and three.
Normal mode three repesents an attractive stretching between atoms one and two, and a repulsive interaction between atoms three and four.
Normal mode four represents a repulsive interaction between atoms one and two, and an attractive interaction between atoms two and three.

Figure 3   Classical harmonic position of atoms $q_<$, q_1, q_2, q_3, q_4, and $q_>$.
Positions are measured in atomic units, periods correspond to one harmonic oscillation of a diatom pair. Atom positions are measured from the center of mass for the chain.

Figure 4   Classical anharmonic position of atoms $q_<$, q_1, q_2, q_3, q_4, and $q_>$.
Positions are measured in atomic units, periods correspond to one harmonic oscillation of a diatom pair. Atom positions are measured from the center of mass for the chain.

Figure 5   Position of the ballistic particle. Atom position is measured in atomic units. Position is measured from the center of mass for the chain.

Figure 6   Classical harmonic bond energy of the intramolecular bond (R12) between atoms q_1 and q_2. Energy is measured in harmonic quanta.

Figure 7   Classical harmonic bond energy of the intramolecular bond (R34) between atoms q_3 and q_4. Energy is measured in harmonic quanta.

Figure 8   Classical harmonic bond energy of the intermolecular bond (R23) between atoms q_2 and q_3. Energy is measured in harmonic quanta.
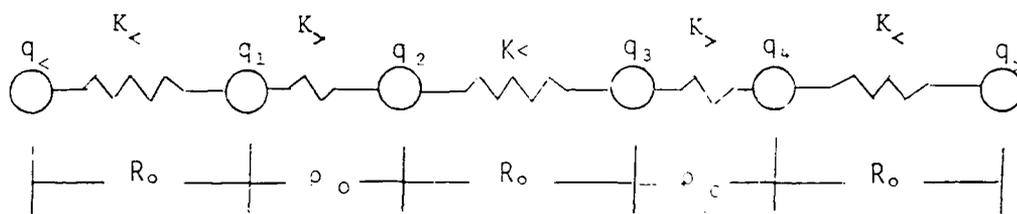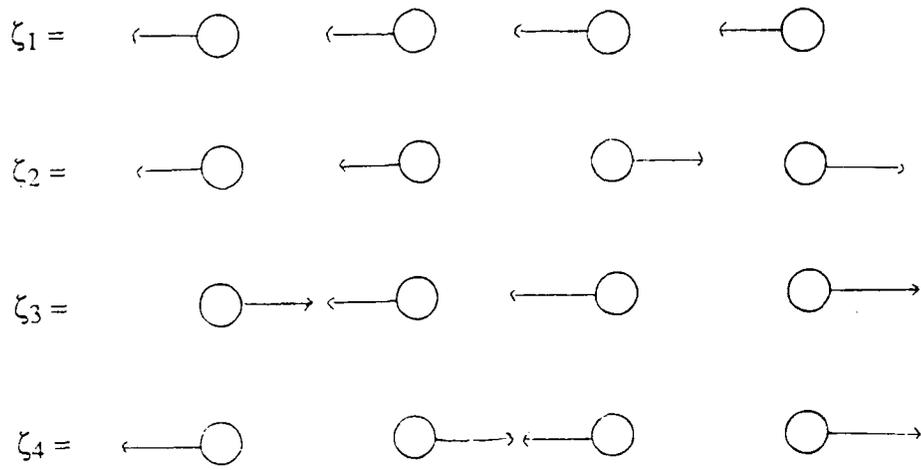
Figure 1

Figure 2

Classical Position of Atoms
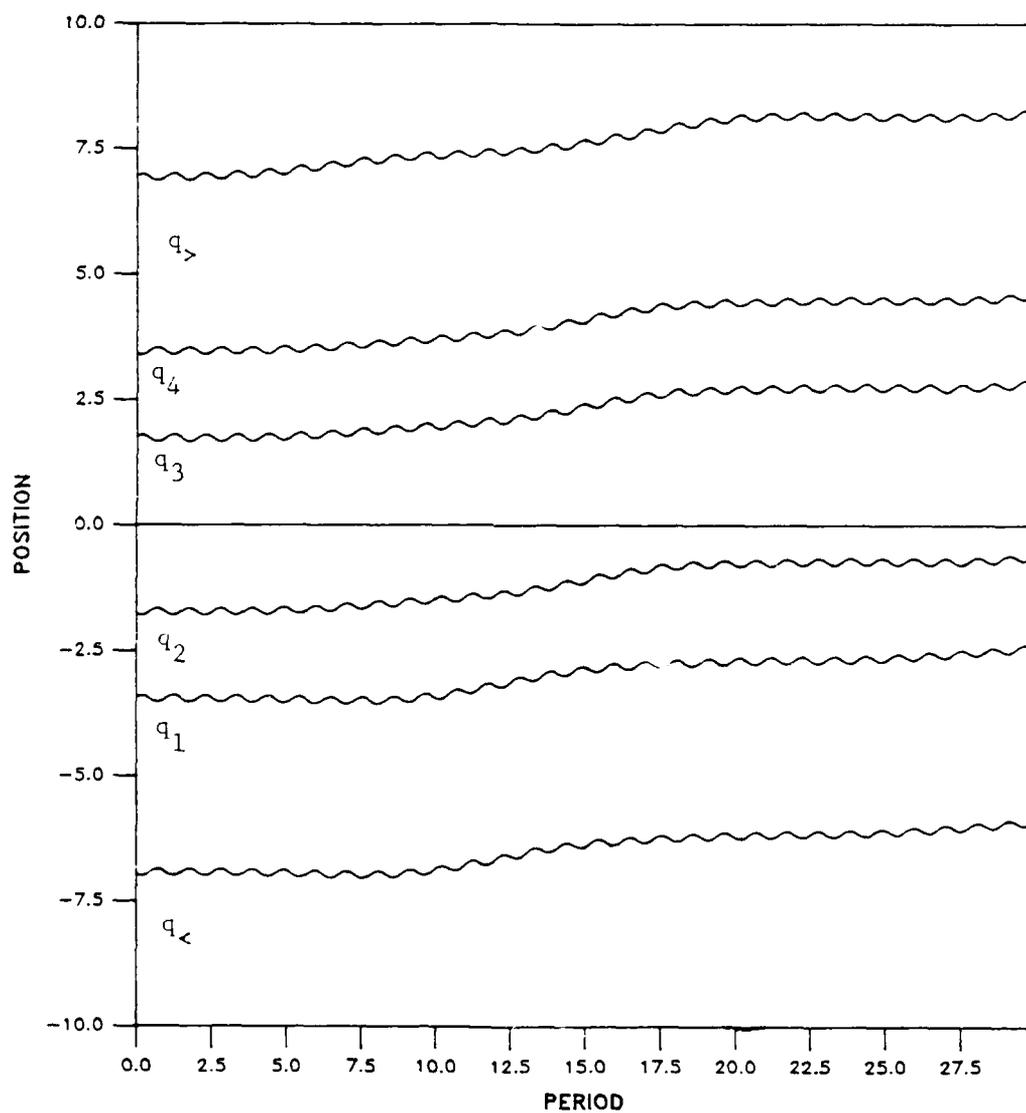
Harmonic

Figure 3

Classical Position of Atoms
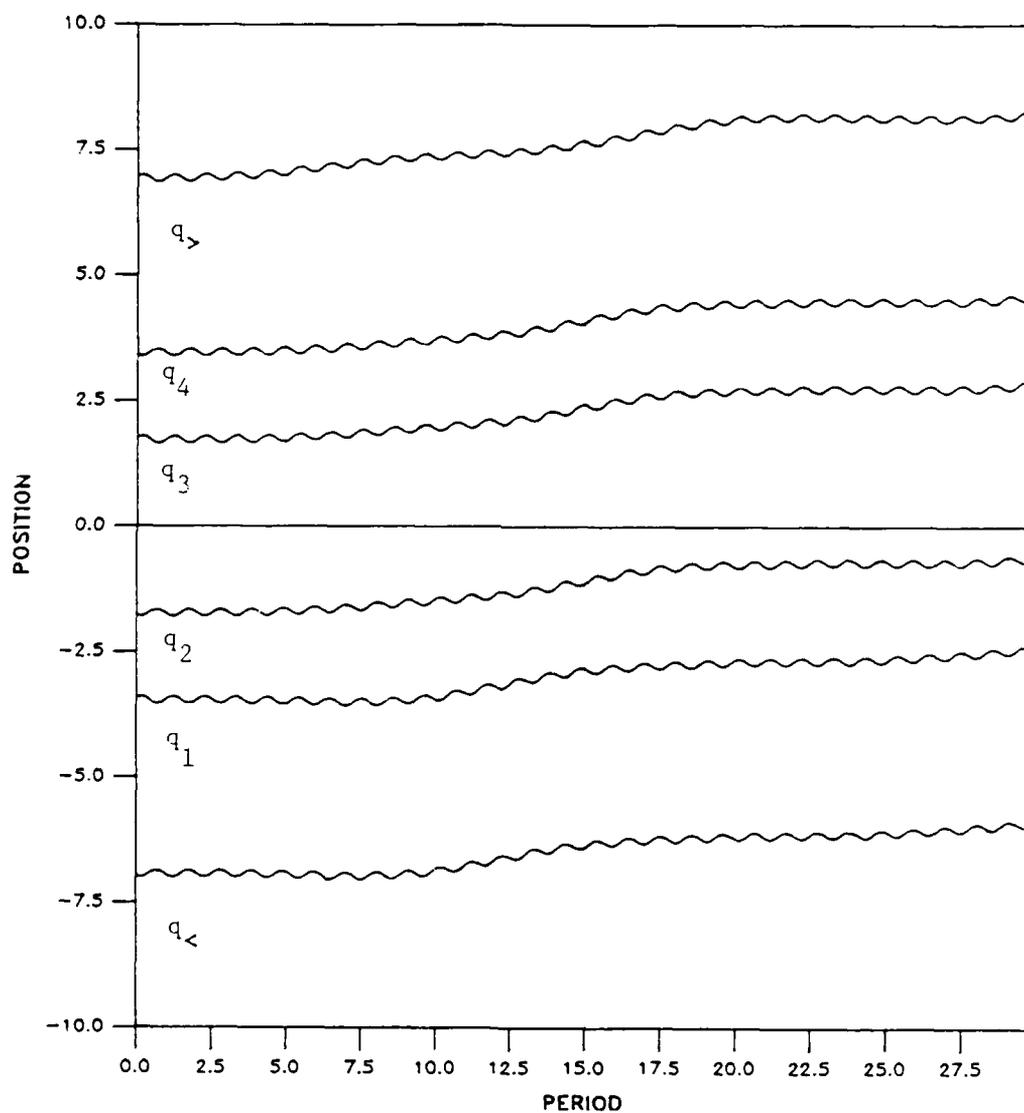
Anharmonic

Figure 4

Position of Impact Atom

Classical
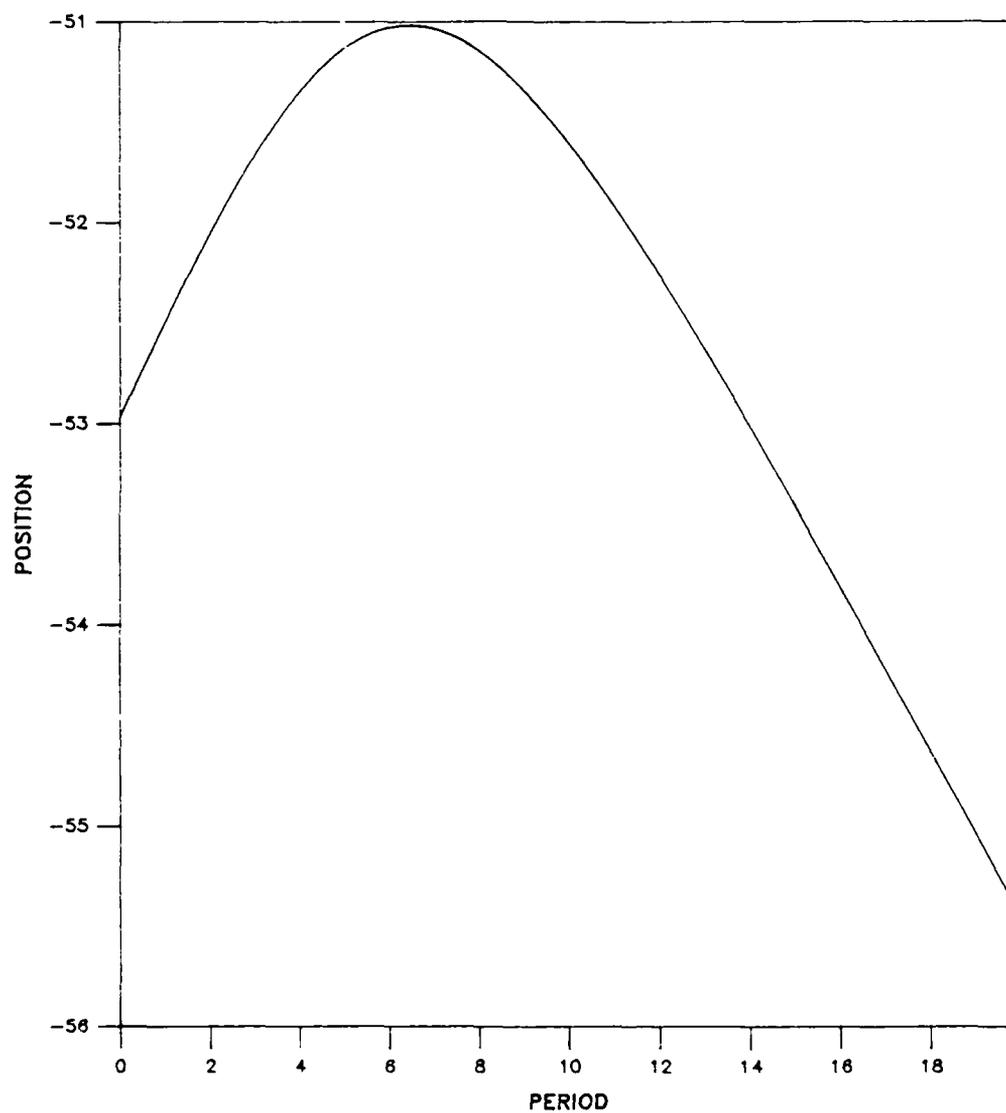
Figure 5

Energy of Bond R12

Classical Harmonic
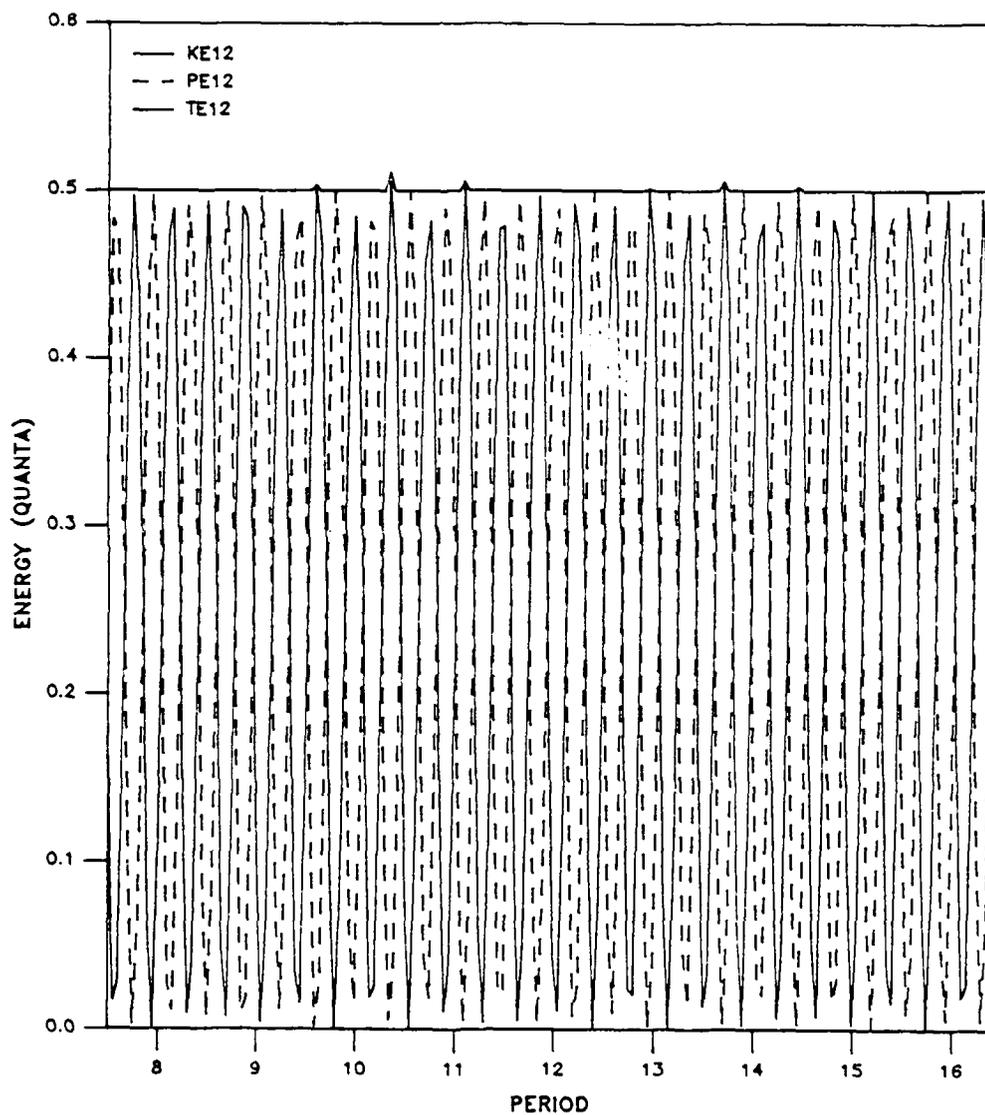
Figure 6

Energy of Bond R34

Classical Harmonic
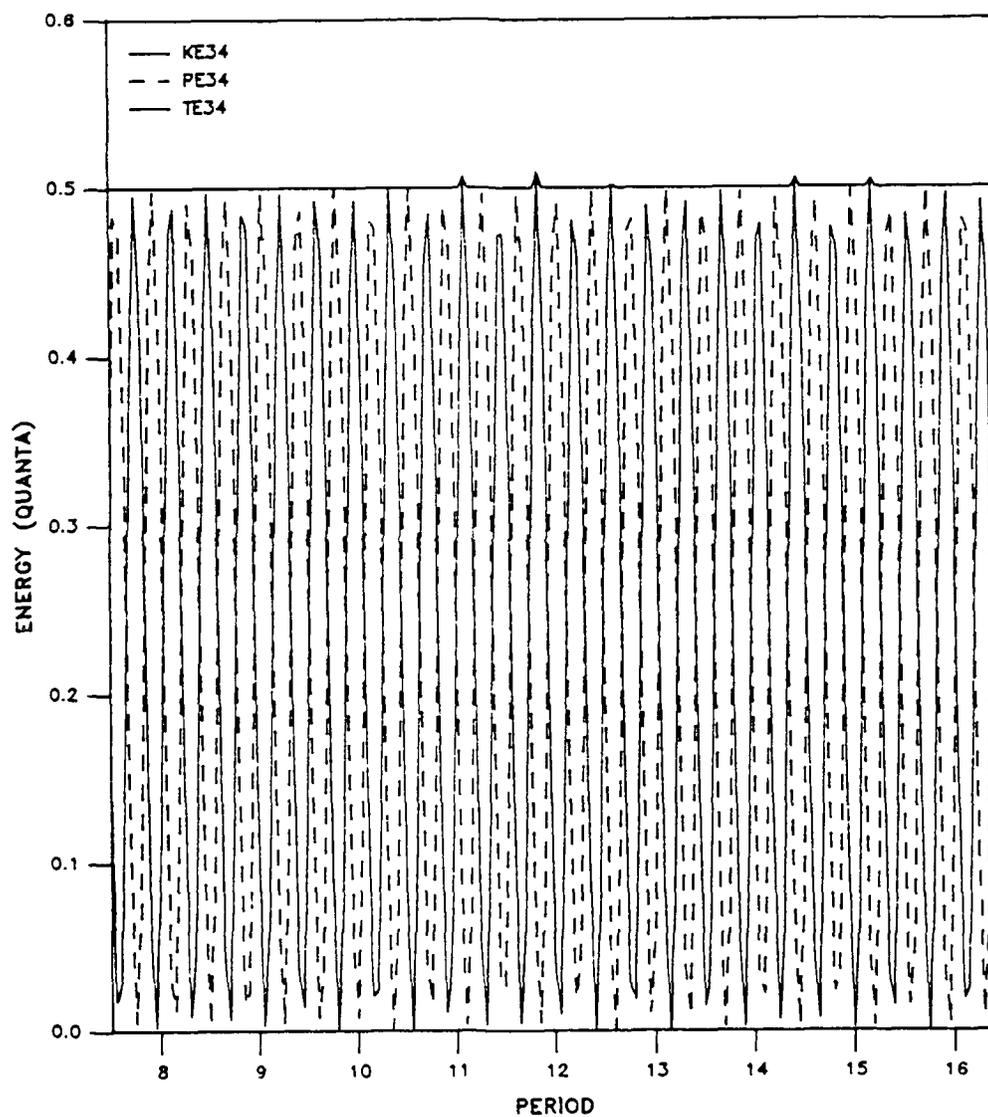
Figure 7

Energy of Bond R23

Classical Harmonic
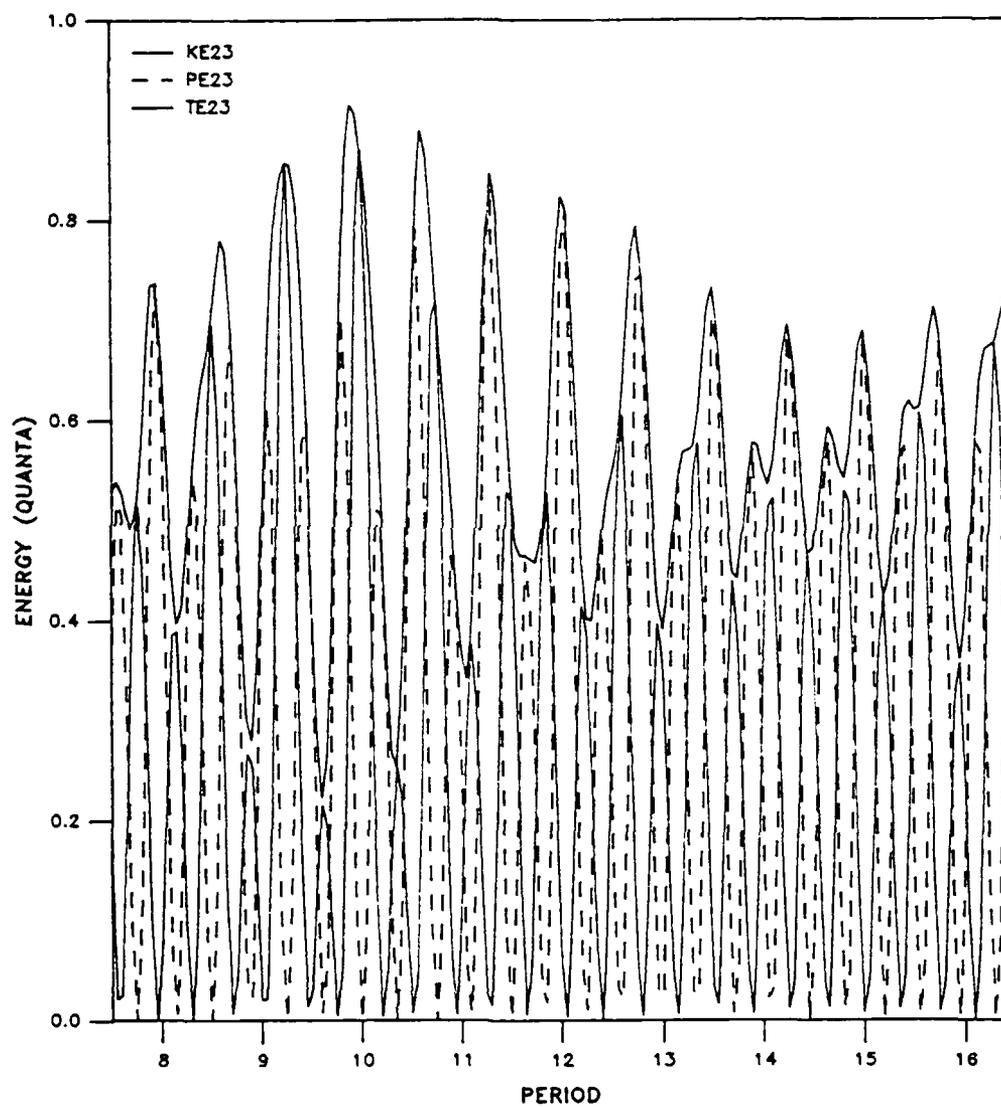
Figure 8

Energy of Bond R12

Classical Anharmonic
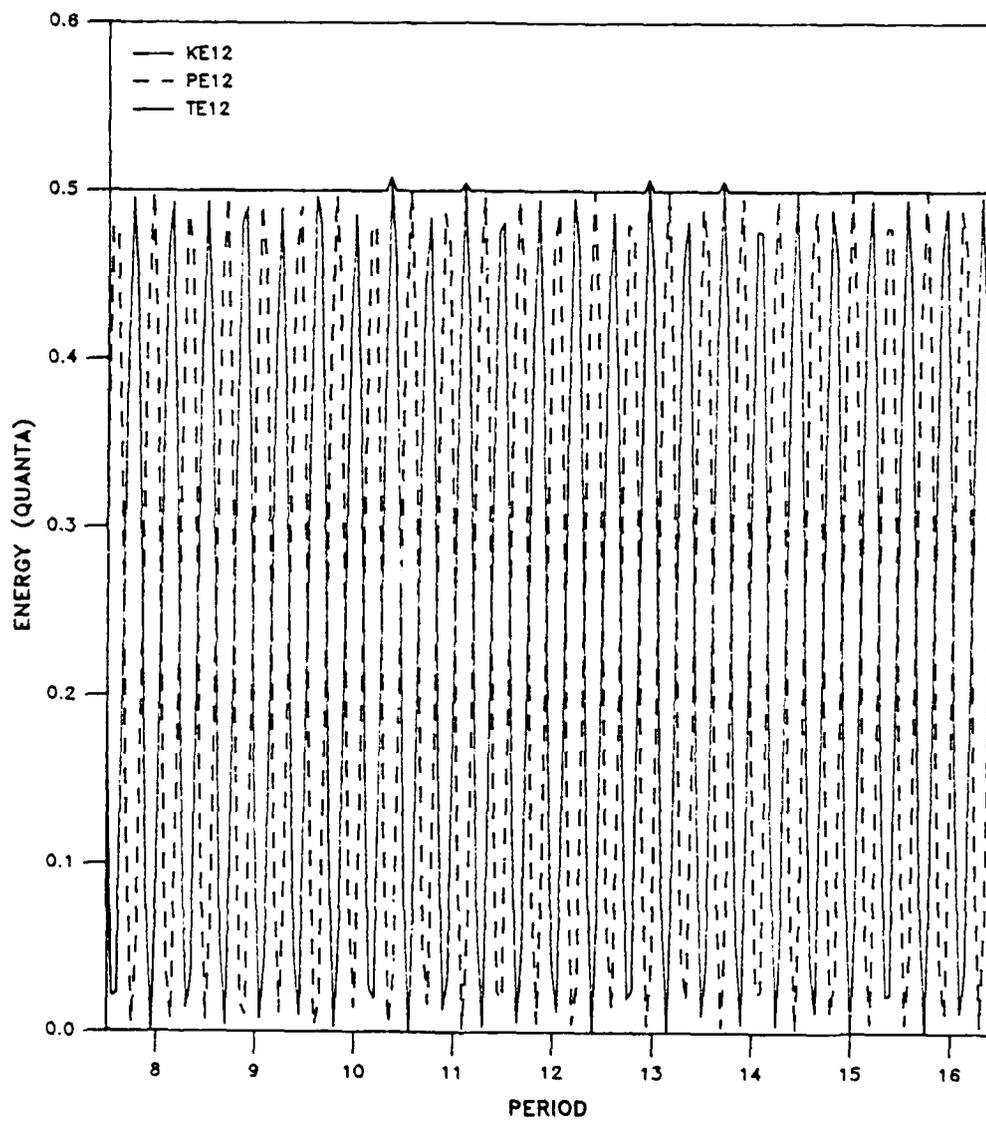
Figure 9

Energy of Bond R34

Classical Anharmonic
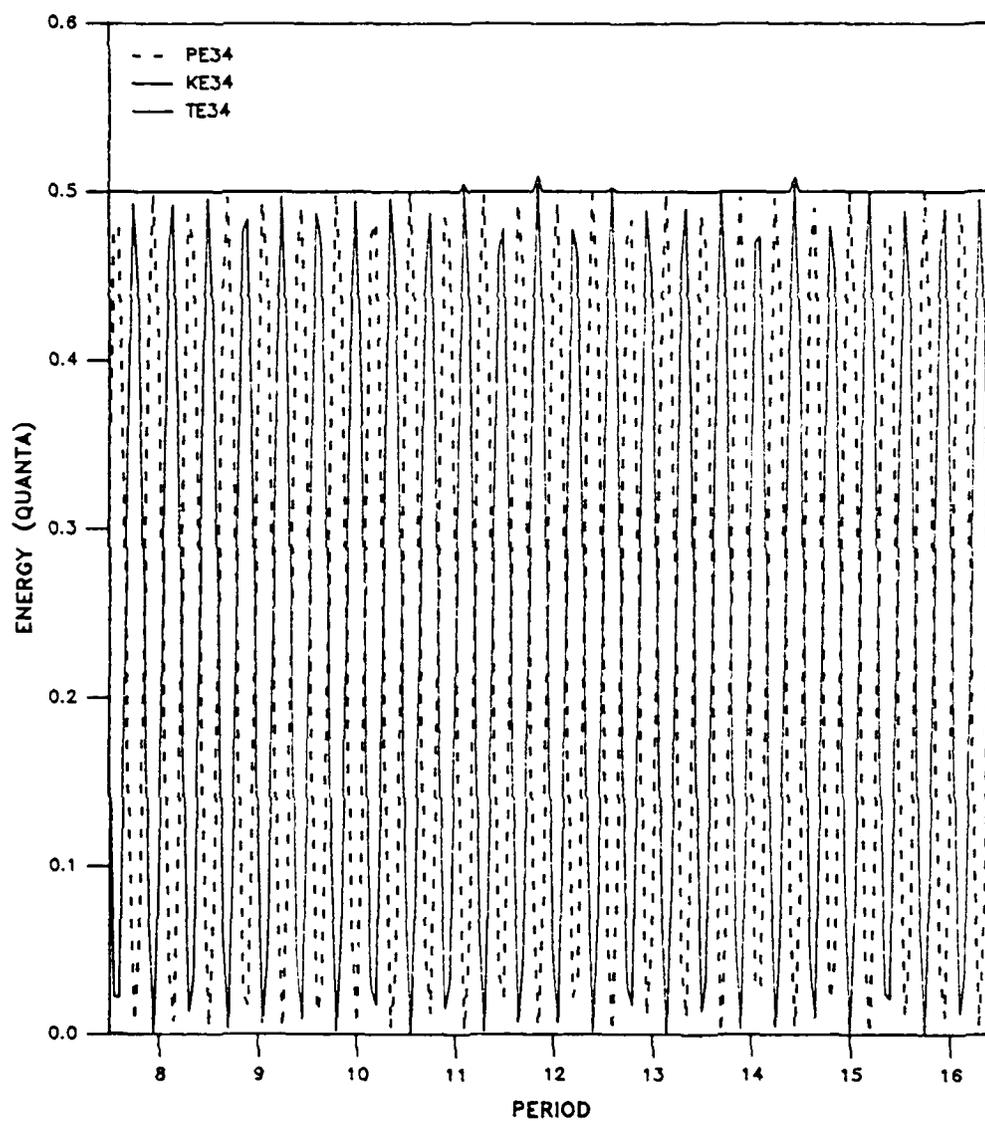
Figure 10

Energy of Bond R23

Classical Anharmonic
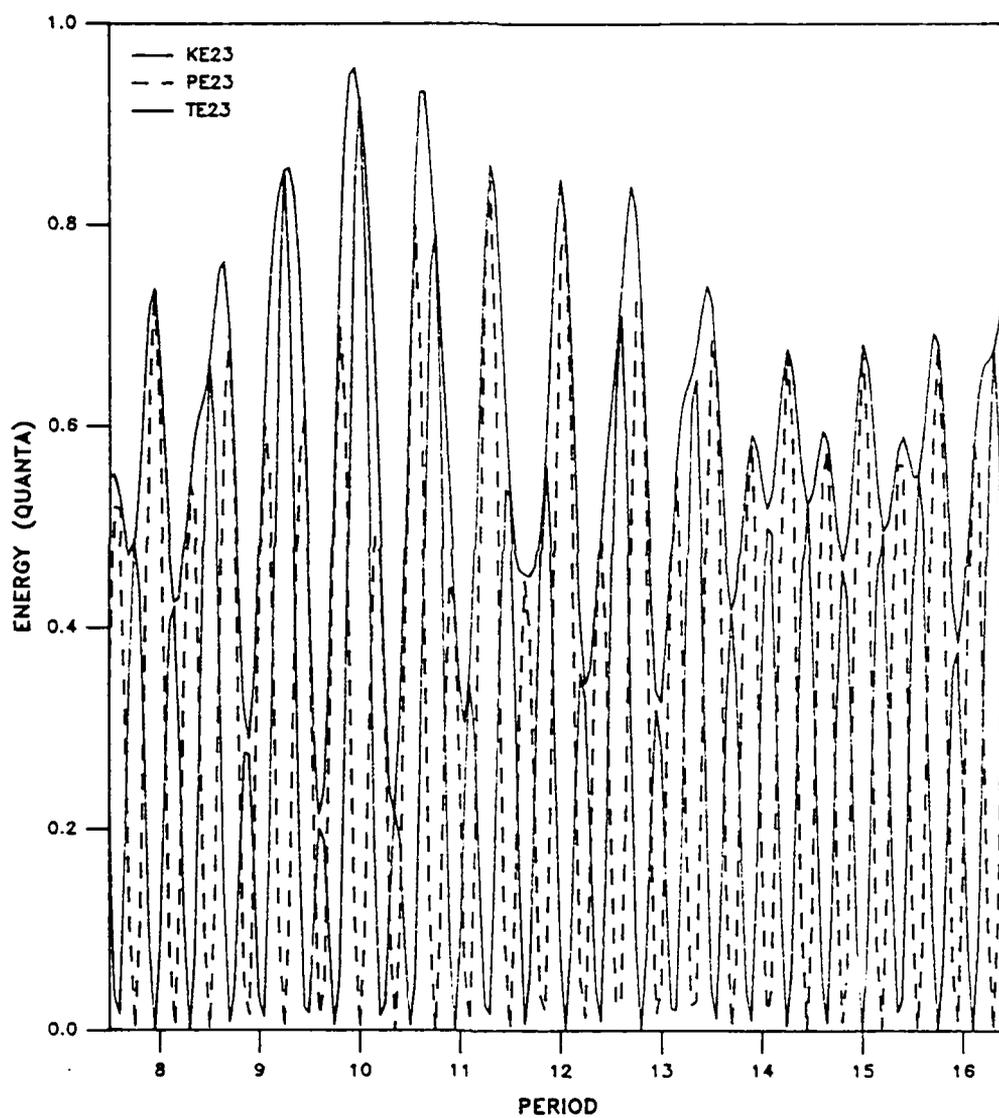
Figure 11

Occupation of States
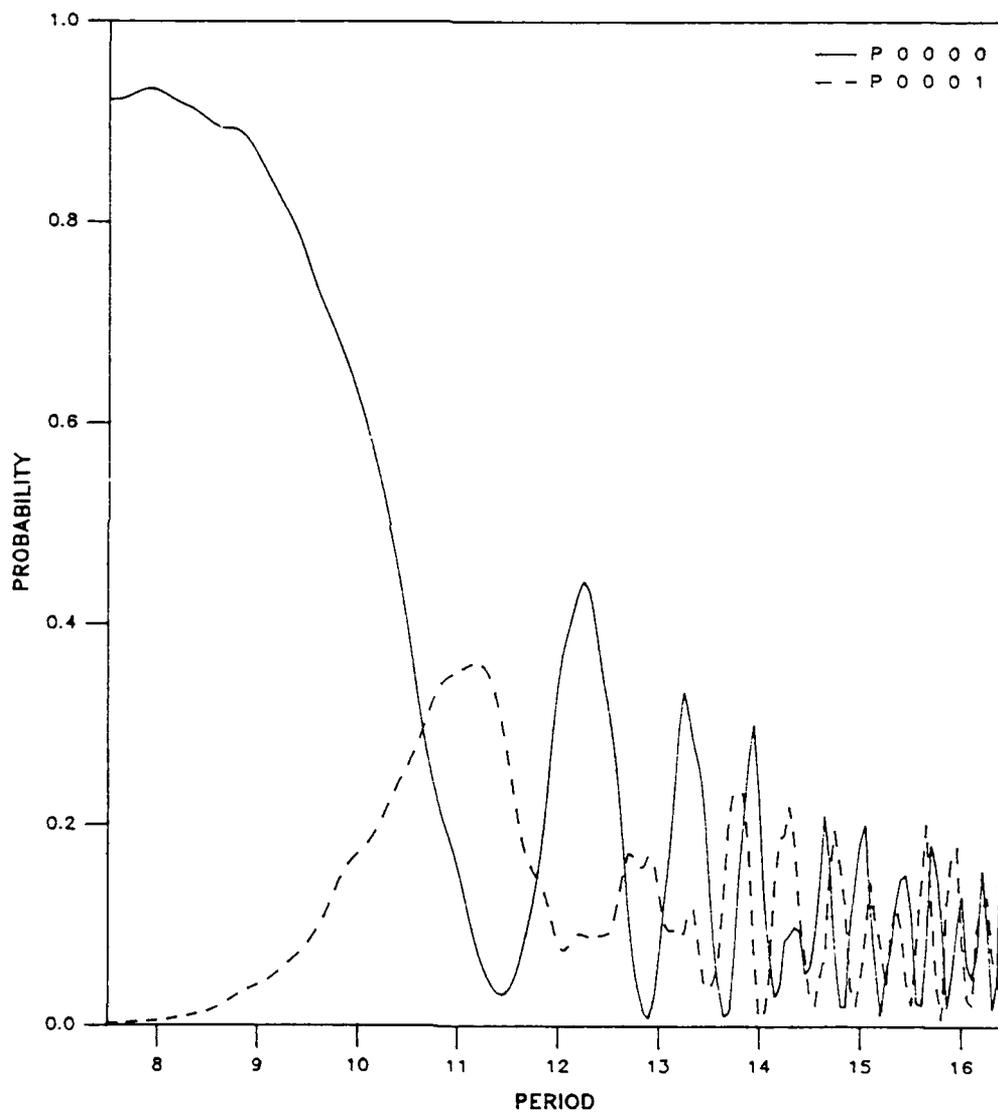
Harmonic

Figure 12

Occupation of States
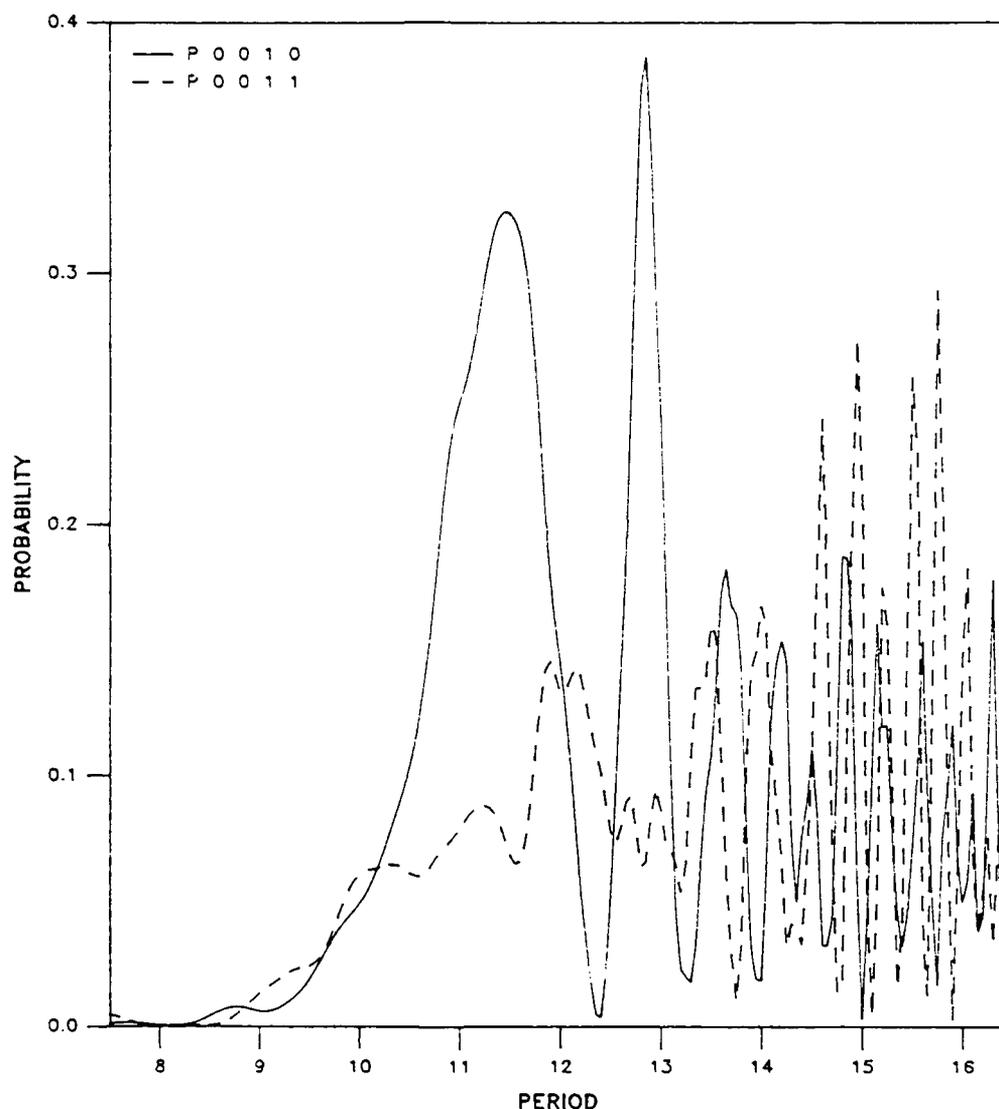
Harmonic

Figure 13

Occupation of States
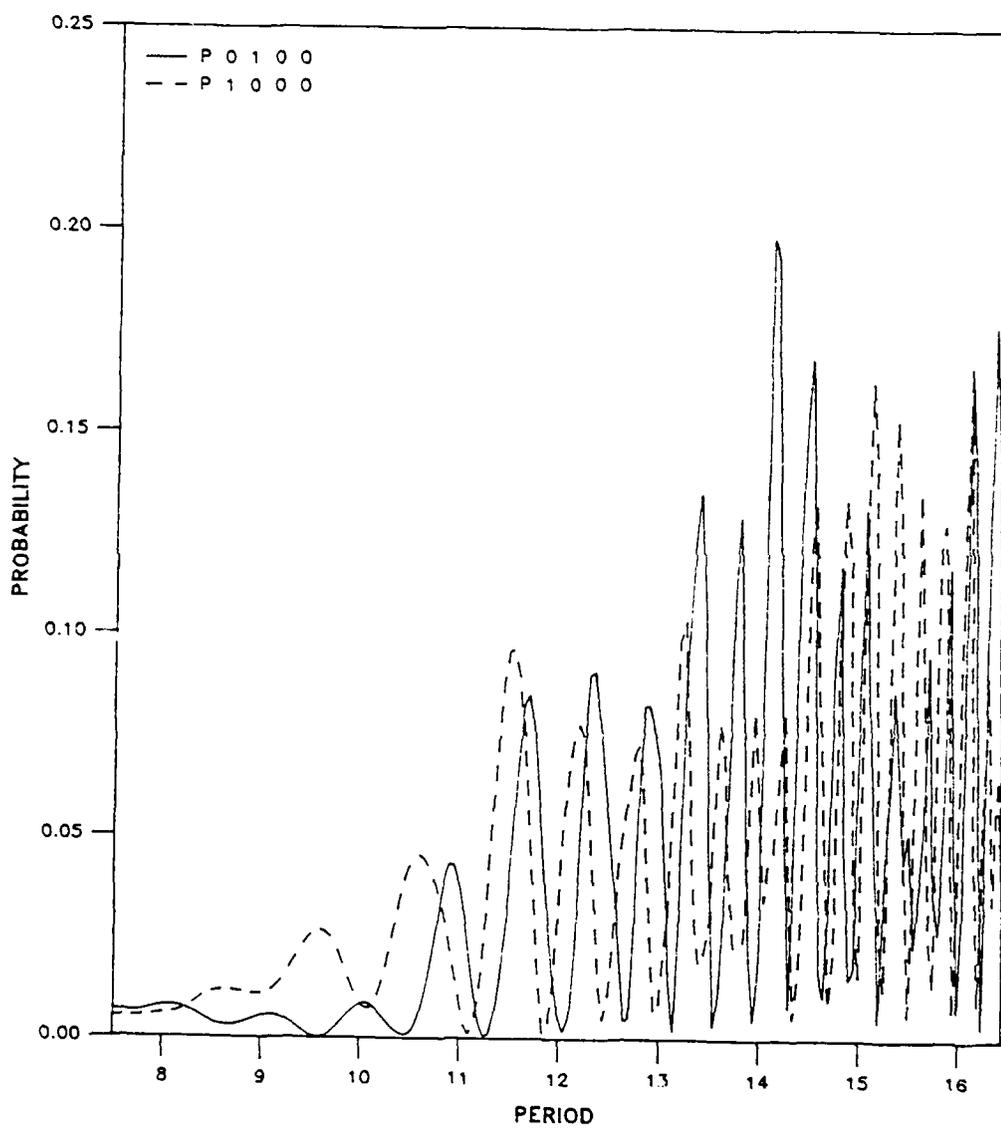
Harmonic

Figure 14

Occupation of States
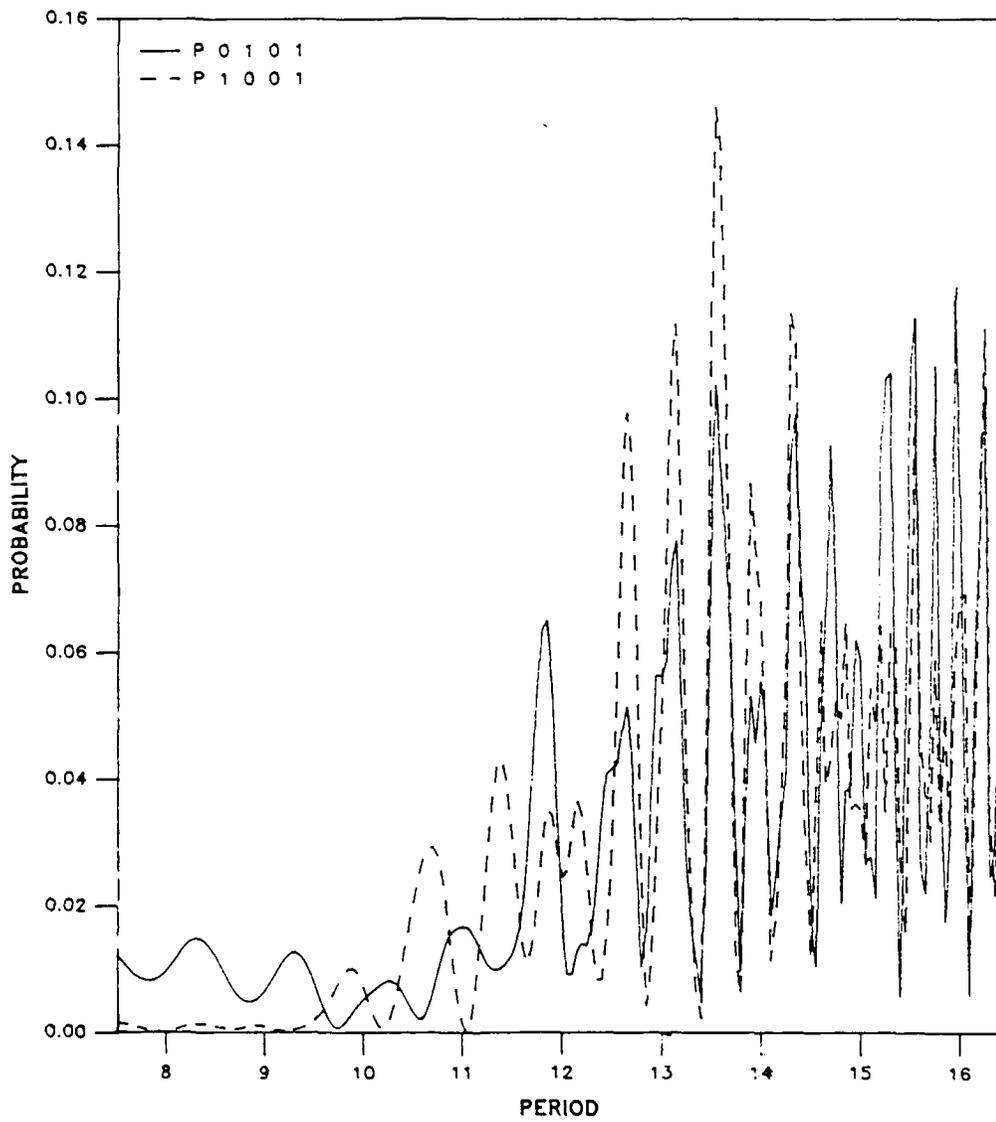
Harmonic

Figure 15

Occupation of States
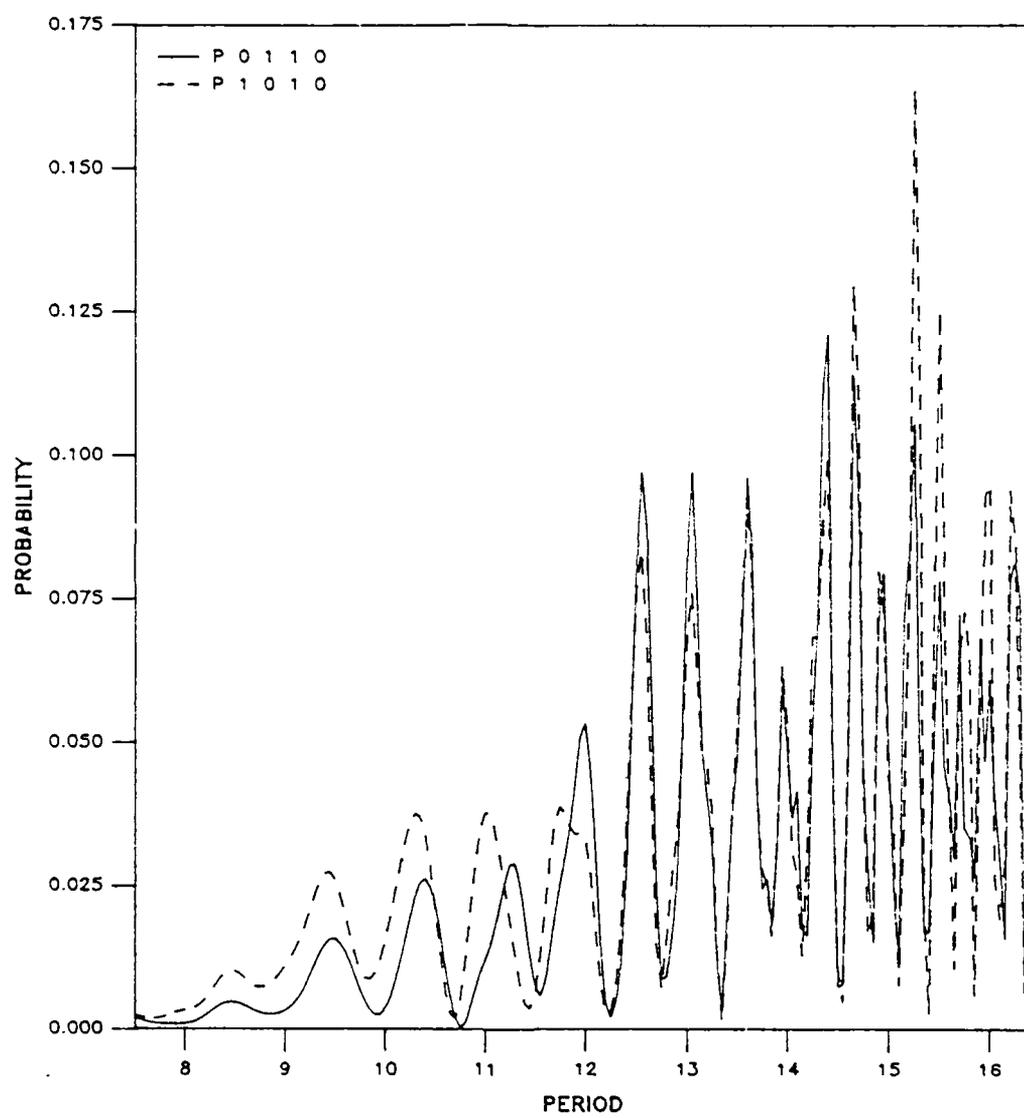
Harmonic

Figure 16

Occupation of States
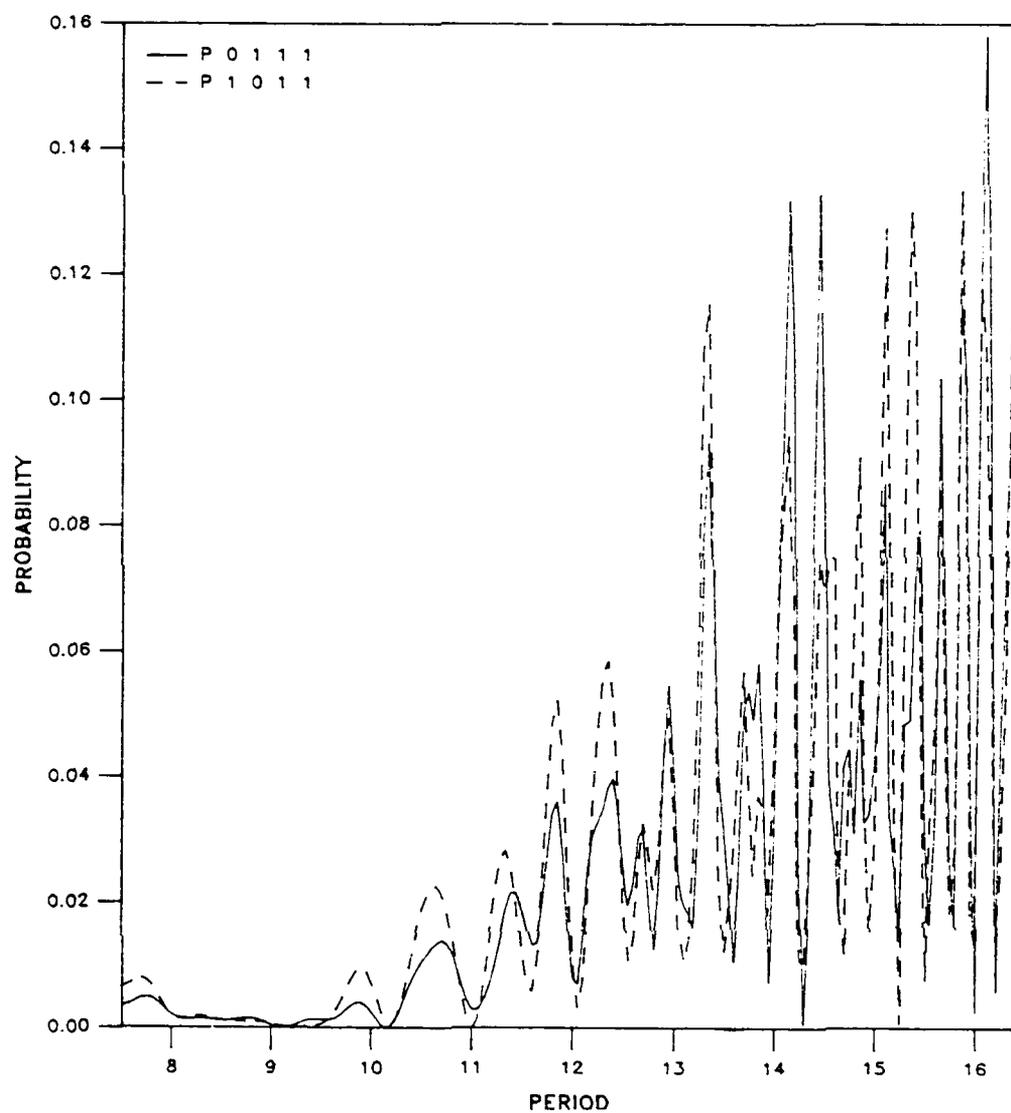
Harmonic

Figure 17

Occupation of States
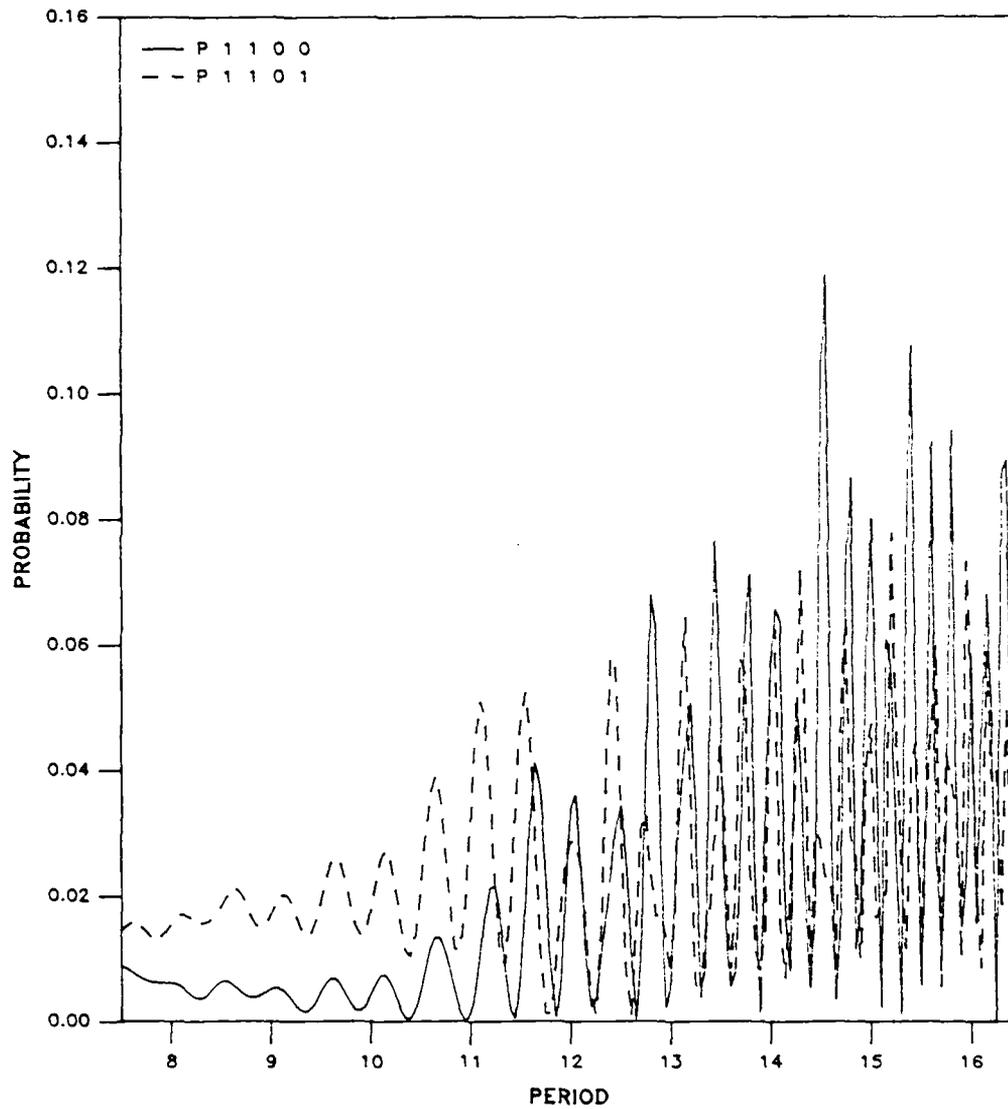
Harmonic

Figure 18

Occupation of States
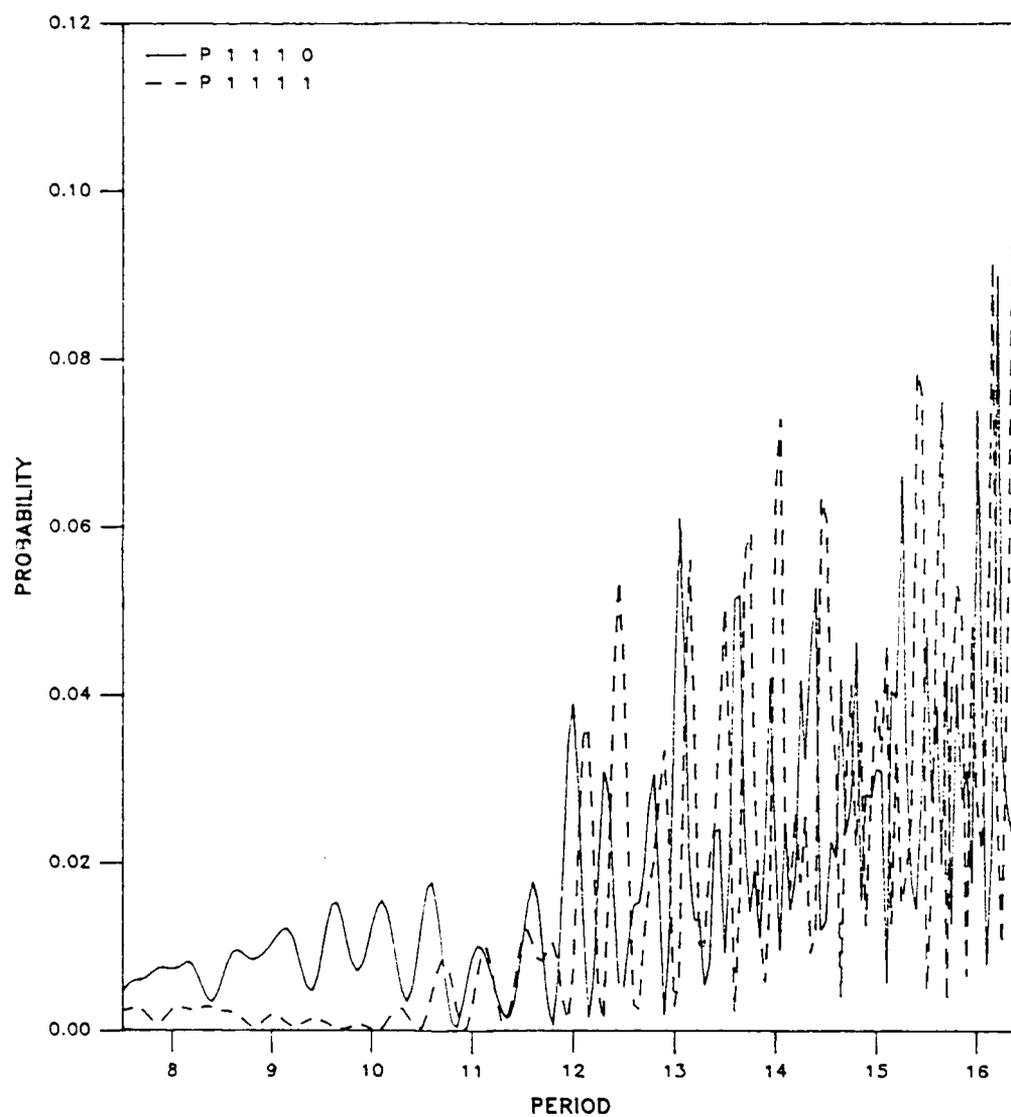
Harmonic

Figure 19

Occupation of States
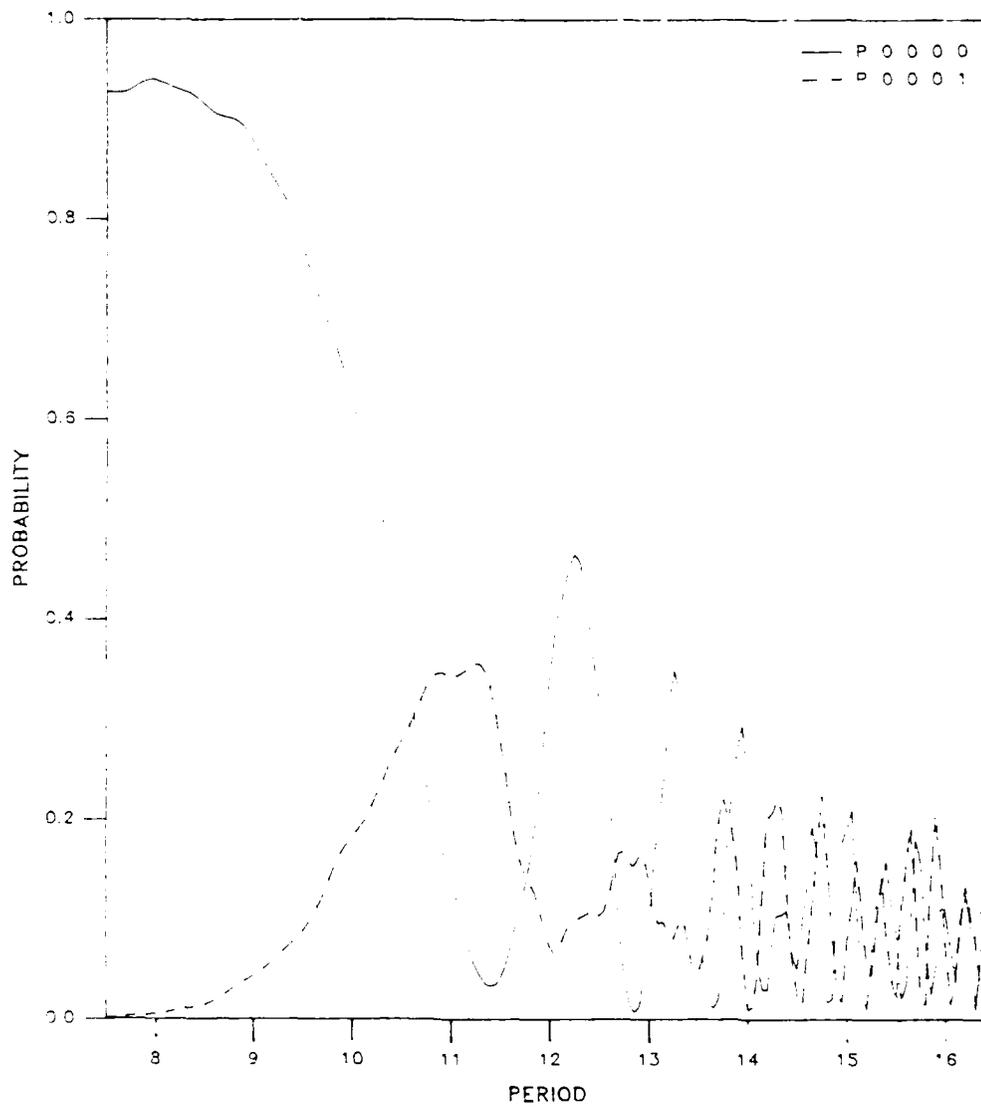
Anharmonic

Figure 20

Occupation of States
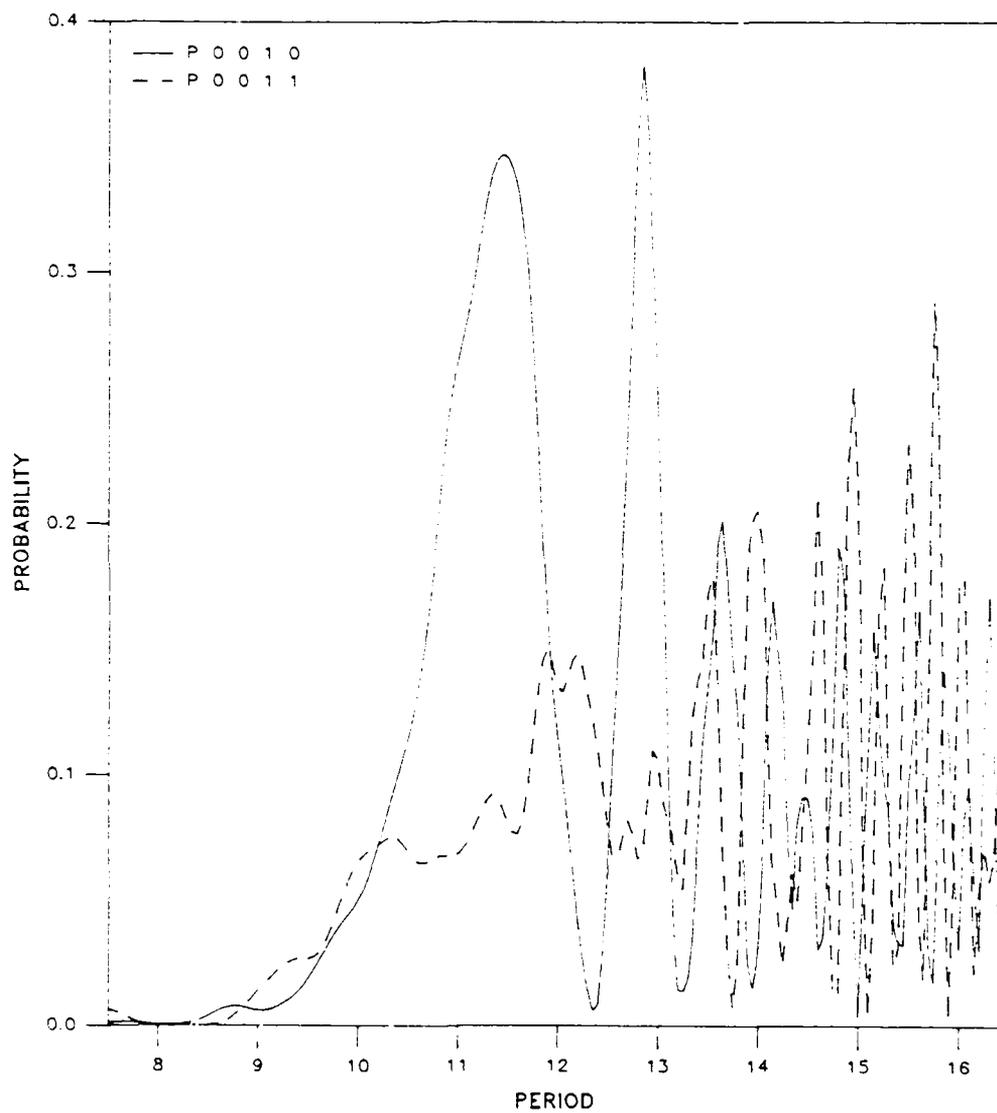
Anharmonic

Figure 21

Occupation of States
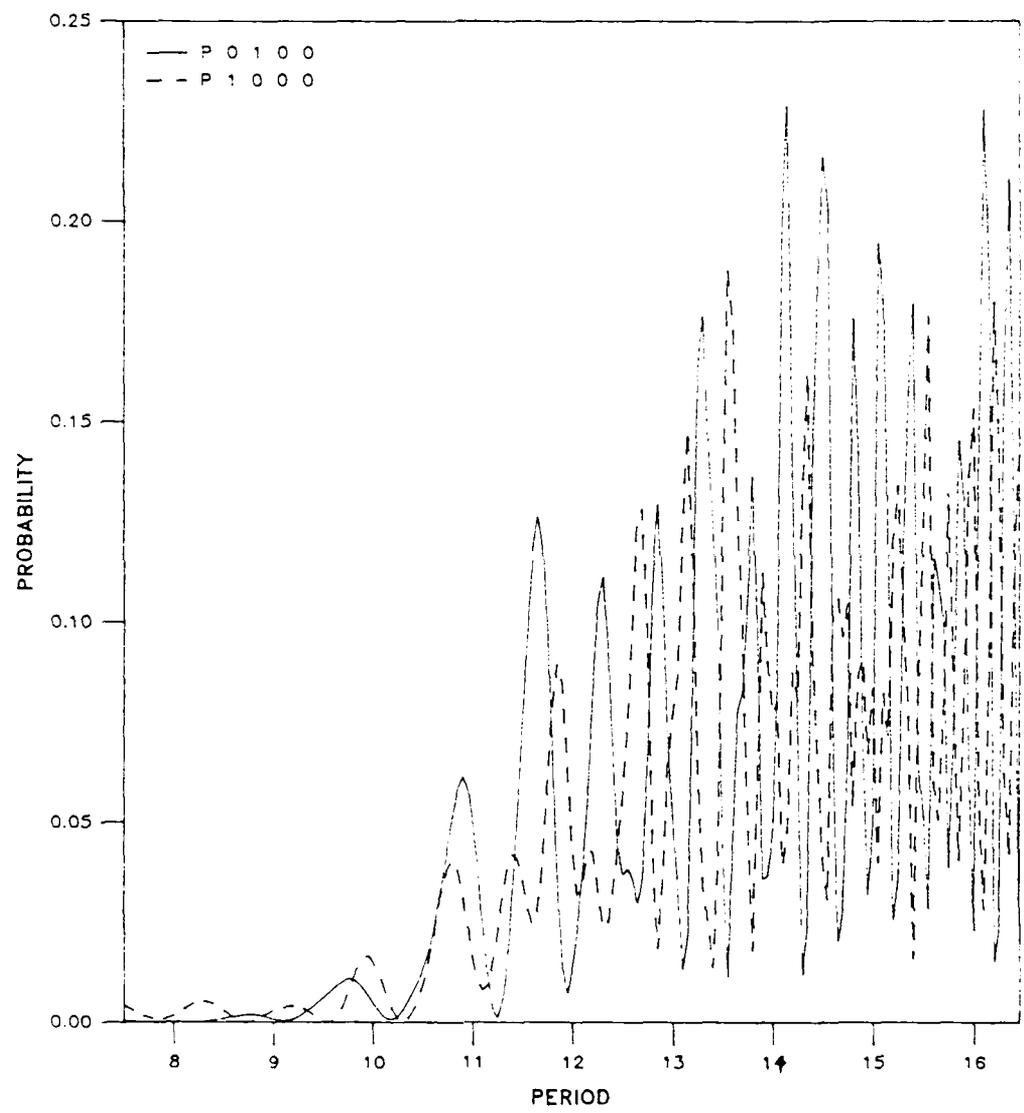
Anharmonic

Figure 22

Occupation of States
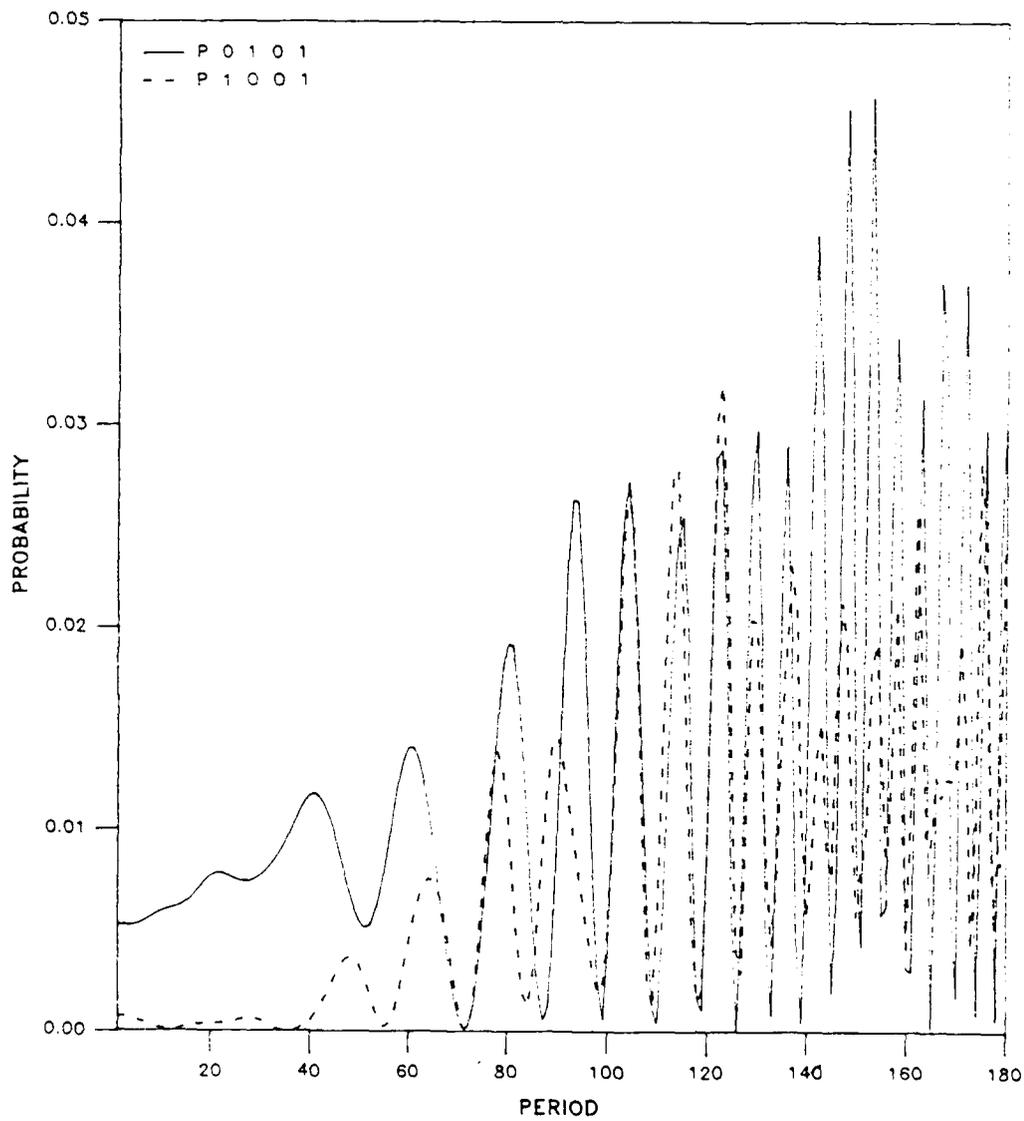
Anharmonic

Figure 23

Occupation of States
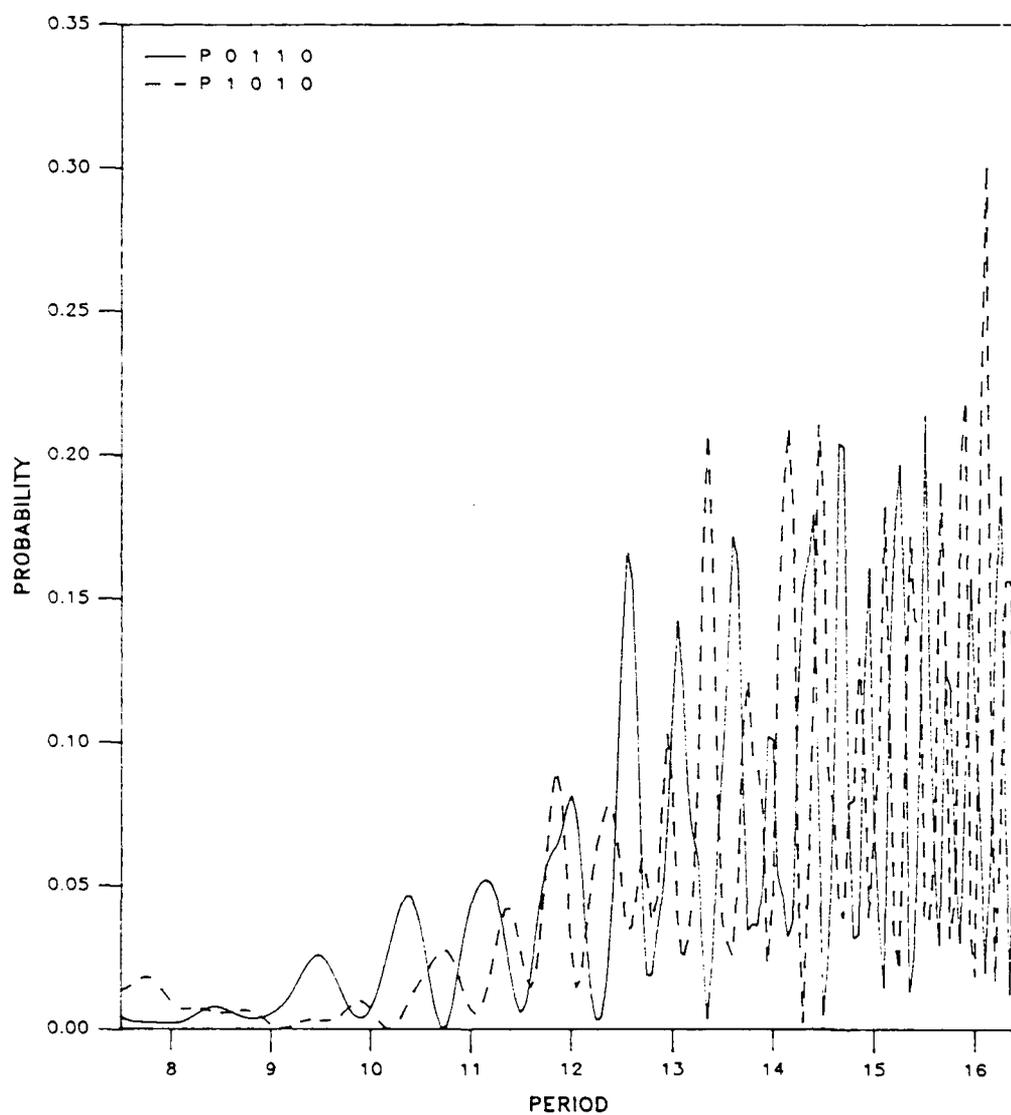
Anharmonic

Figure 24

Occupation of States
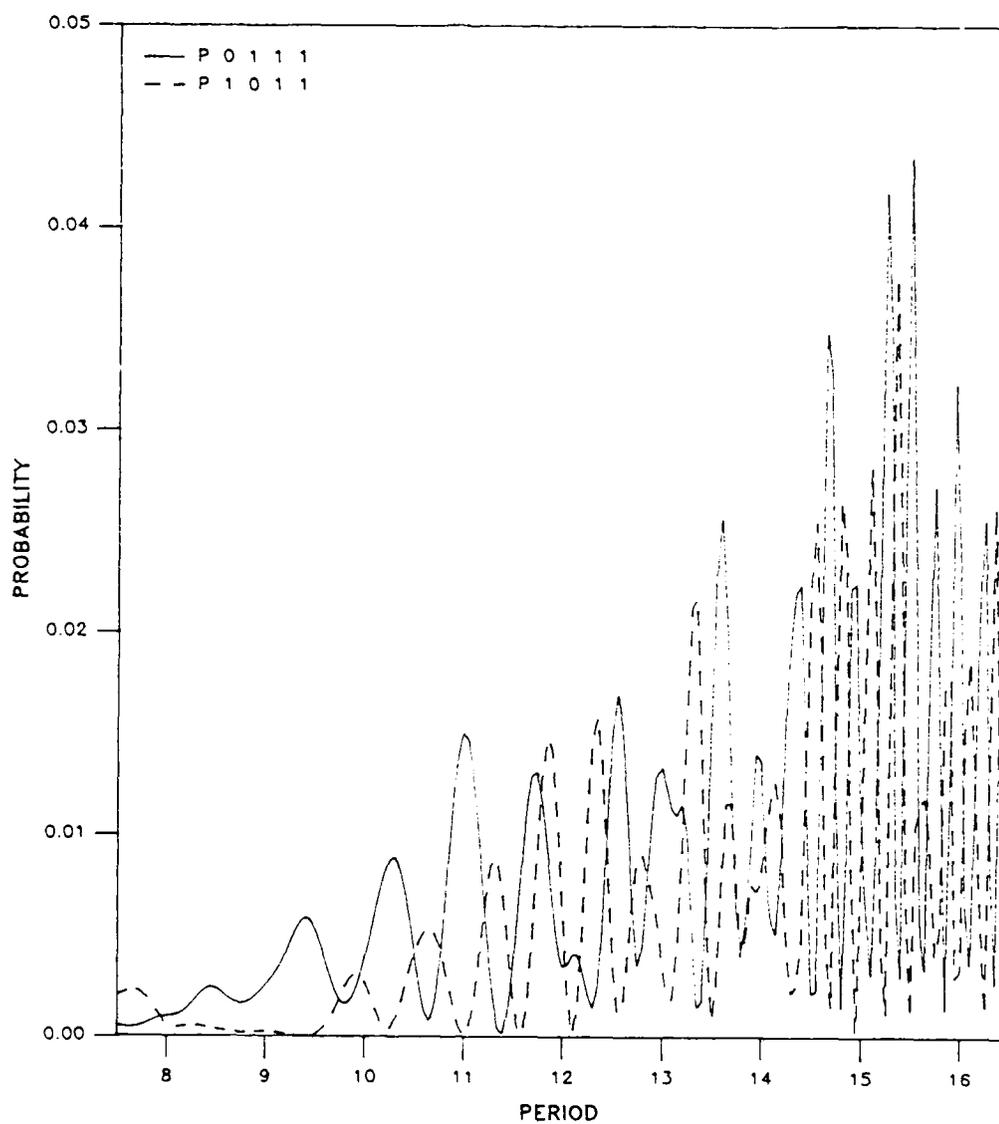
Anharmonic

Figure 25

Occupation of States
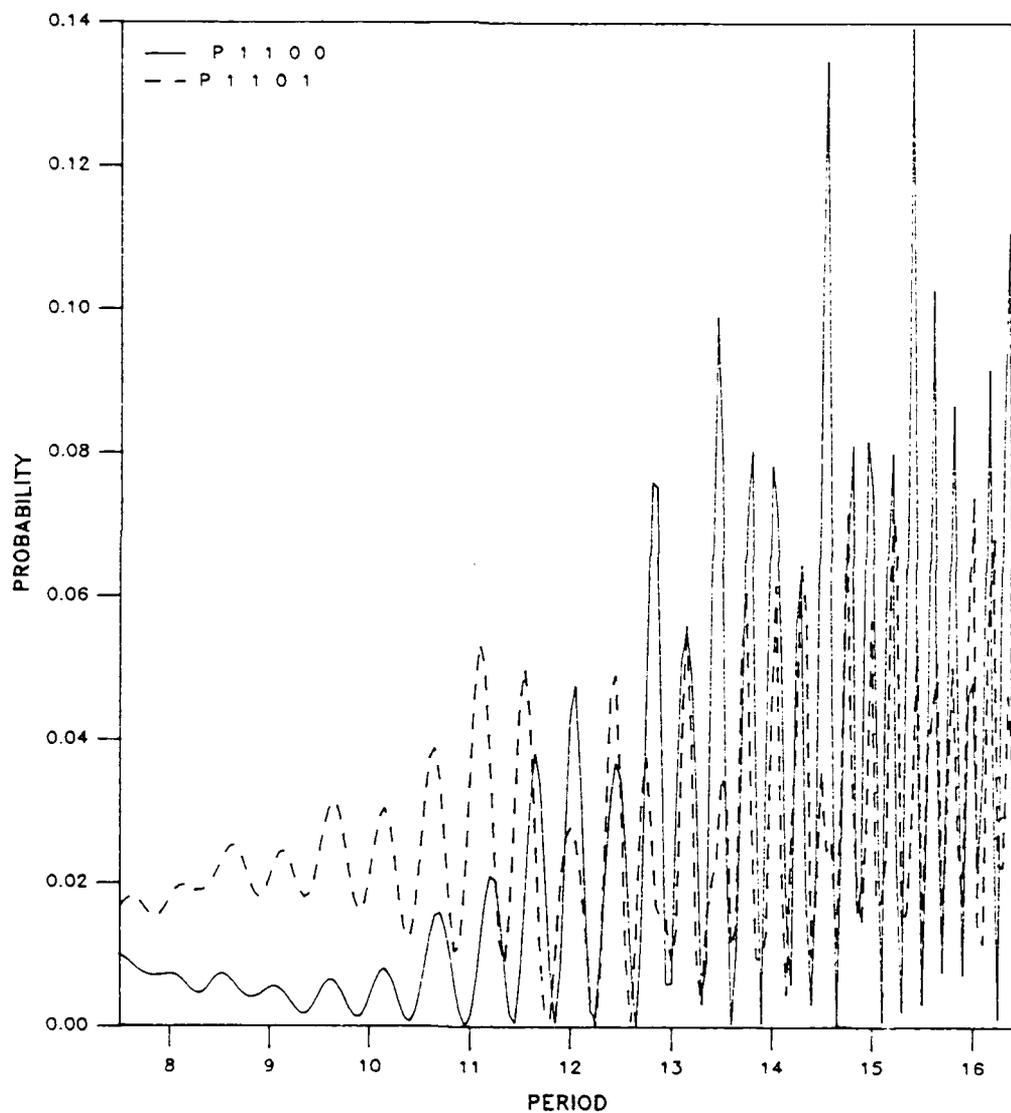
Anharmonic

Figure 26

Occupation of States
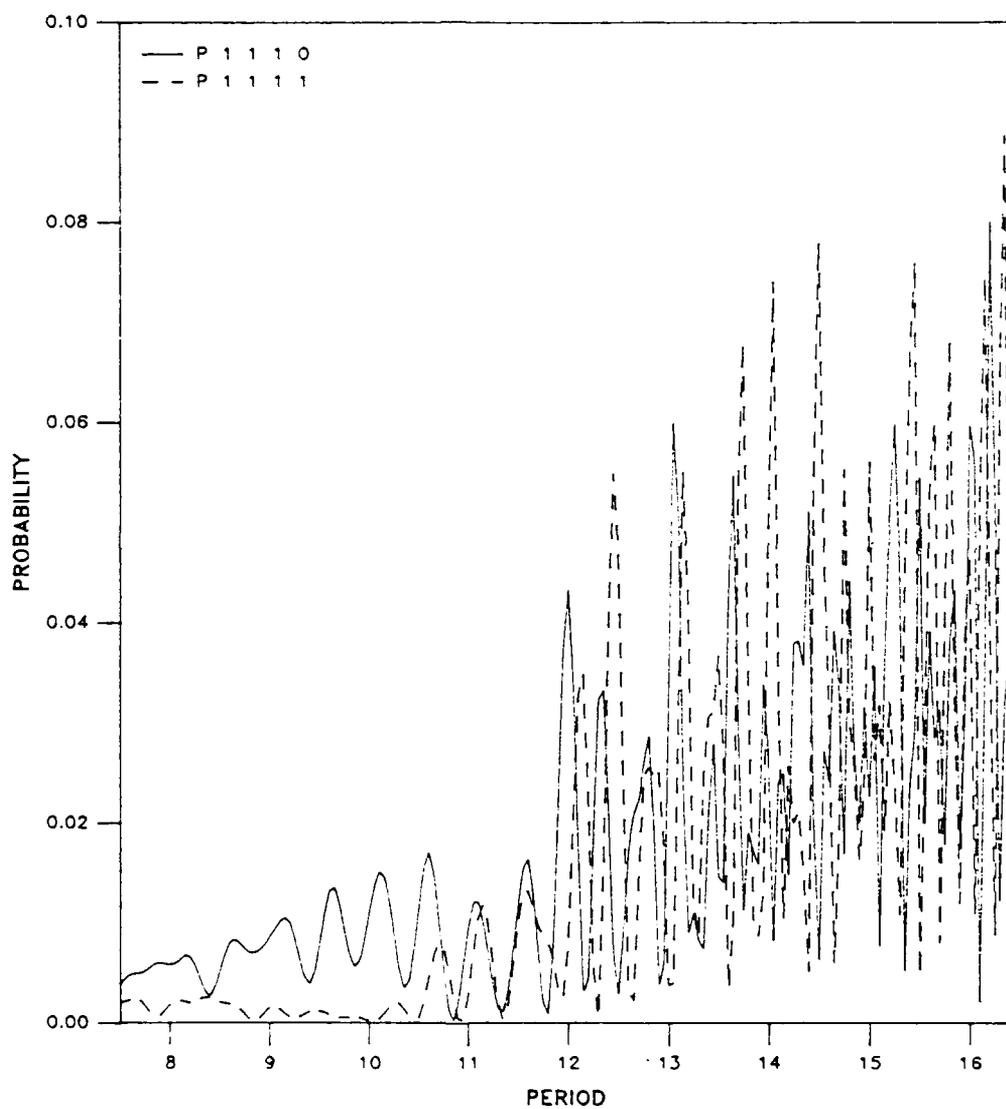
Anharmonic

Figure 27

Occupation of States
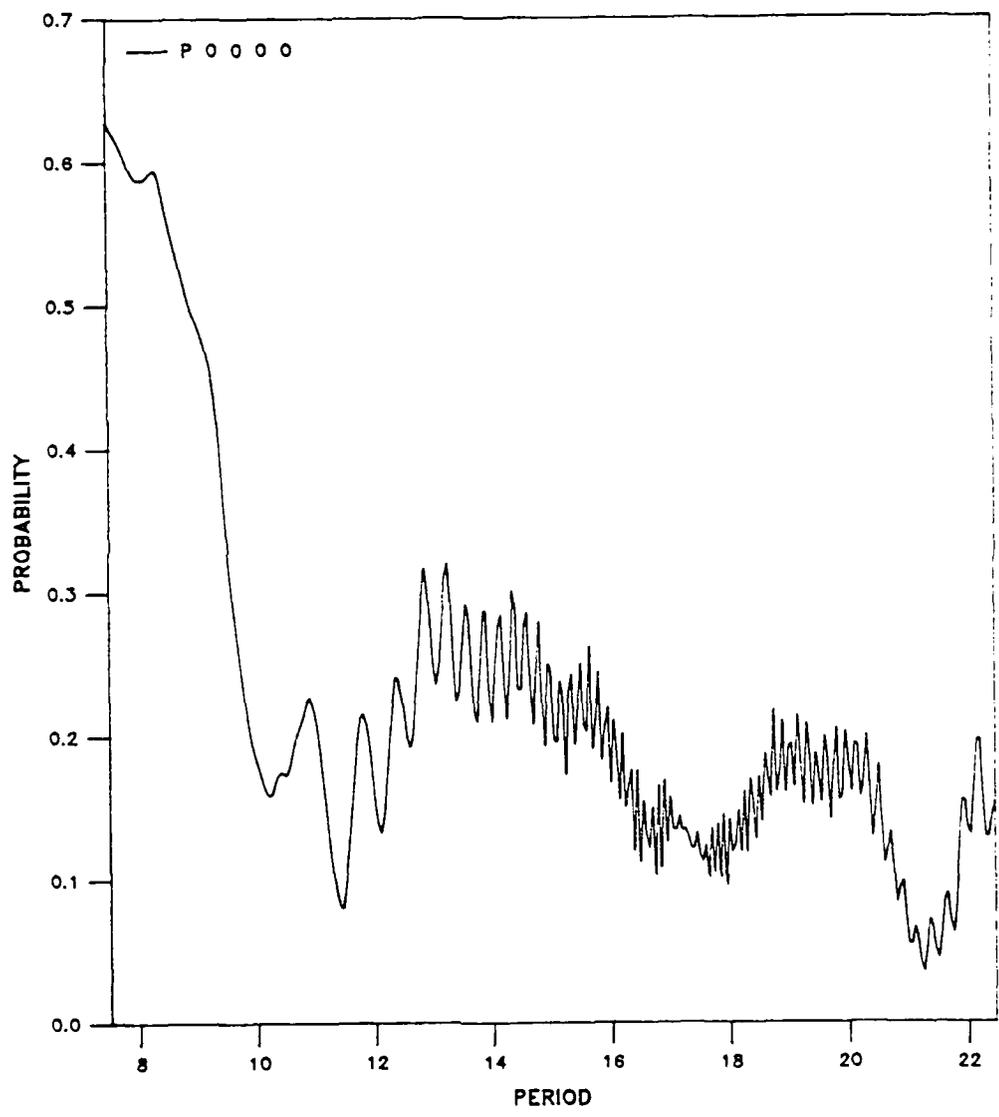
Anharmonic

Figure 28

Occupation of States
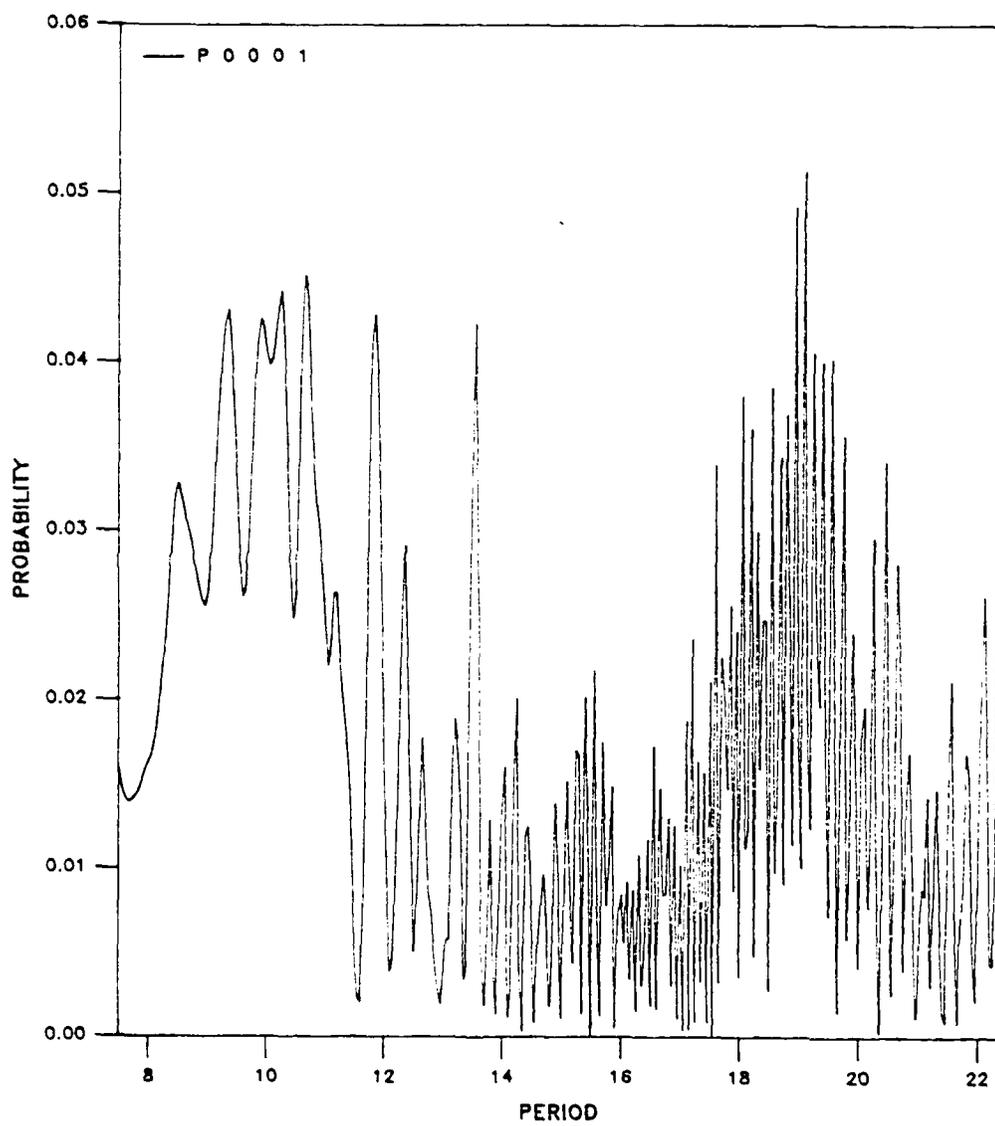
Anharmonic

Figure 29

Occupation of States
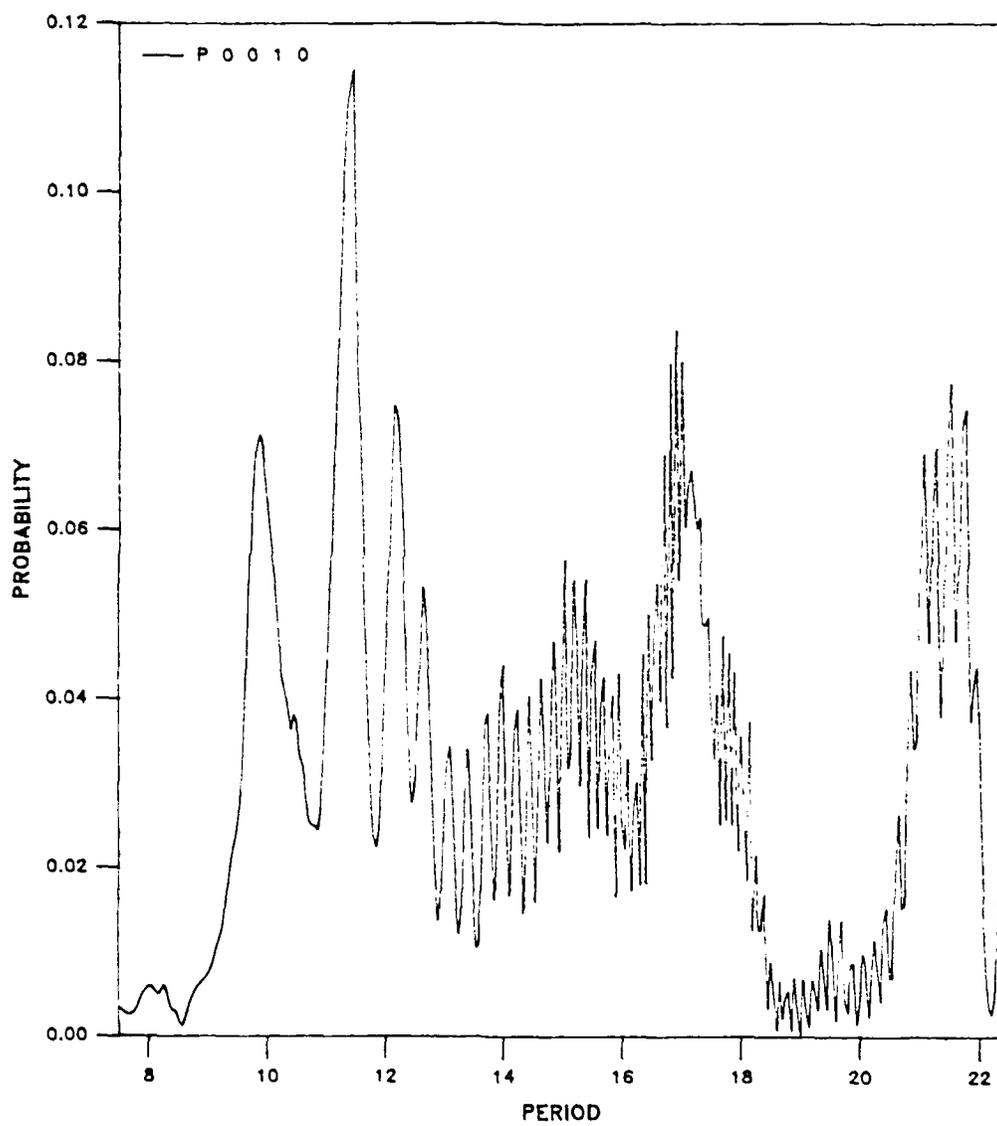
Anharmonic

Figure 30

Occupation of States
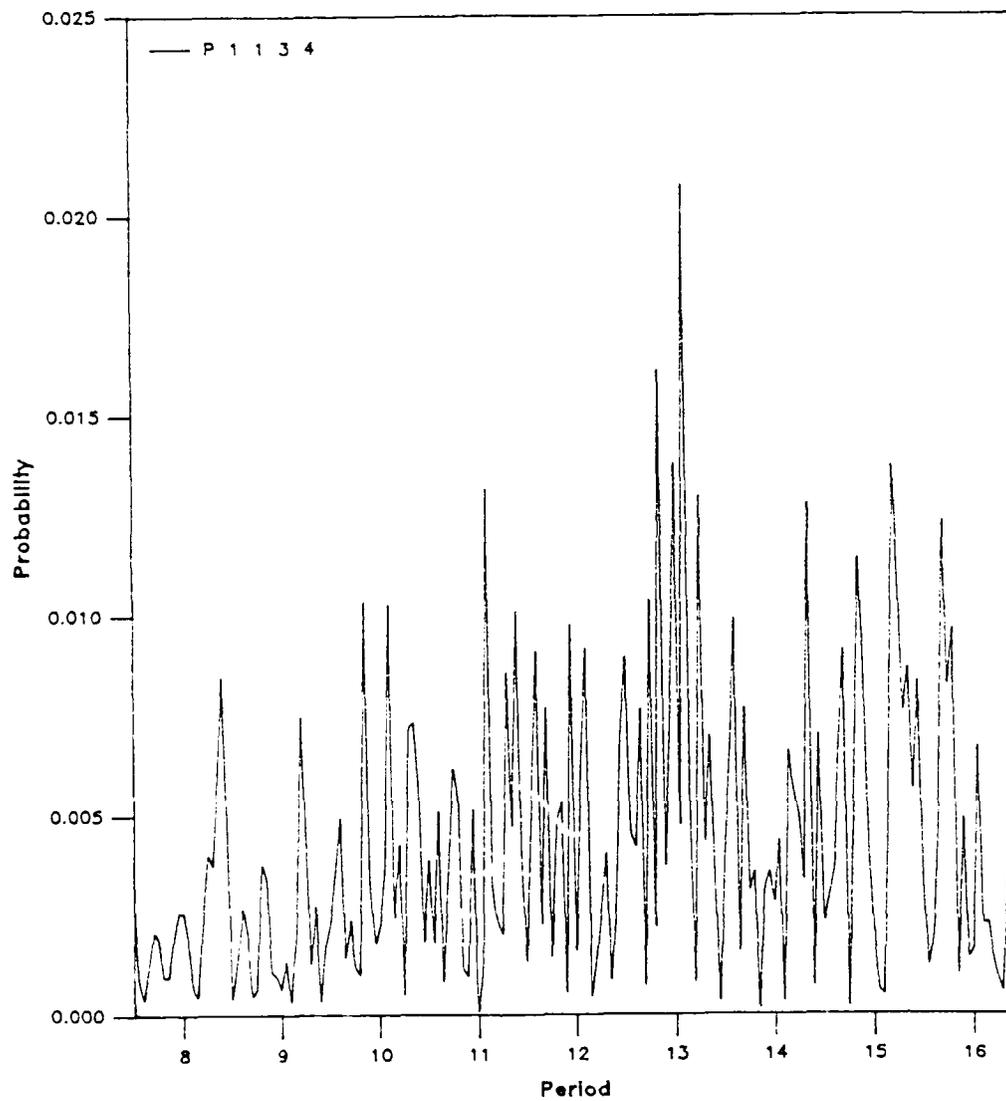
Anharmonic

Figure 31

Occupation of States
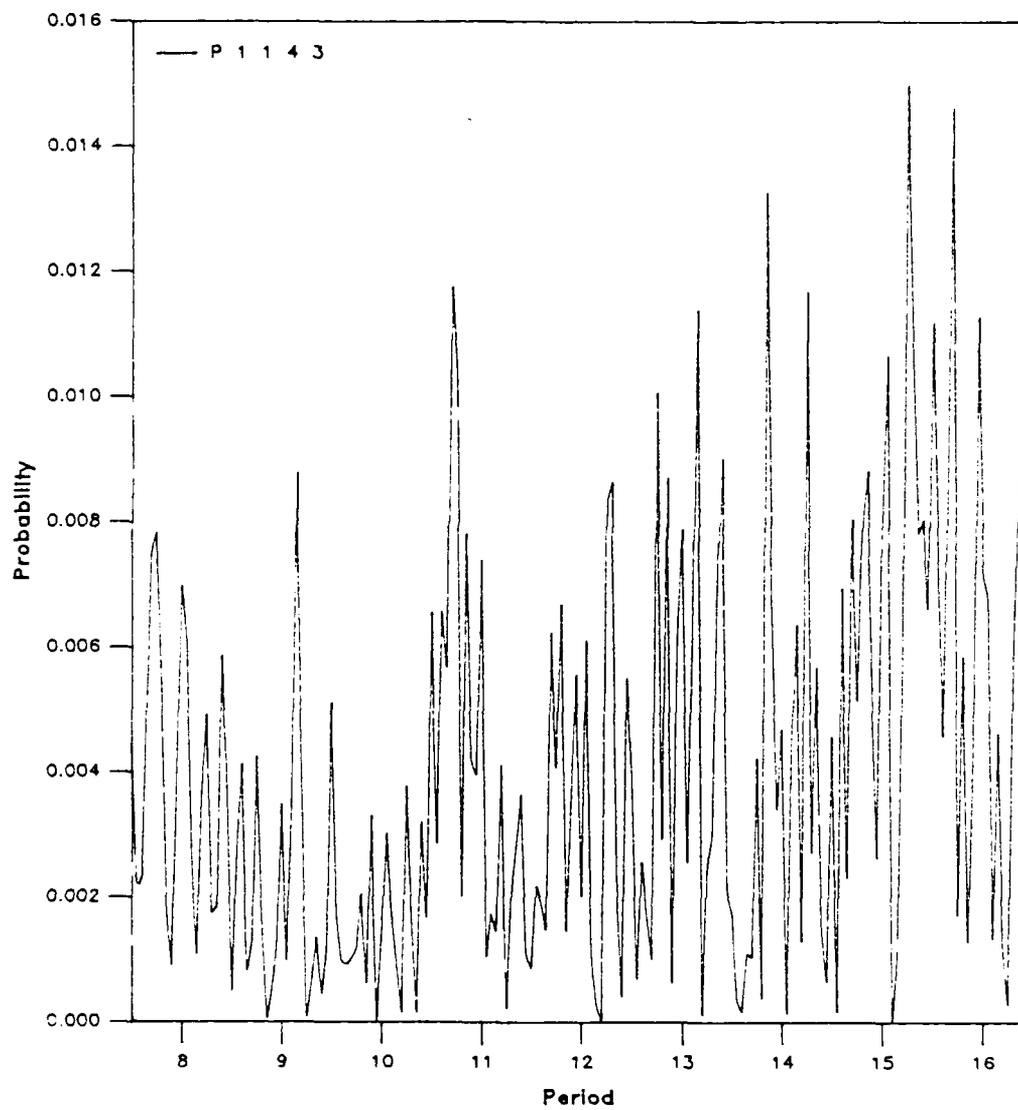
Anharmonic

Figure 32

Occupation of States
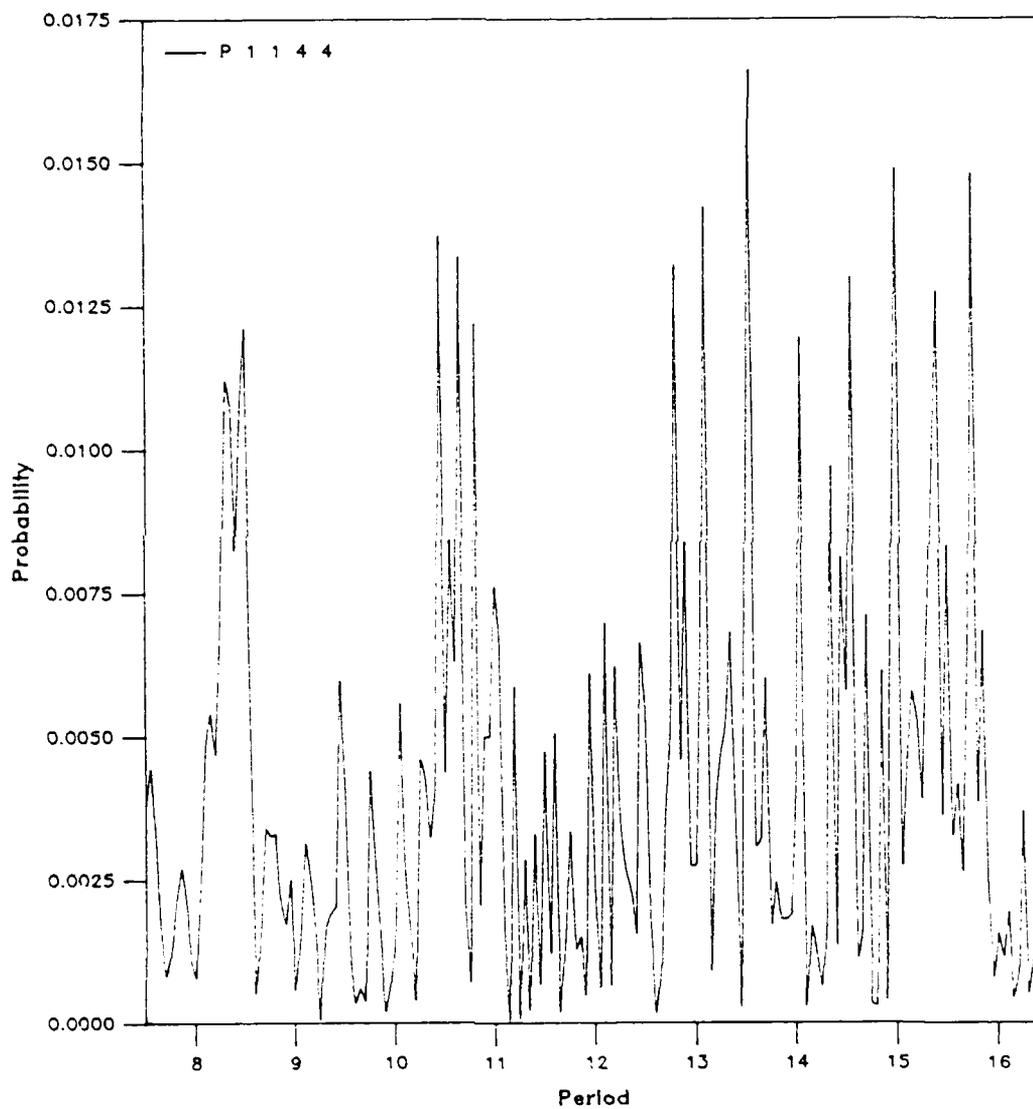
Anharmonic

Figure 33

Position of Atoms
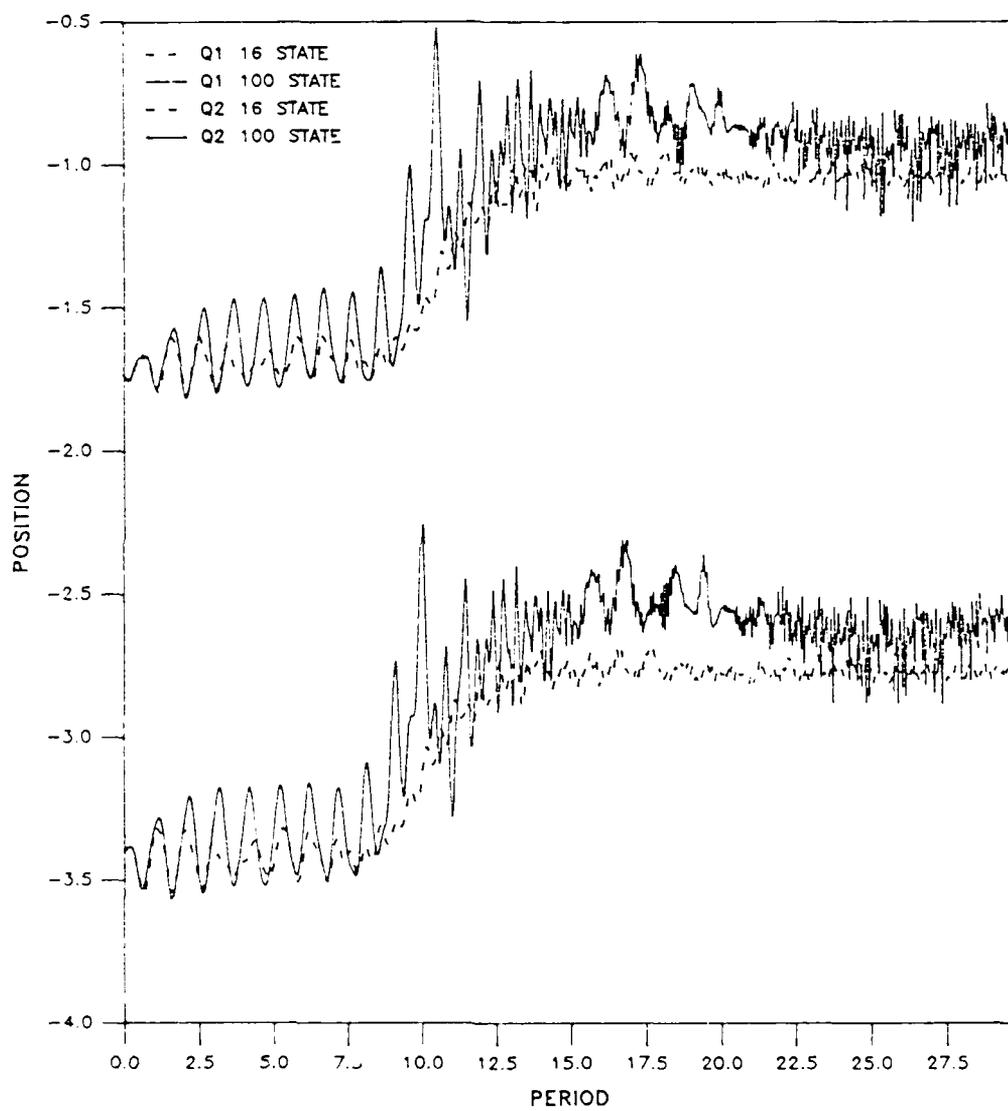
Harmonic

Figure 34

Position of Atoms
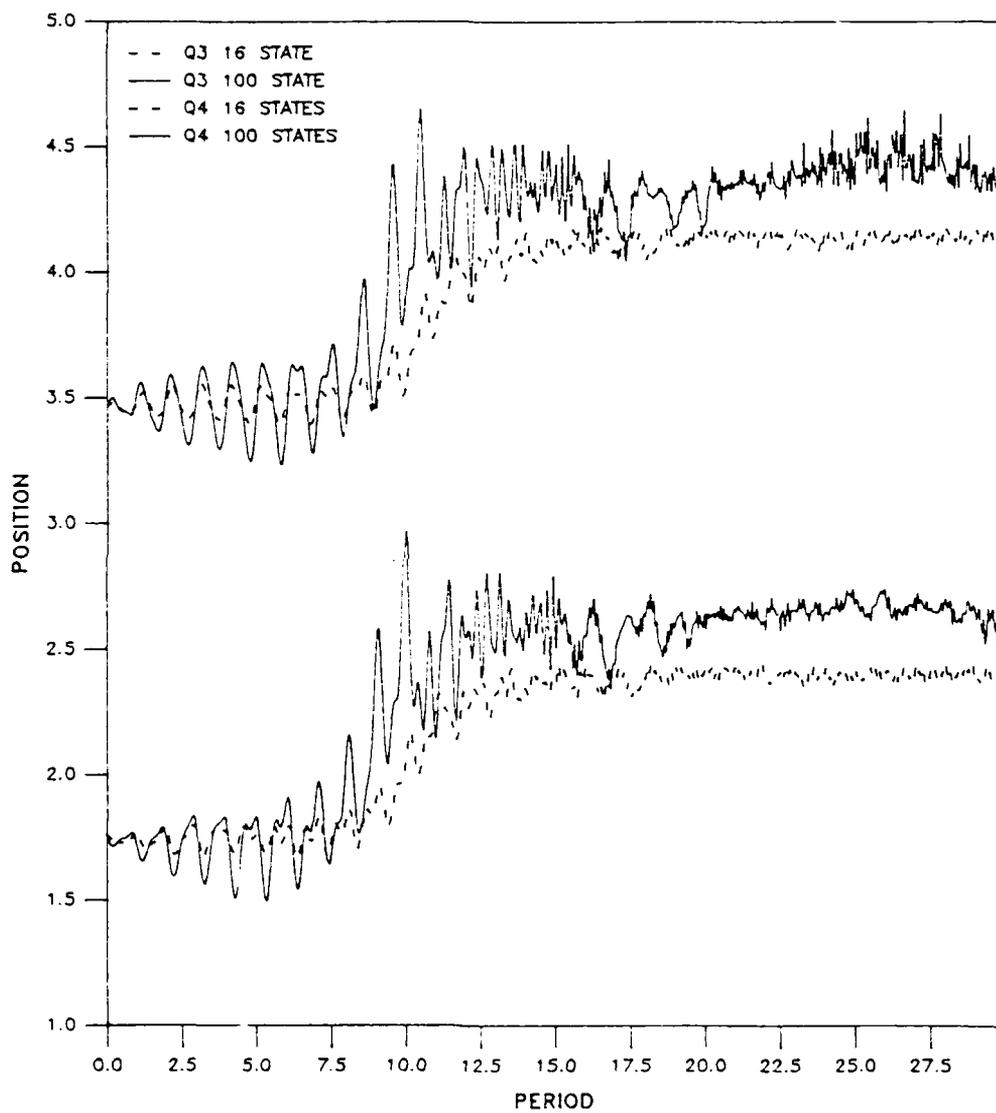
Harmonic

Figure 35

Position of Atoms
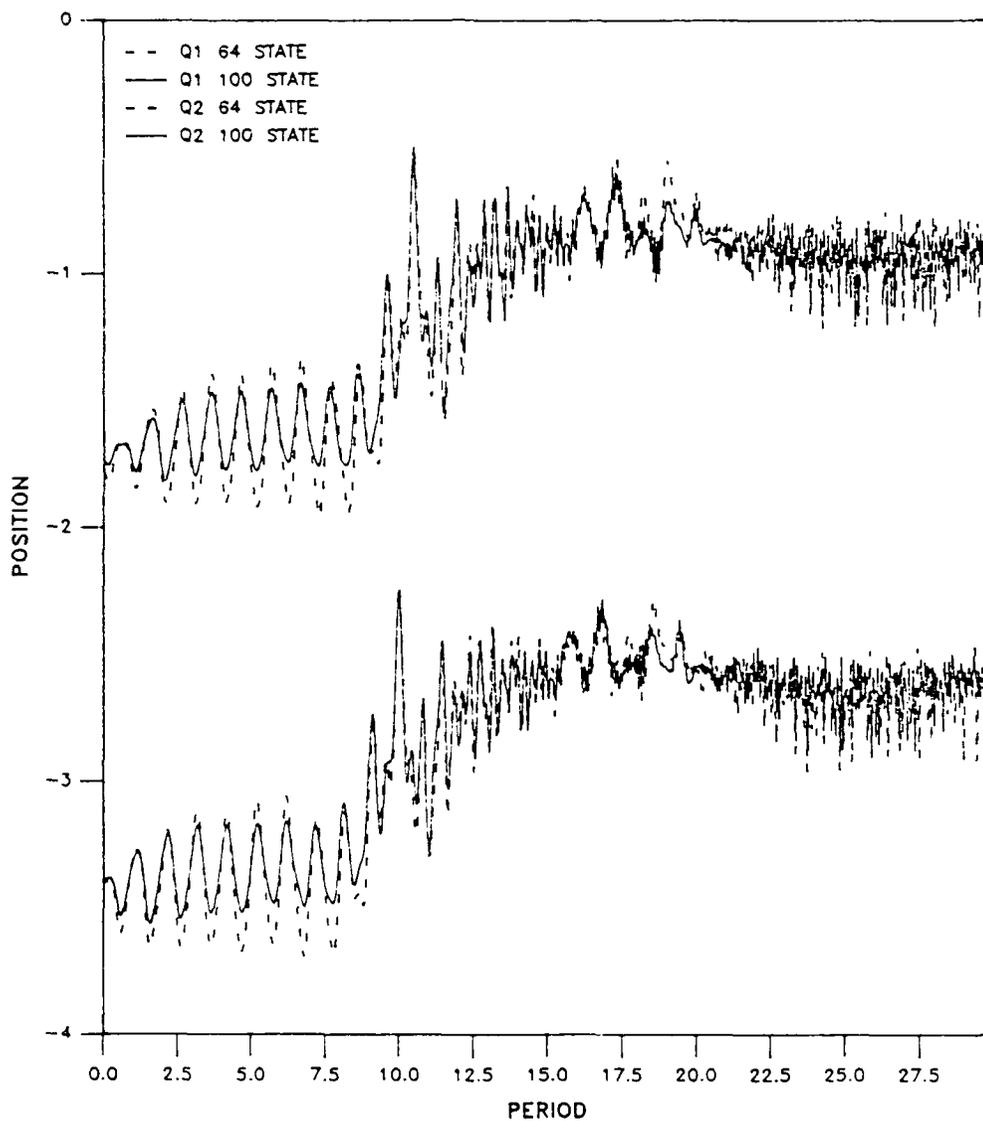
Harmonic

Figure 36

Position of Atoms
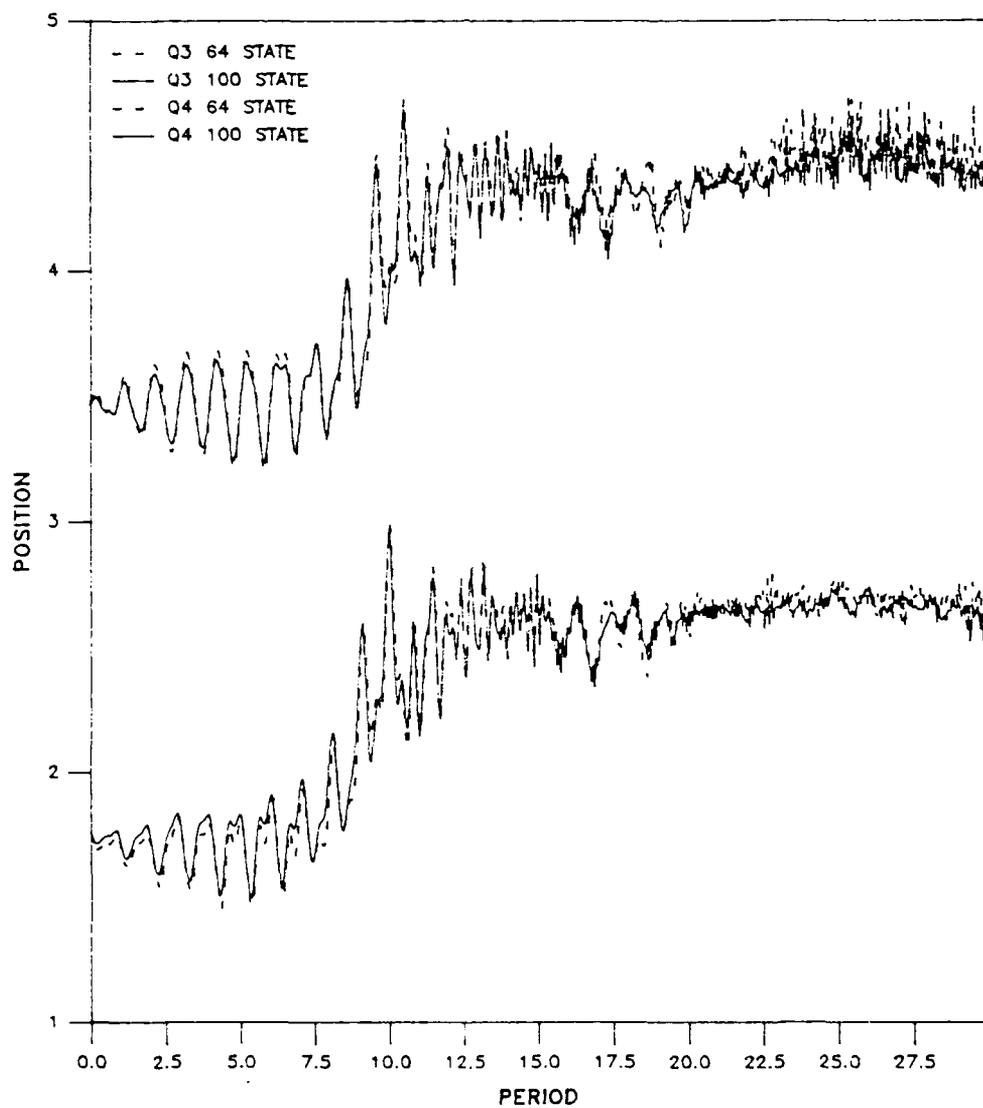
Harmonic

Figure 37

Position of Atoms
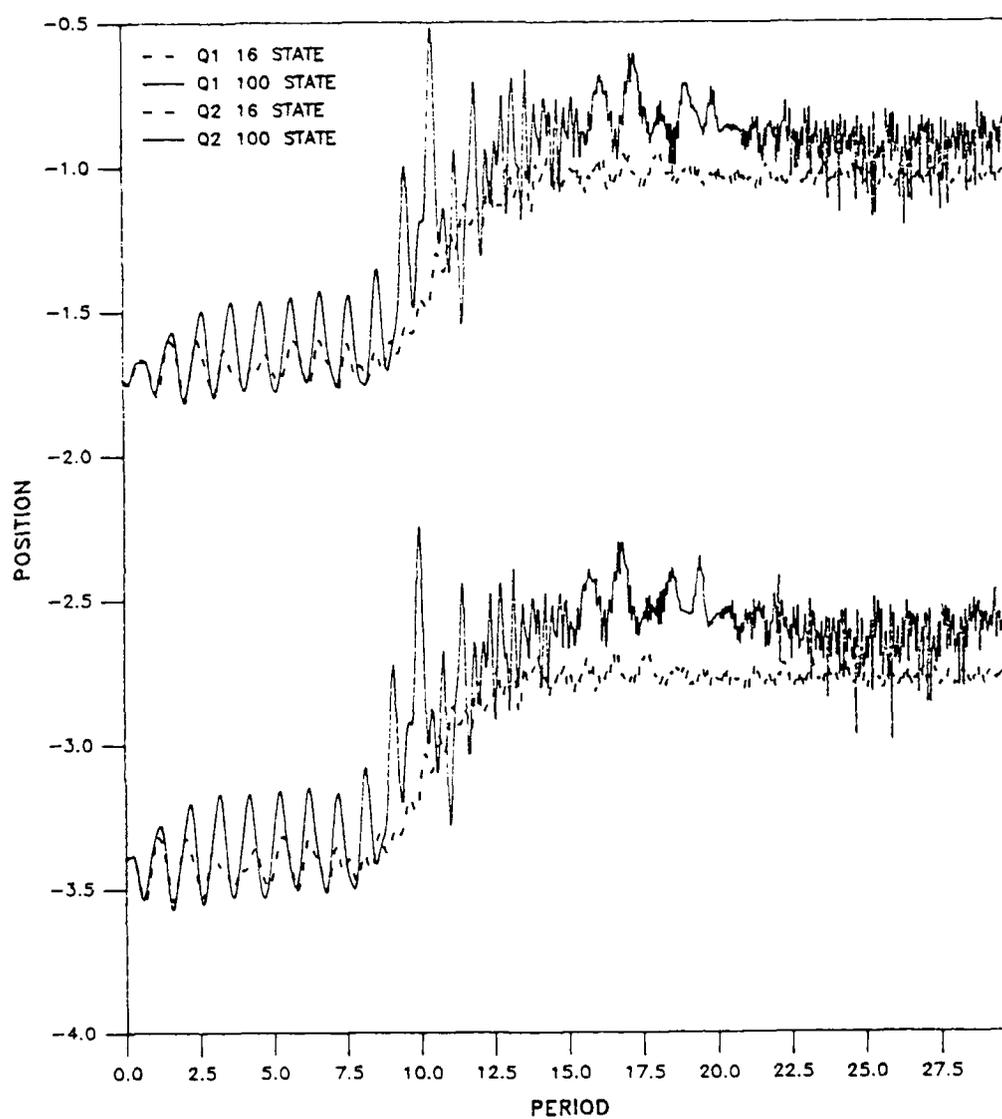
Anharmonic

Figure 38

Position of Atoms
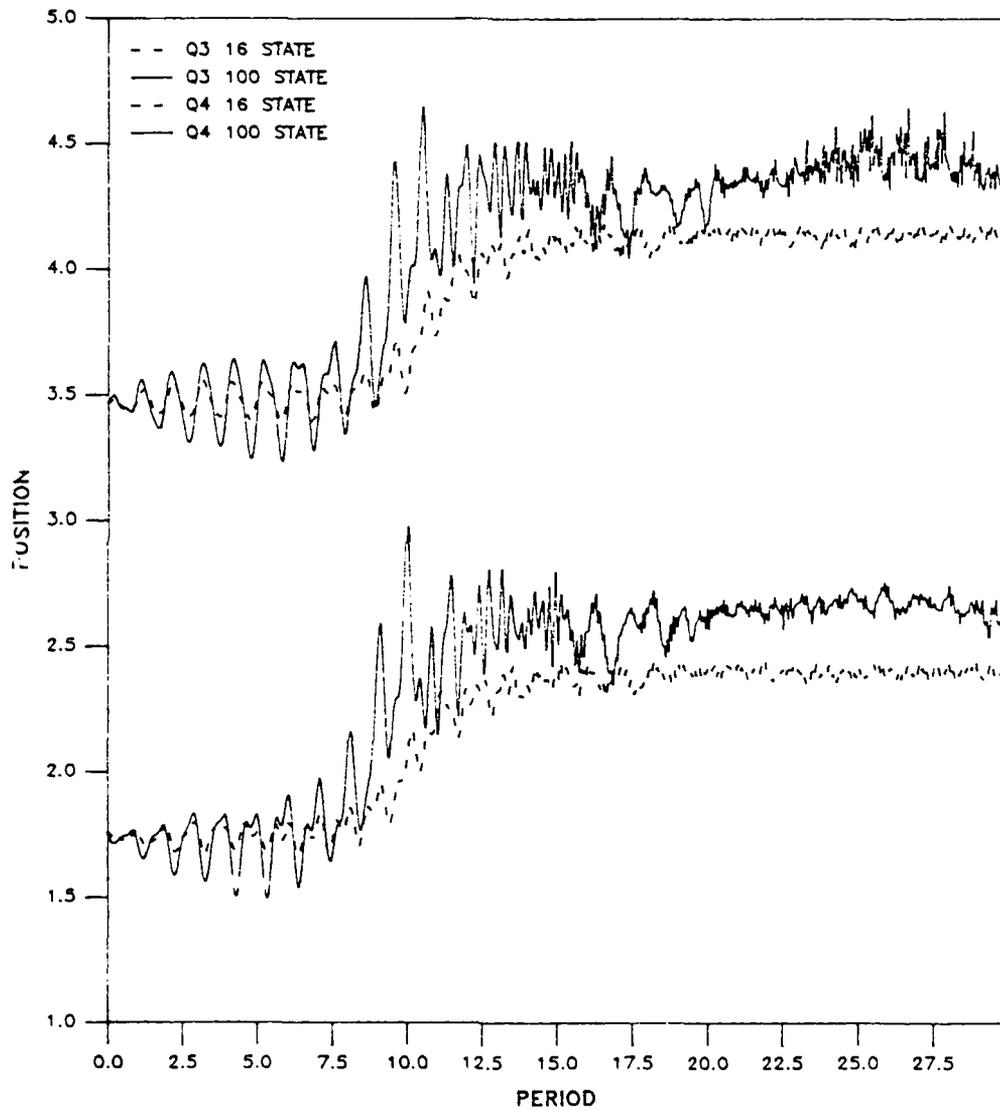
Anharmonic

Figure 39

Position of Atoms
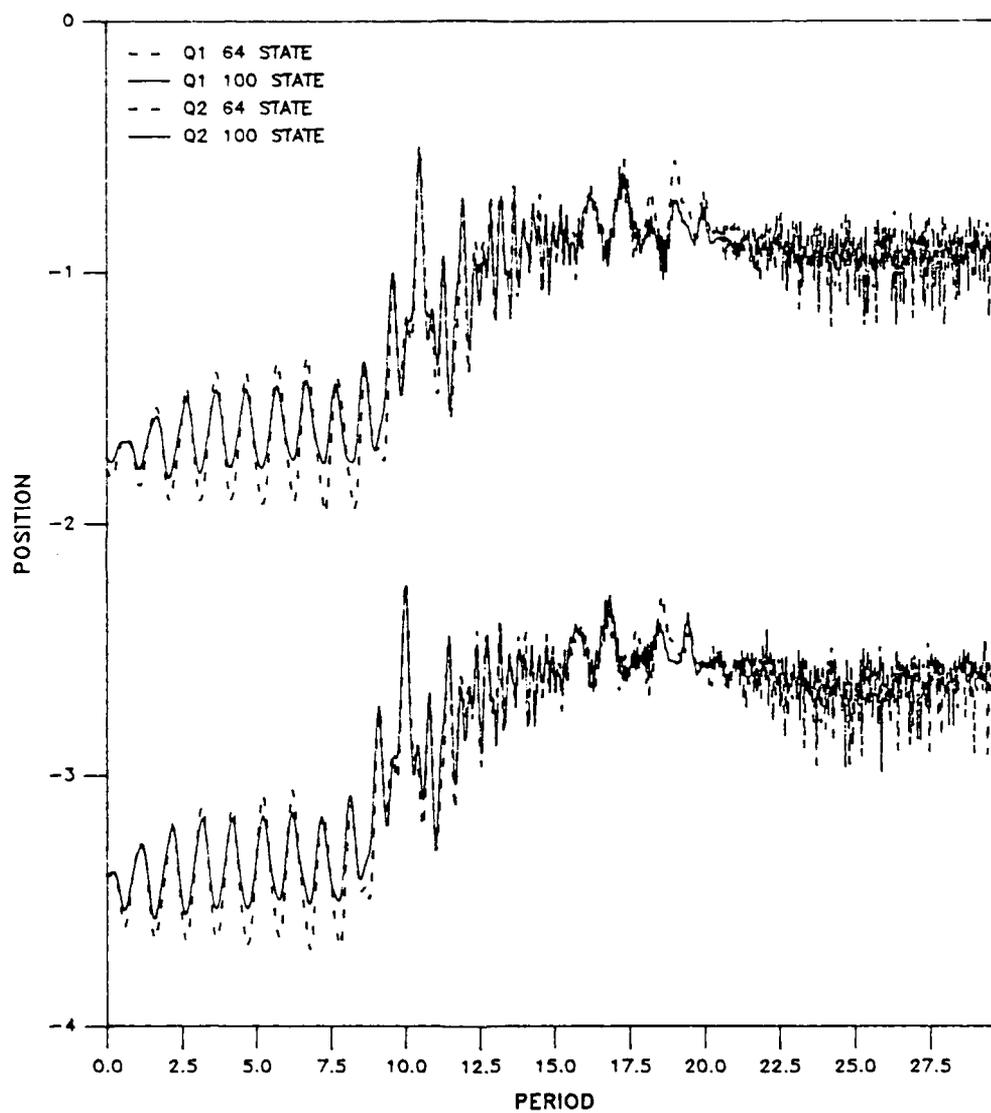
Anharmonic

Figure 40

Position of Atoms
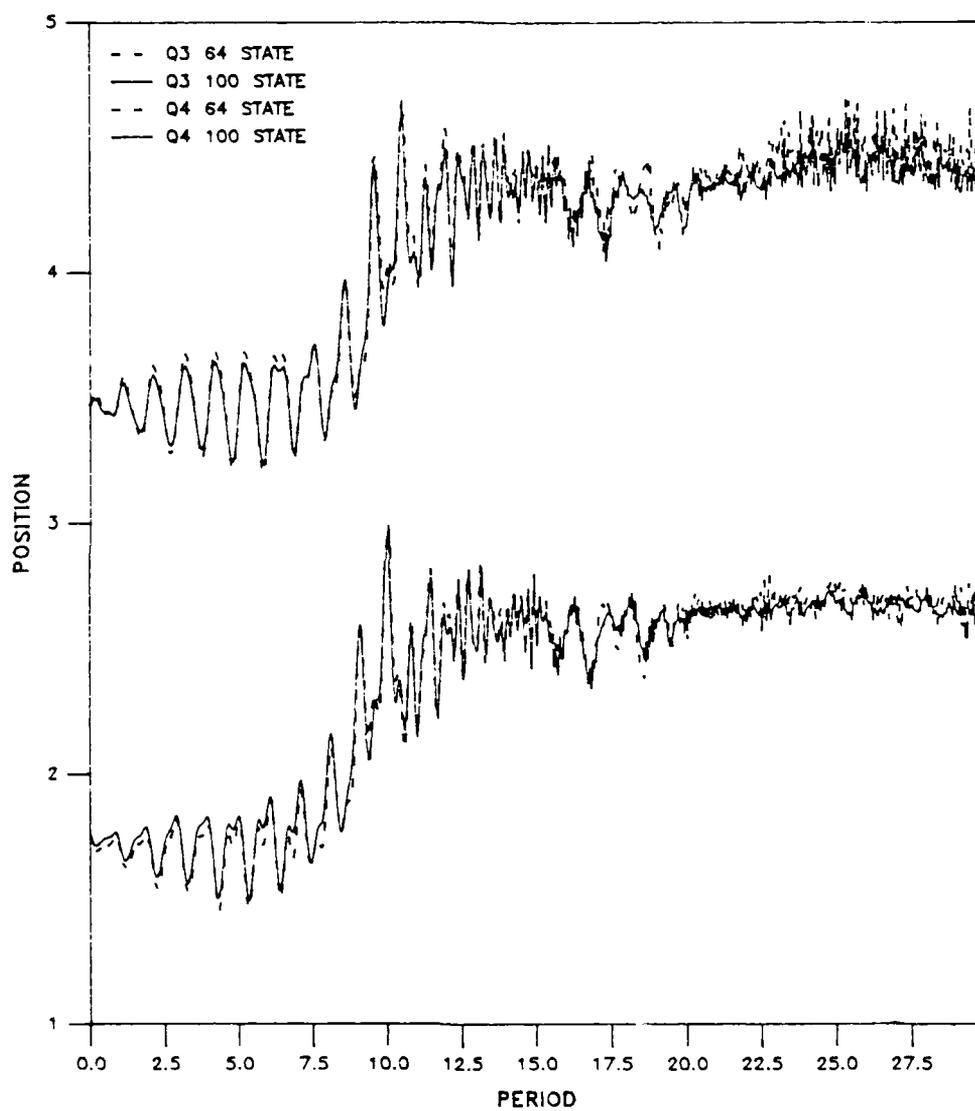
Anharmonic

Figure 41

Position of Atoms
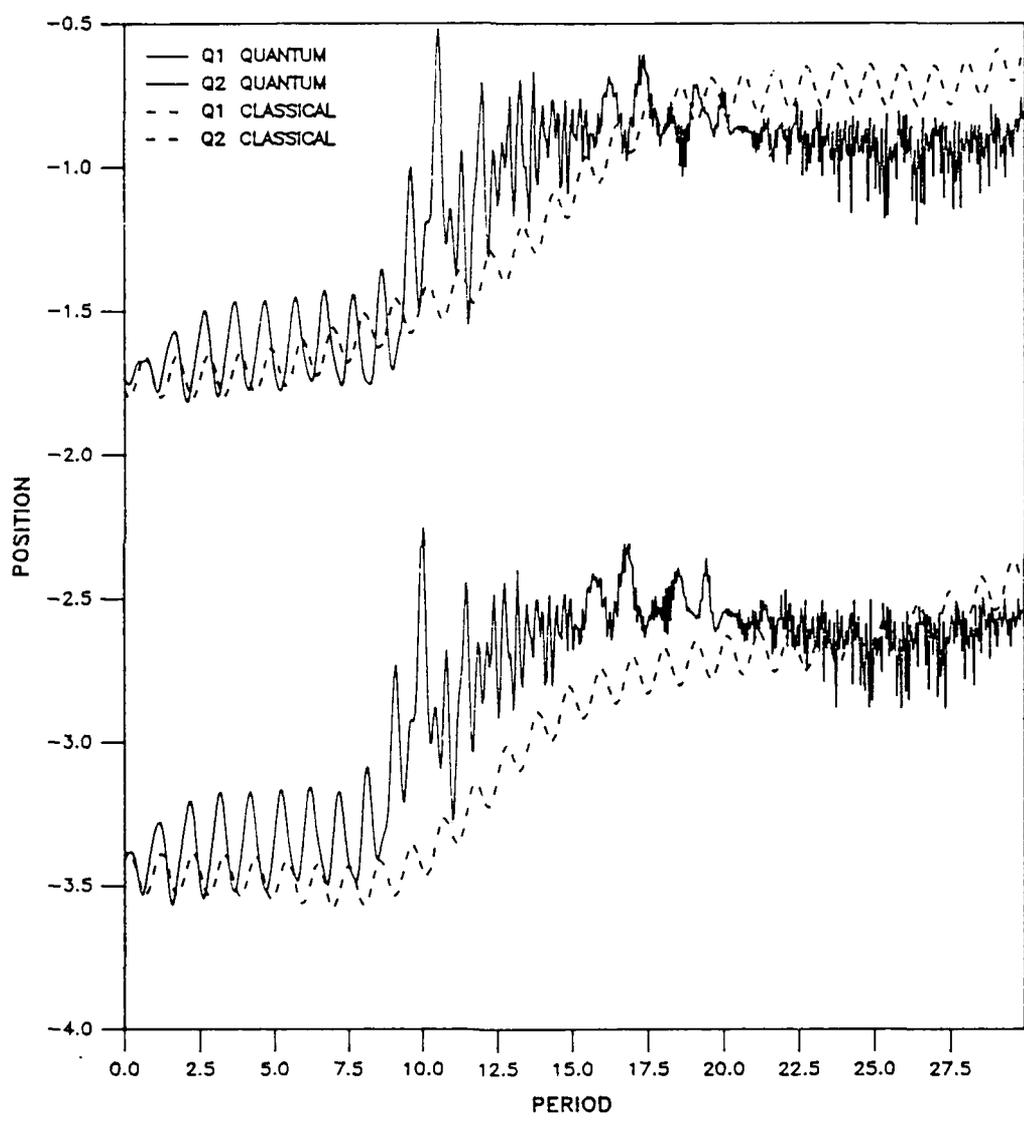
Harmonic

Figure 42

Position of Atoms
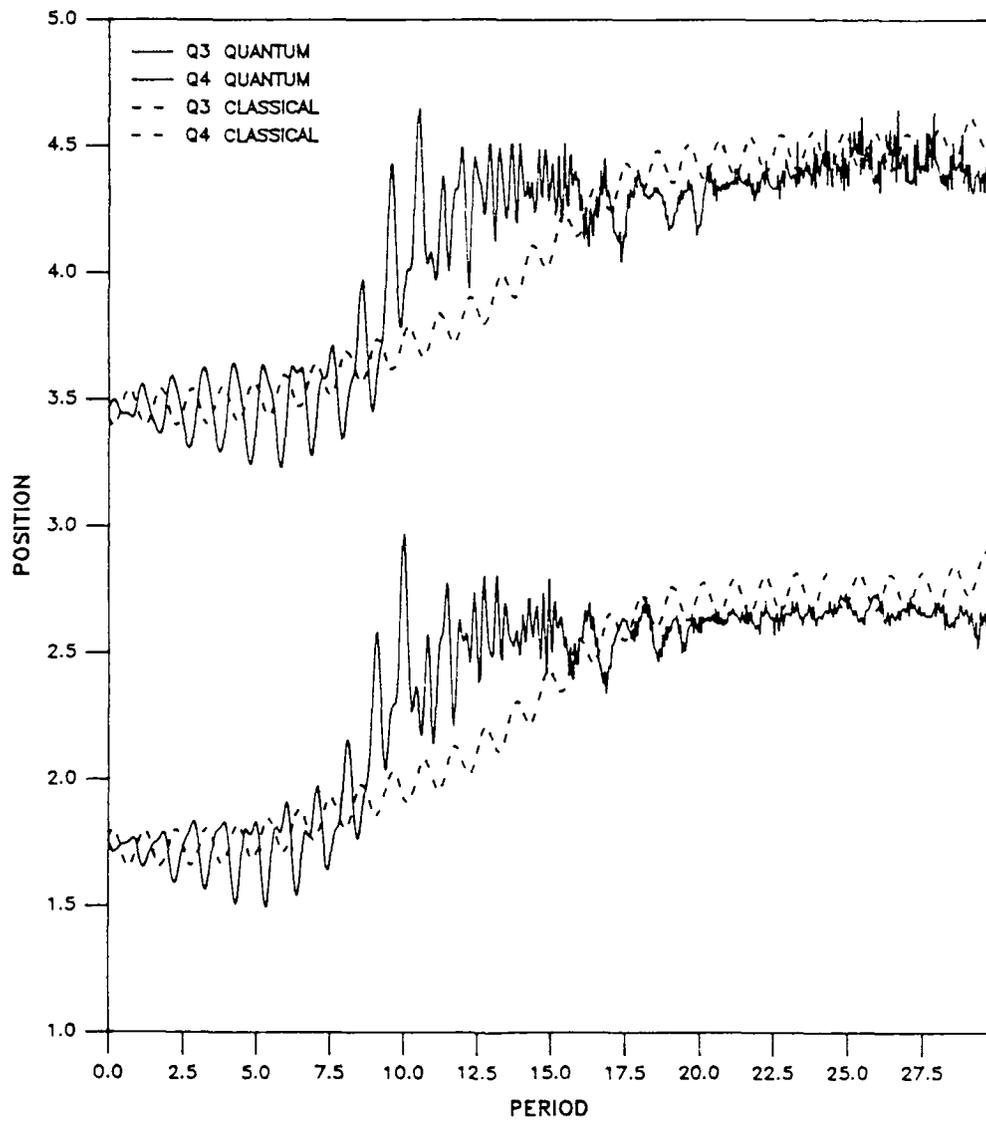
Harmonic

Figure 43

Position of Atoms
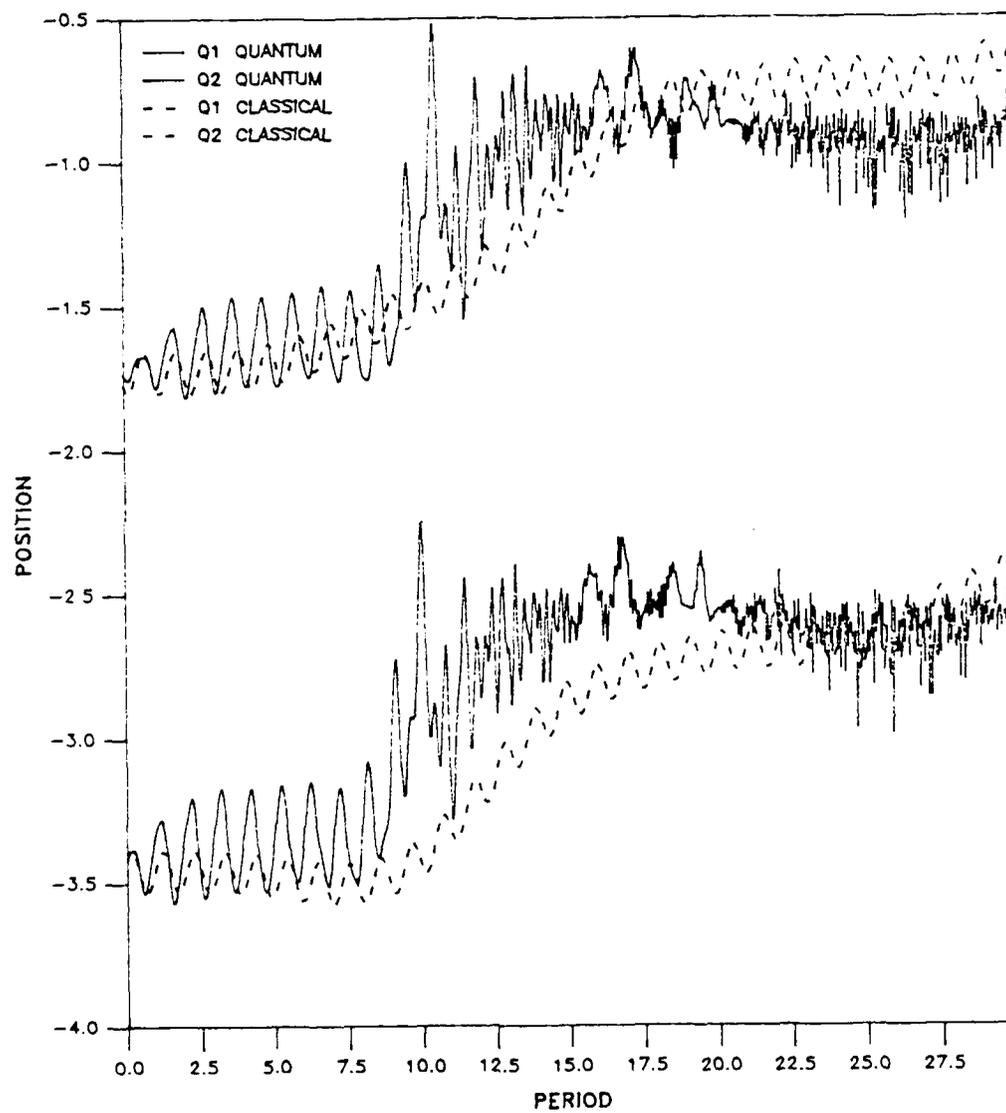
Anharmonic

Figure 44

Position of Atoms
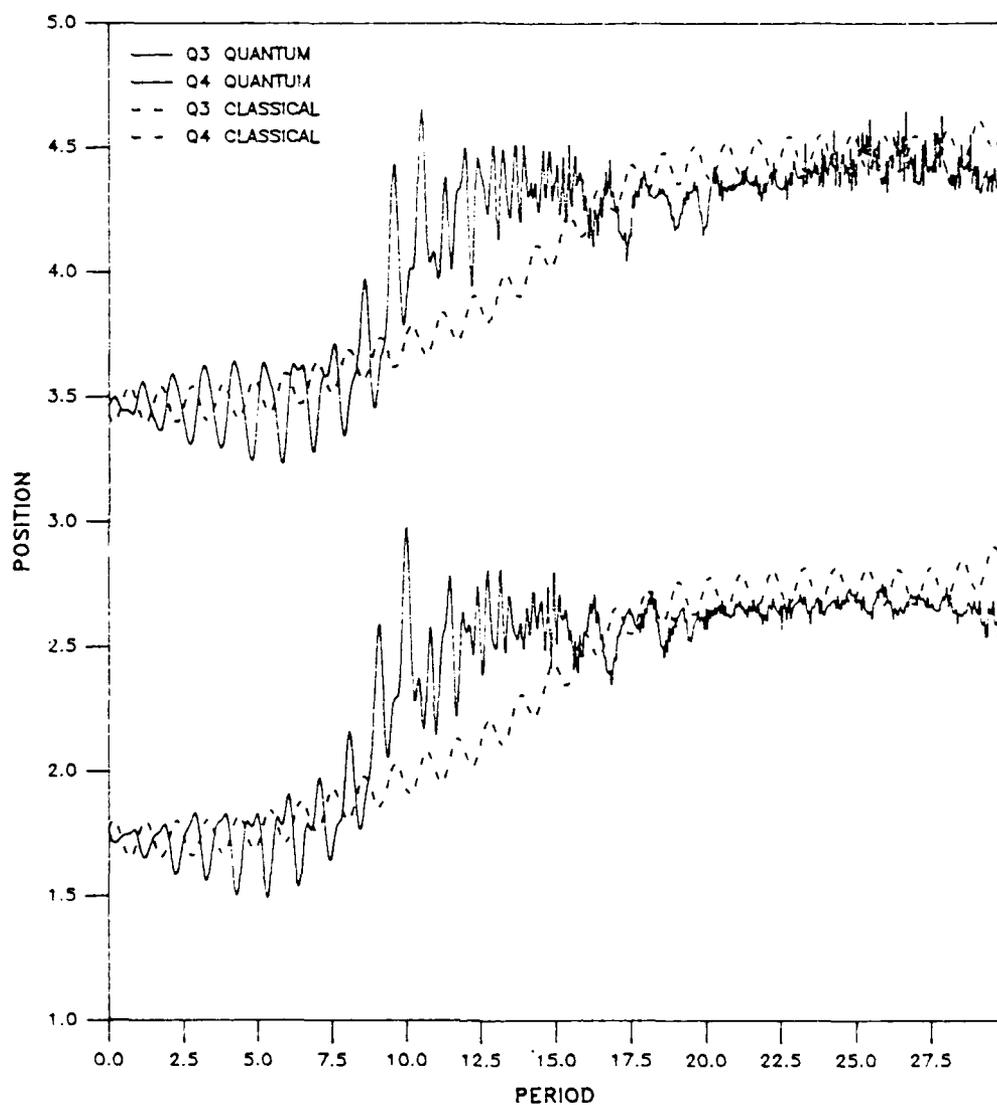
Anharmonic

Figure 45

Quantum Position Differences

Anharmonic Minus Harmonic
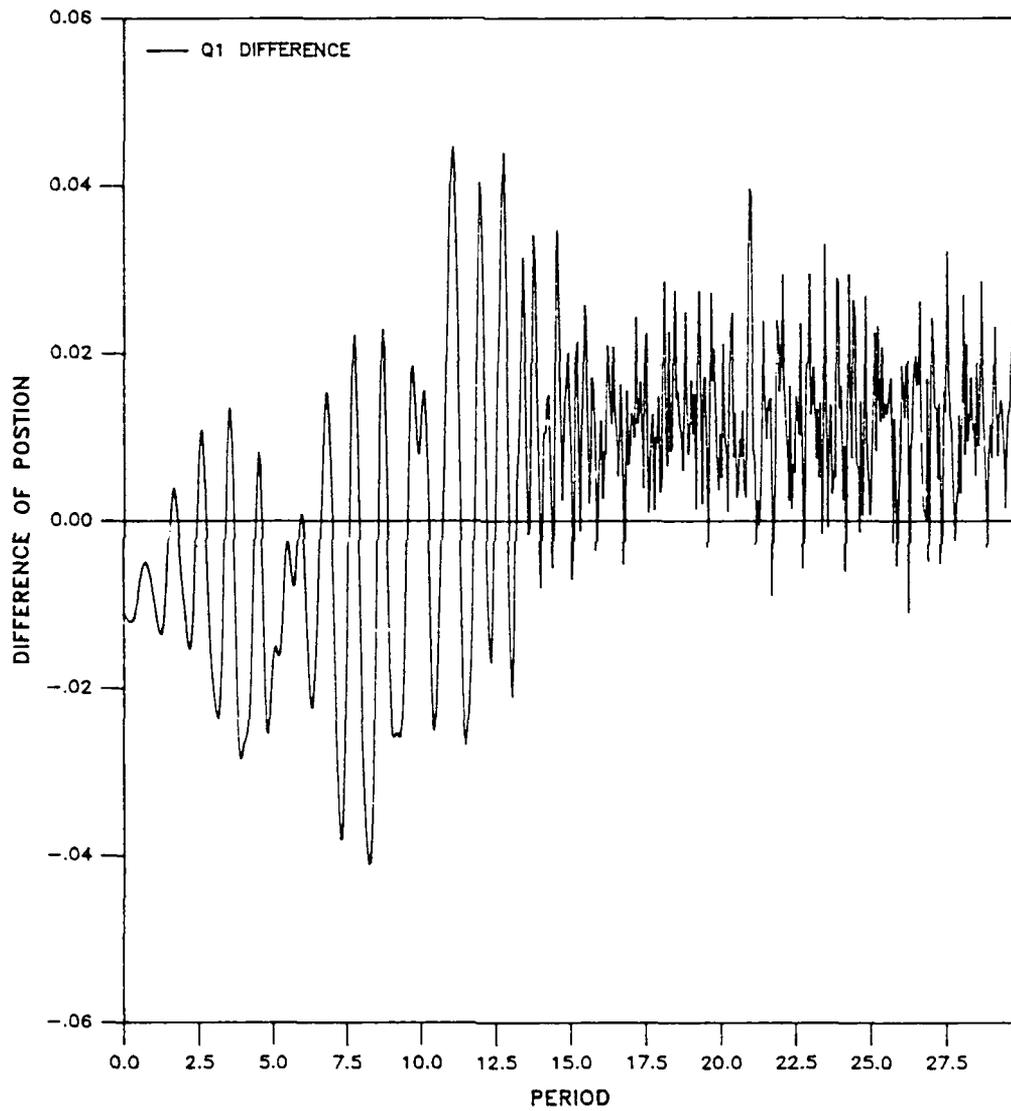
Figure 46

Quantum Position Differences

Anharmonic Minus Harmonic
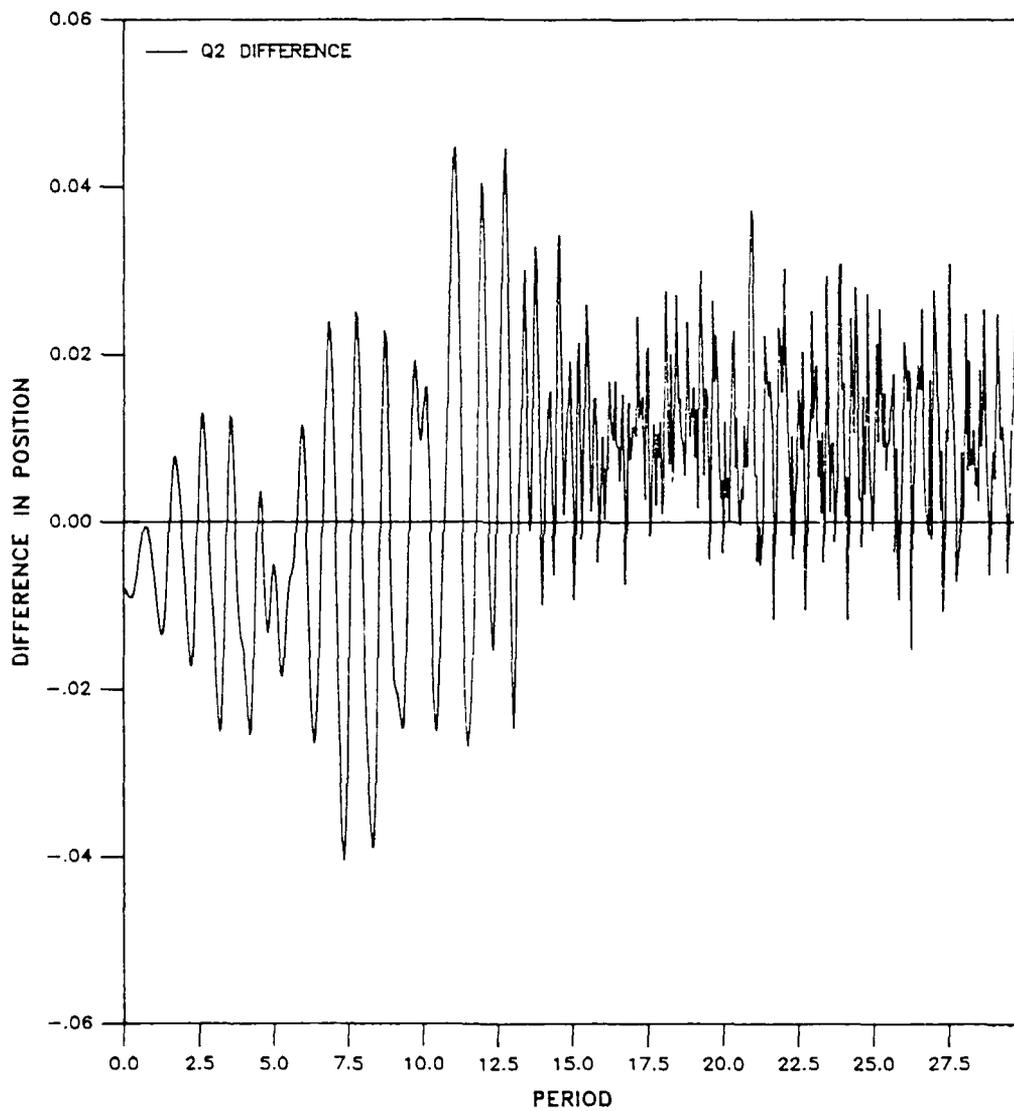
Figure 47

Quantum Position Differences

Anharmonic Minus Harmonic
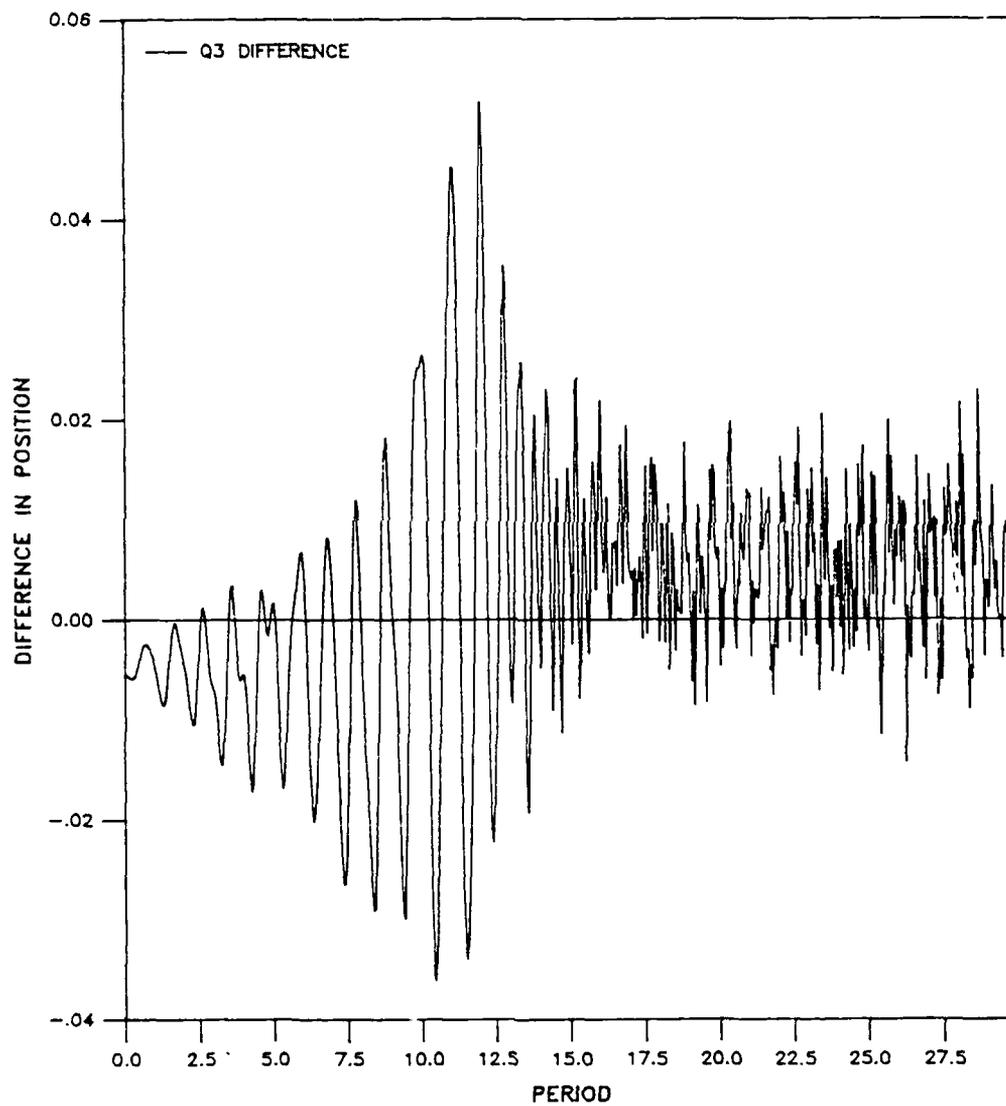
Figure 48

Quantum Position Differences

Anharmonic Minus Harmonic
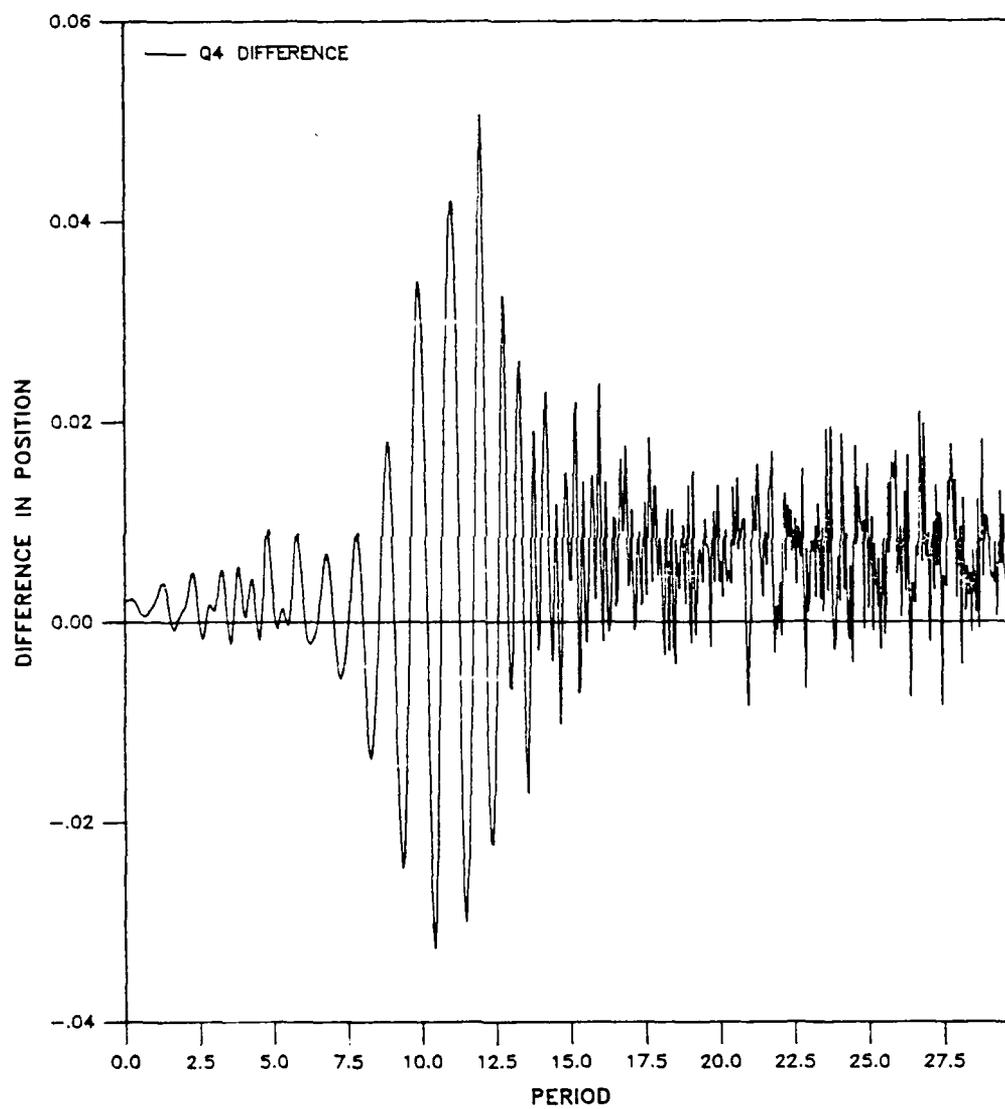
Figure 49

Harmonic Position of Atoms
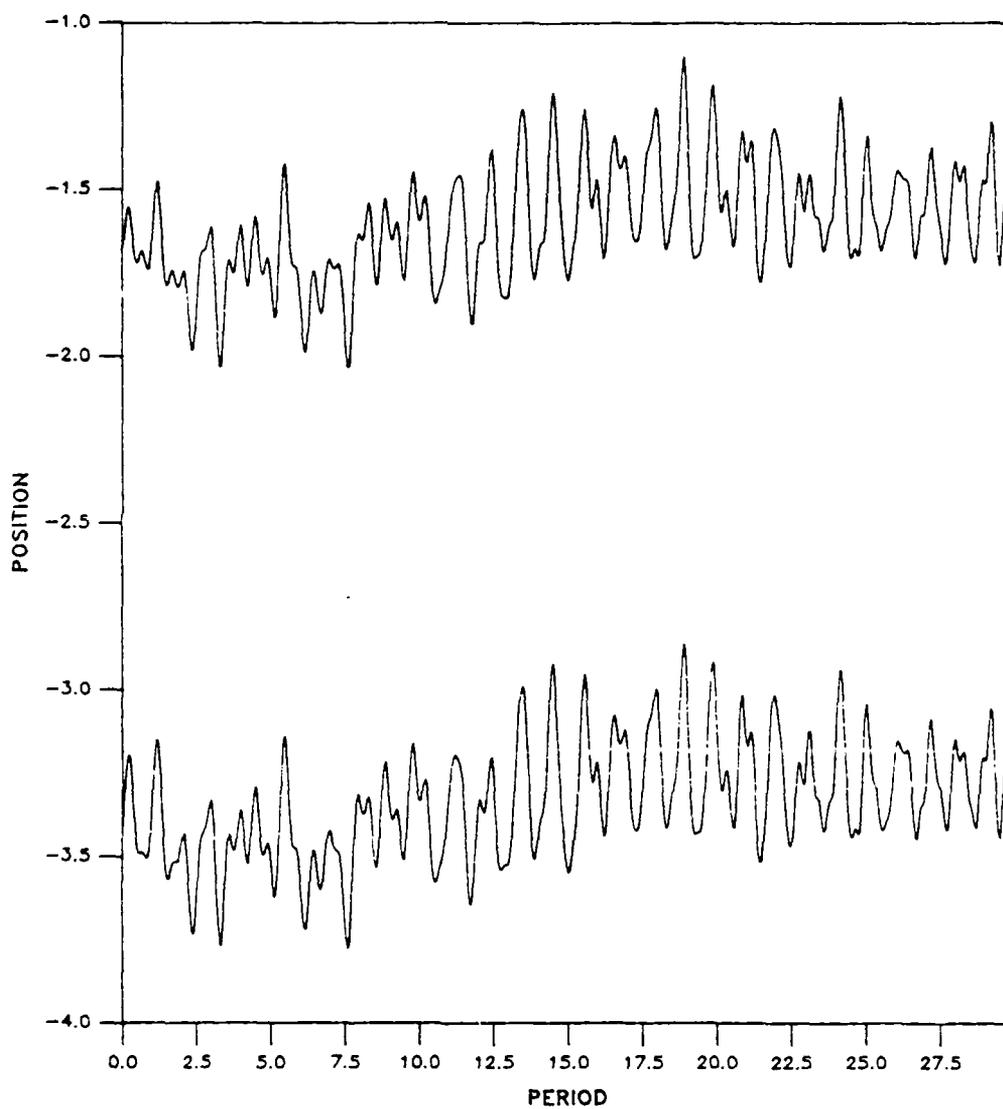
Q>= 0 at all time

Figure 50

Harmonic Position of Atoms

Q>=0 at all time
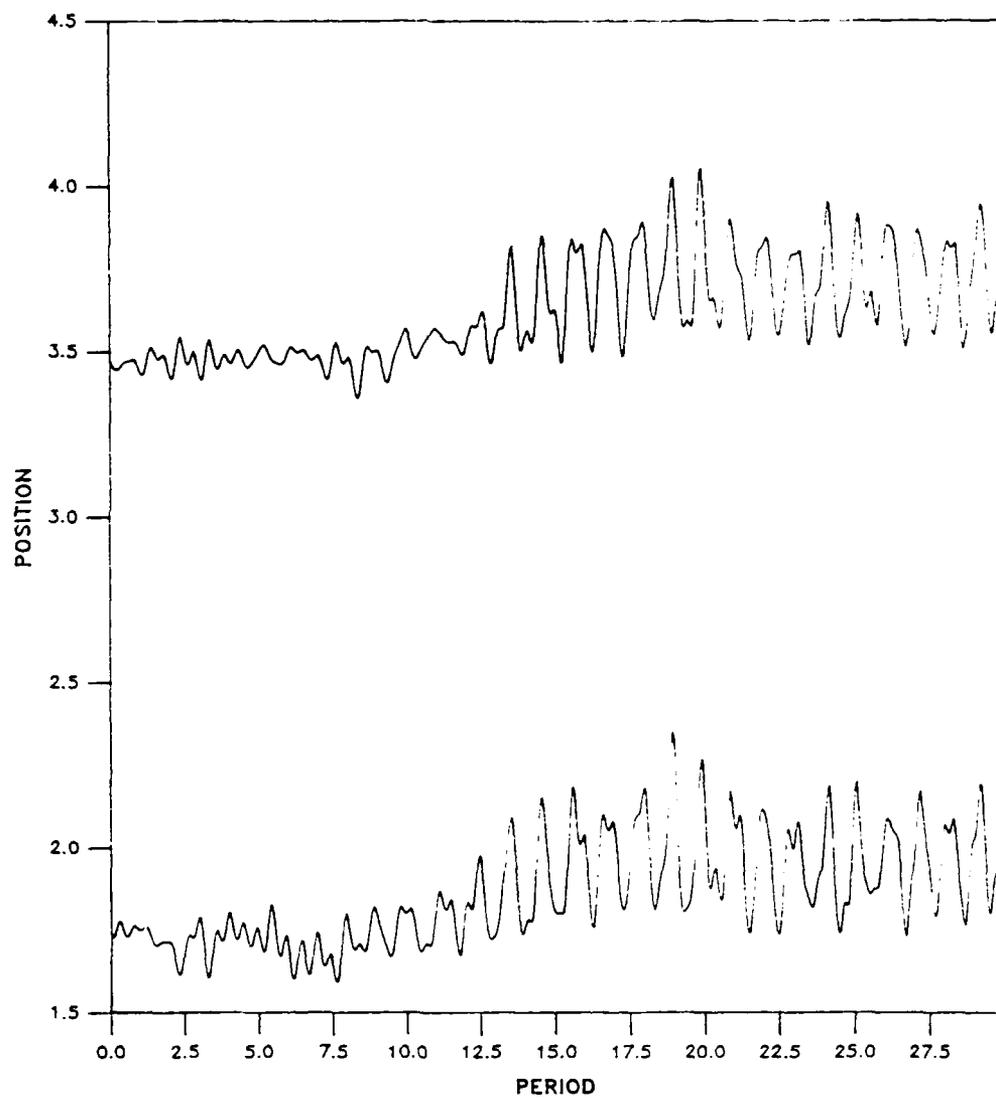
Figure 51

Harmonic Position of Atoms
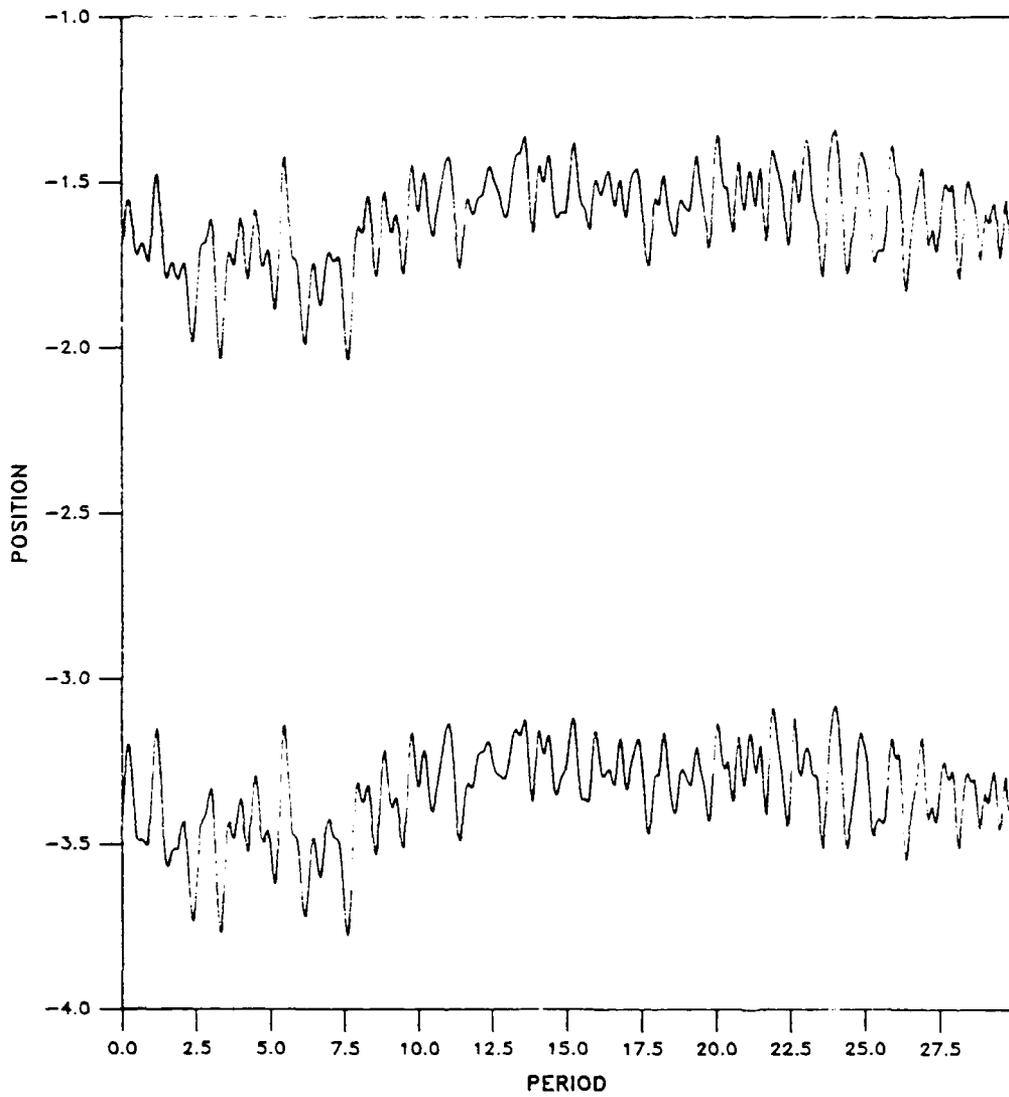
Q>=.5 at t>10 periods

Figure 52

Harmonic Position of Atoms
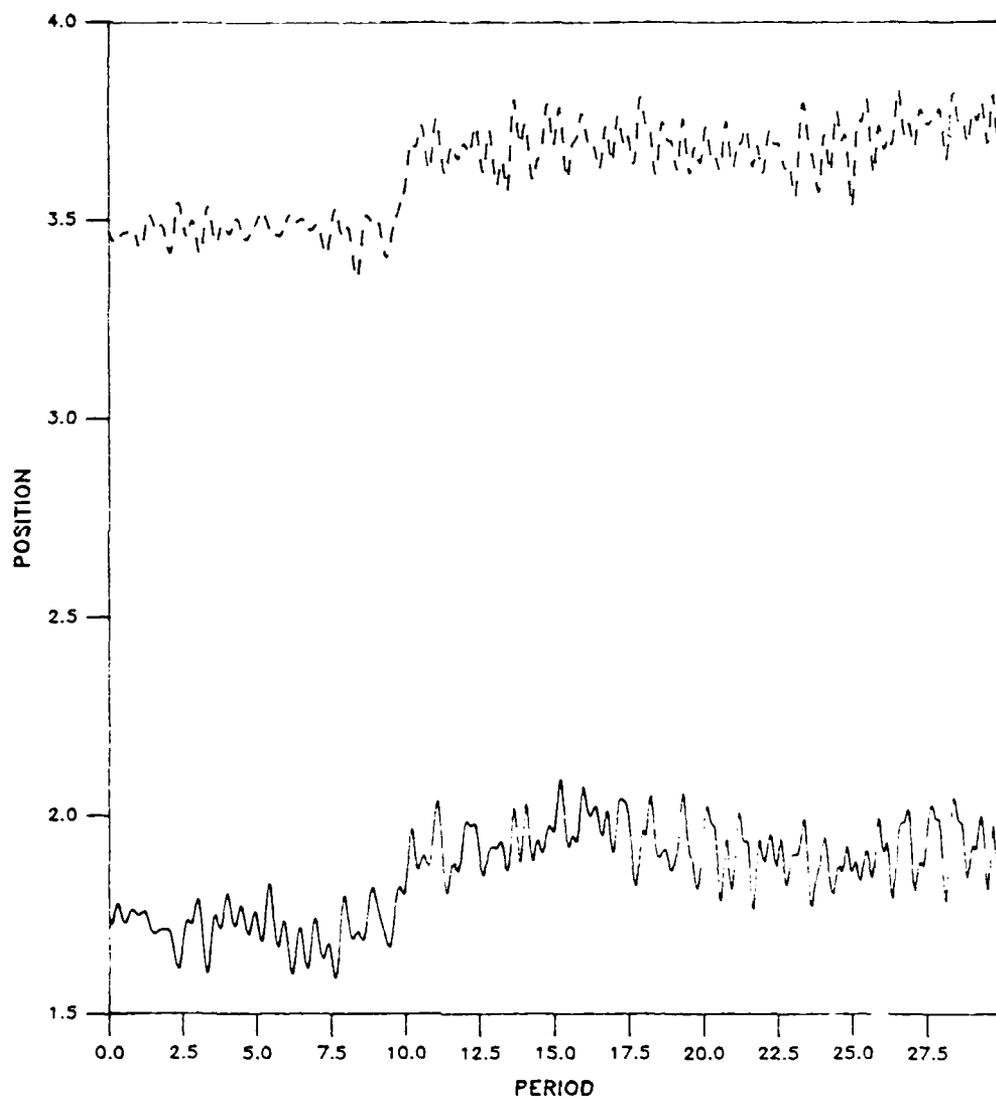
Q>=.5 at t>10 periods

Figure 53

Harmonic Position of Atoms

Q> at a ramp starting at t=10 periods

Figure 54

100
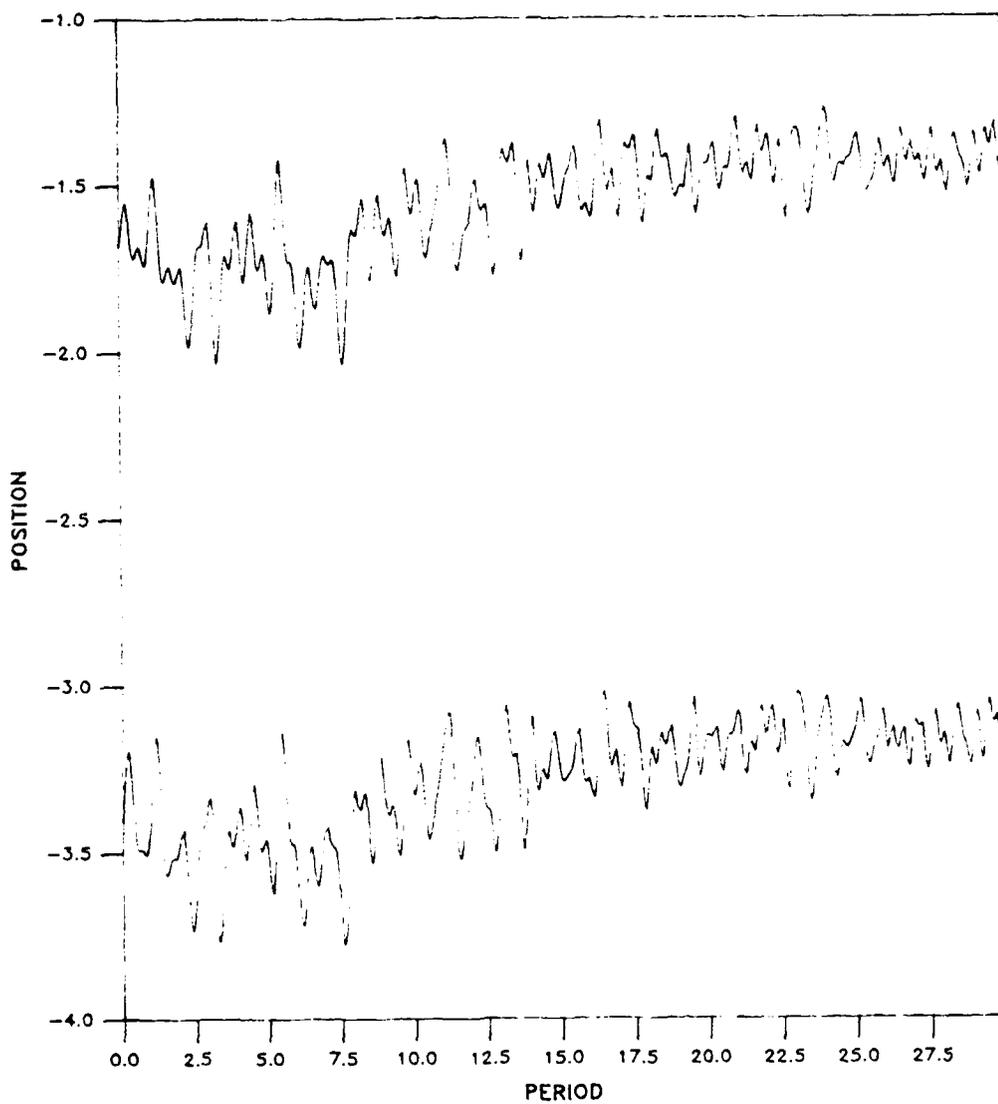
Harmonic Position of Atoms

Q>= at a ramp starting at t=10 periods
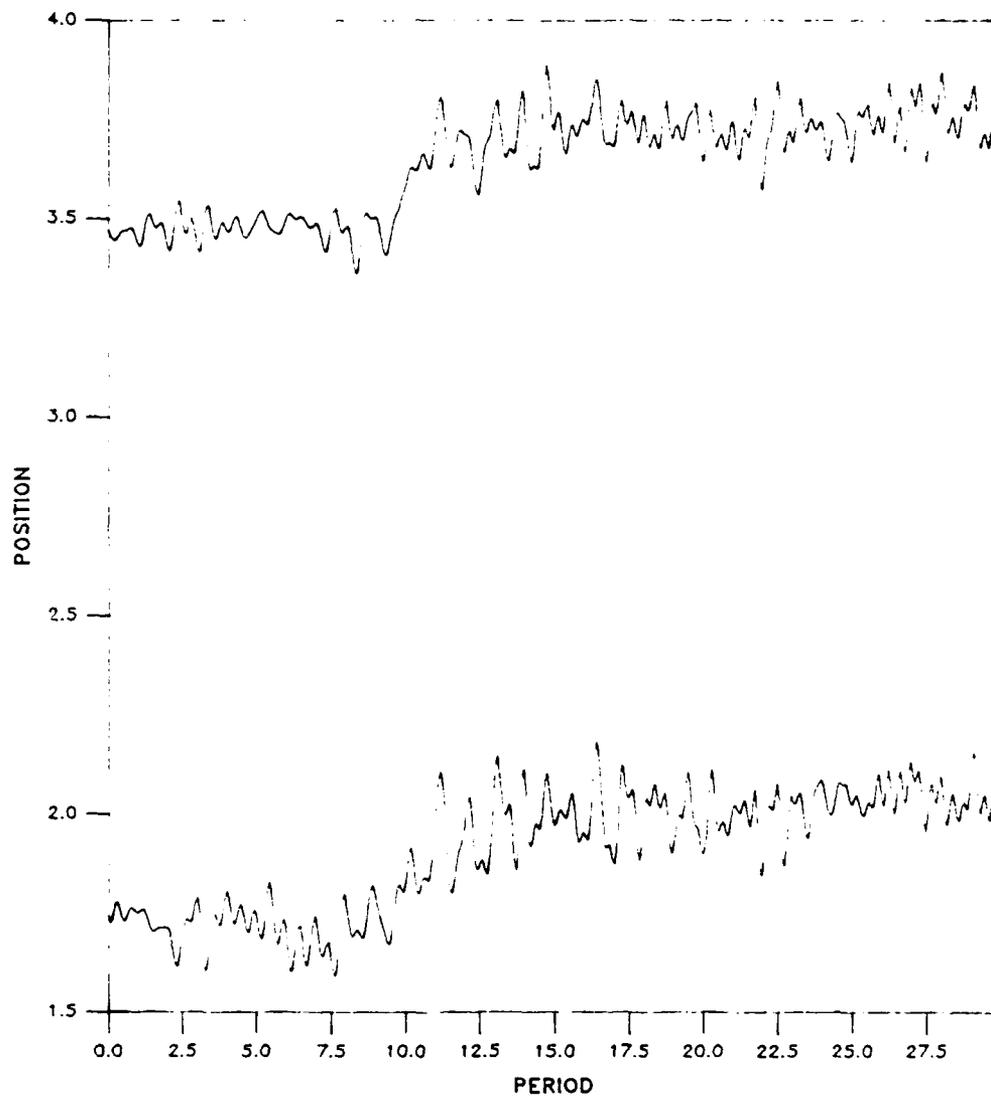
Figure 55

Position of Atoms

Harmonic, DG Shifted 3 Periods Left
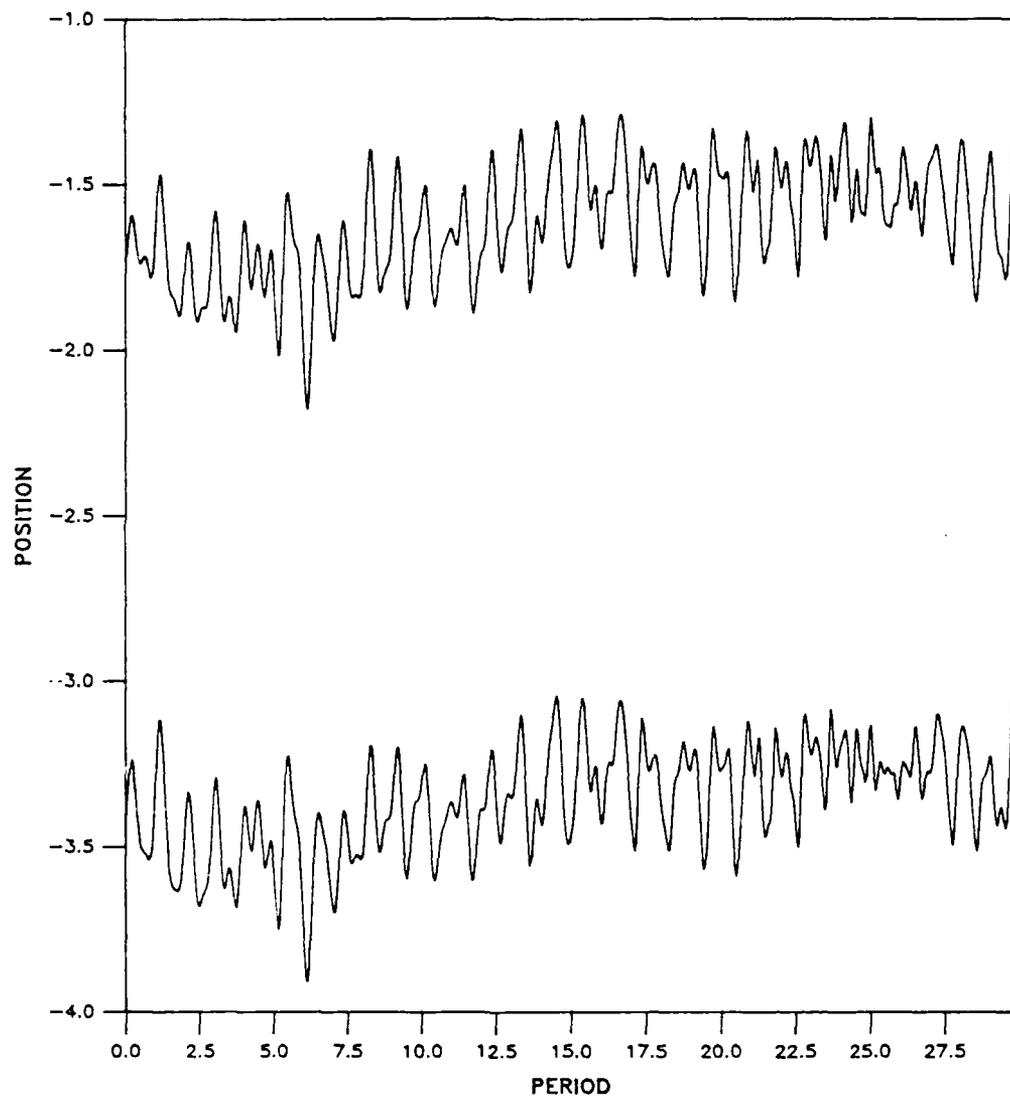
Figure 56

Position of Atoms

HARMONIC, DG SHIFTED 3 PERIODS
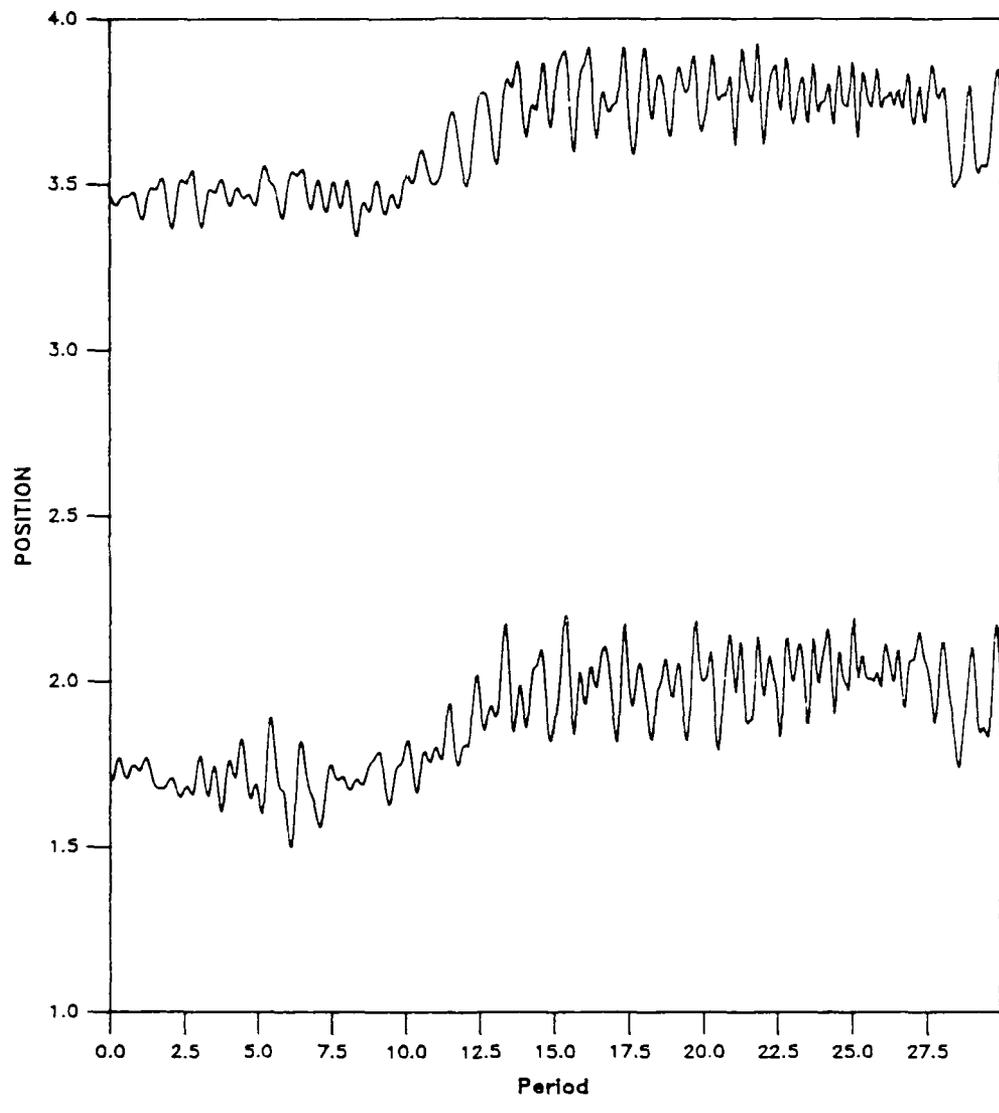
Figure 57

Position of Atoms

Harmonic, DG Shifted 3 Periods Right
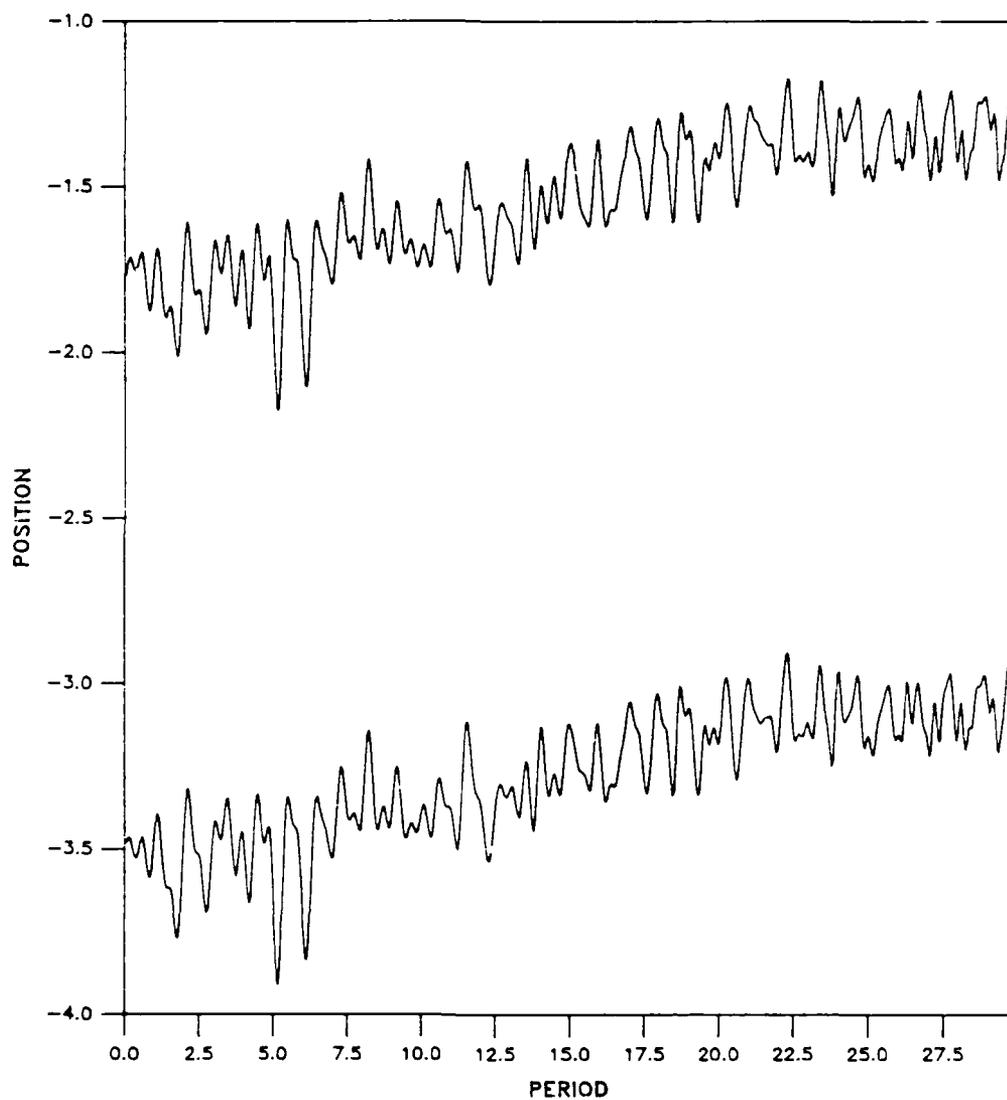
Figure 58

Position of Atoms

Harmonic, DG Shifted 3 Periods Right
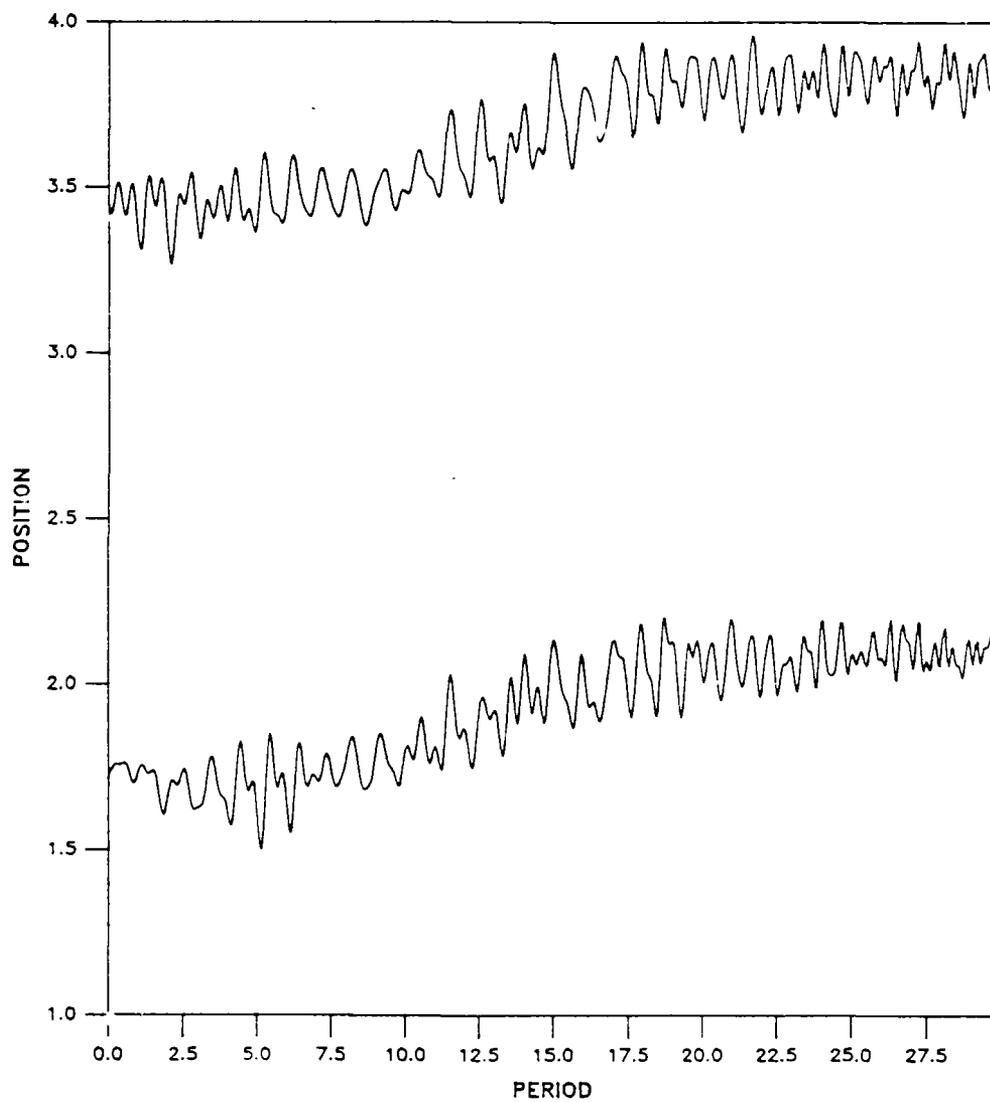
Figure 59

Position of Atoms
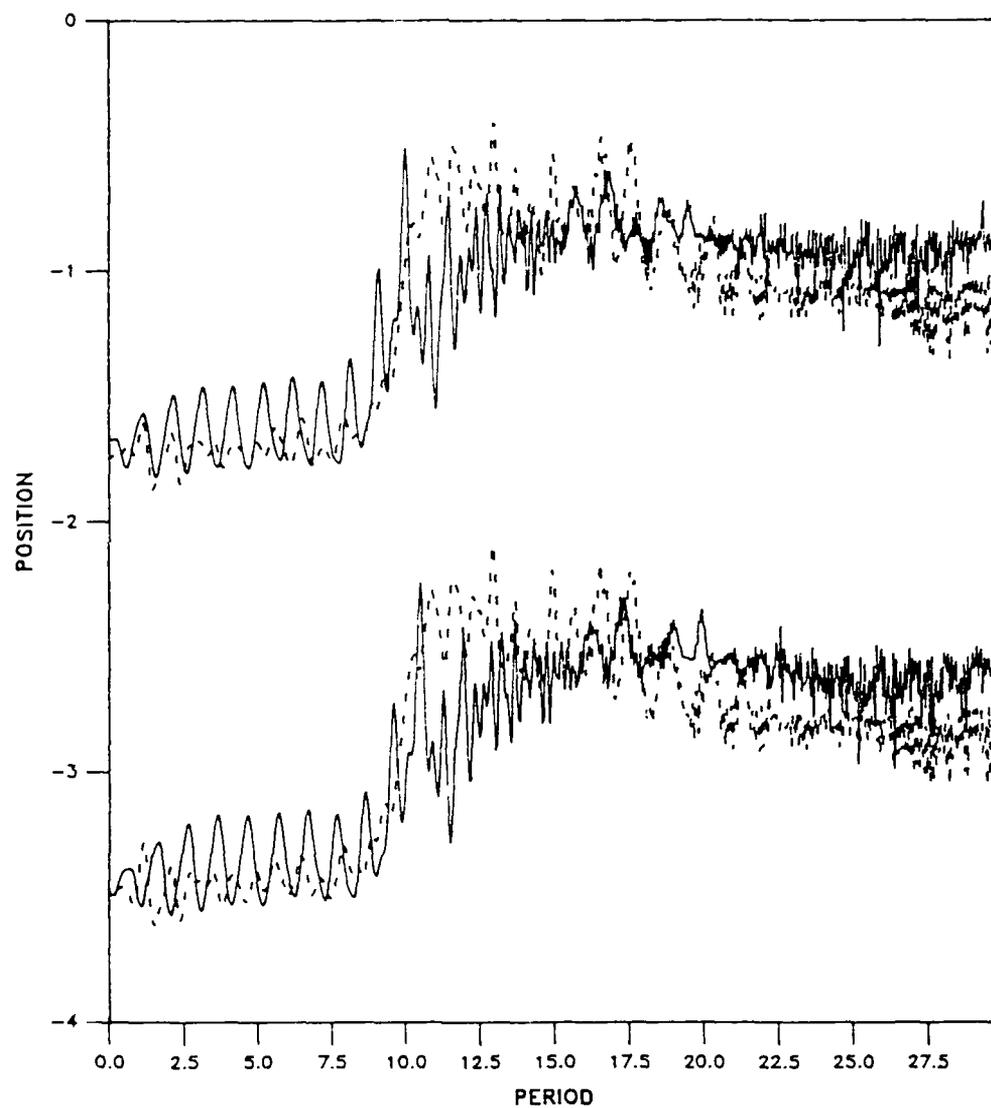
Anharmonic

Figure 60

Position of Atoms
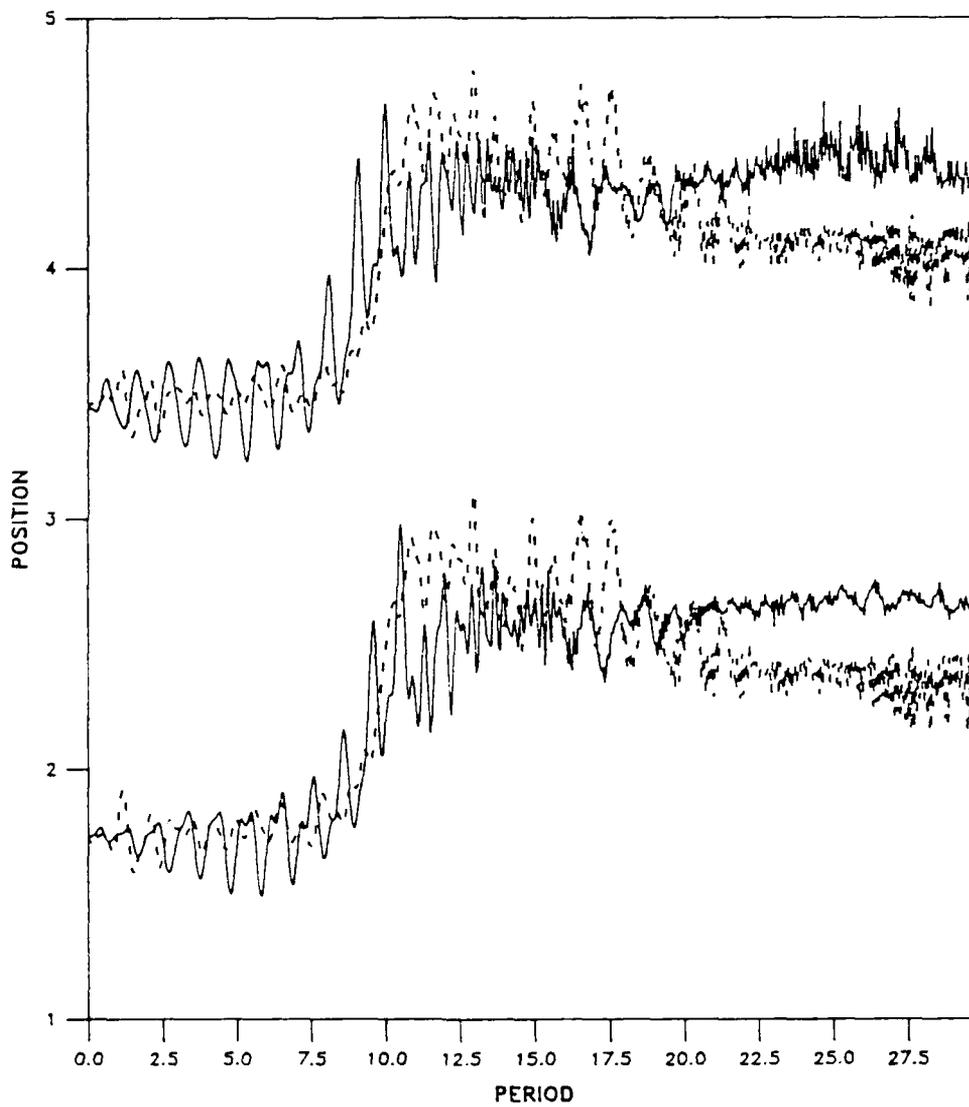
## Anharmonic

Figure 61

Energy of Mode One

Harmonic
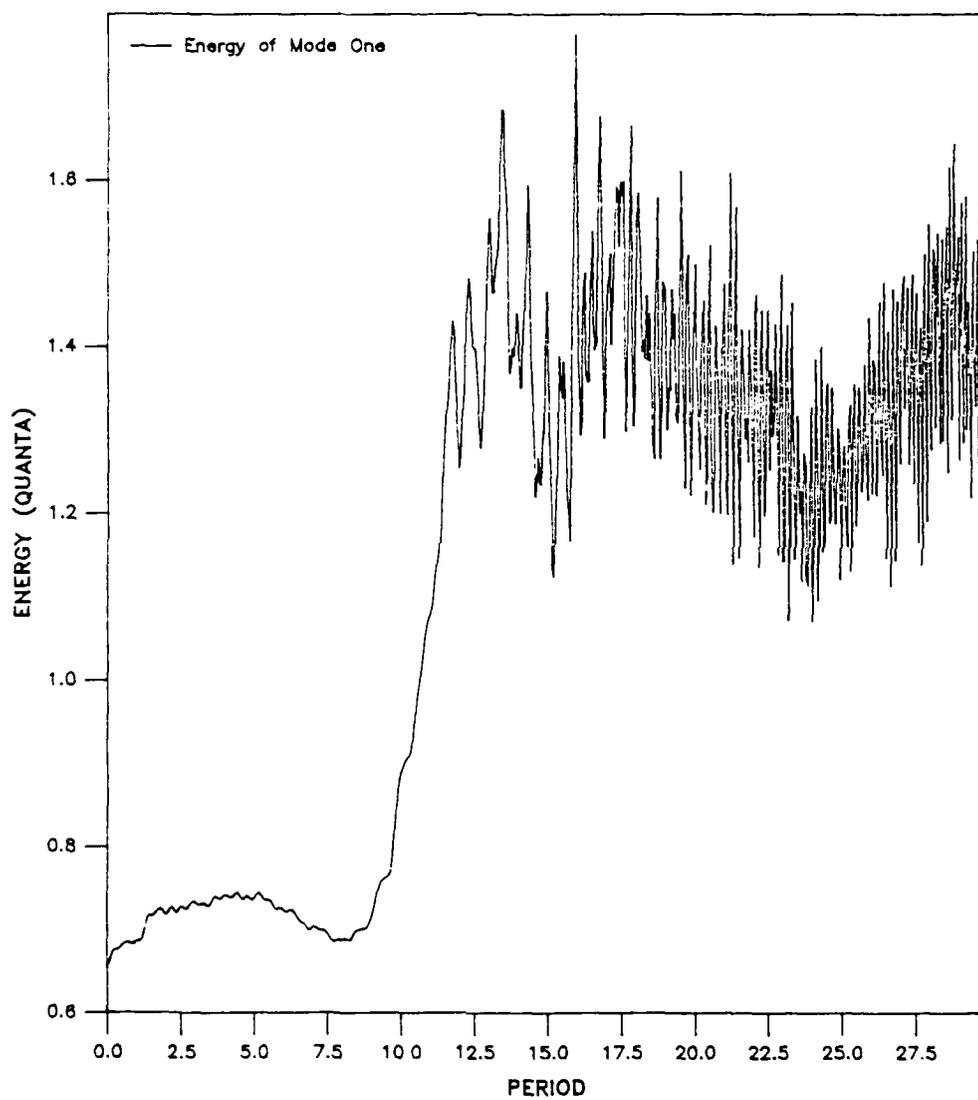

Figure 62

Energy of Mode Two

Harmonic
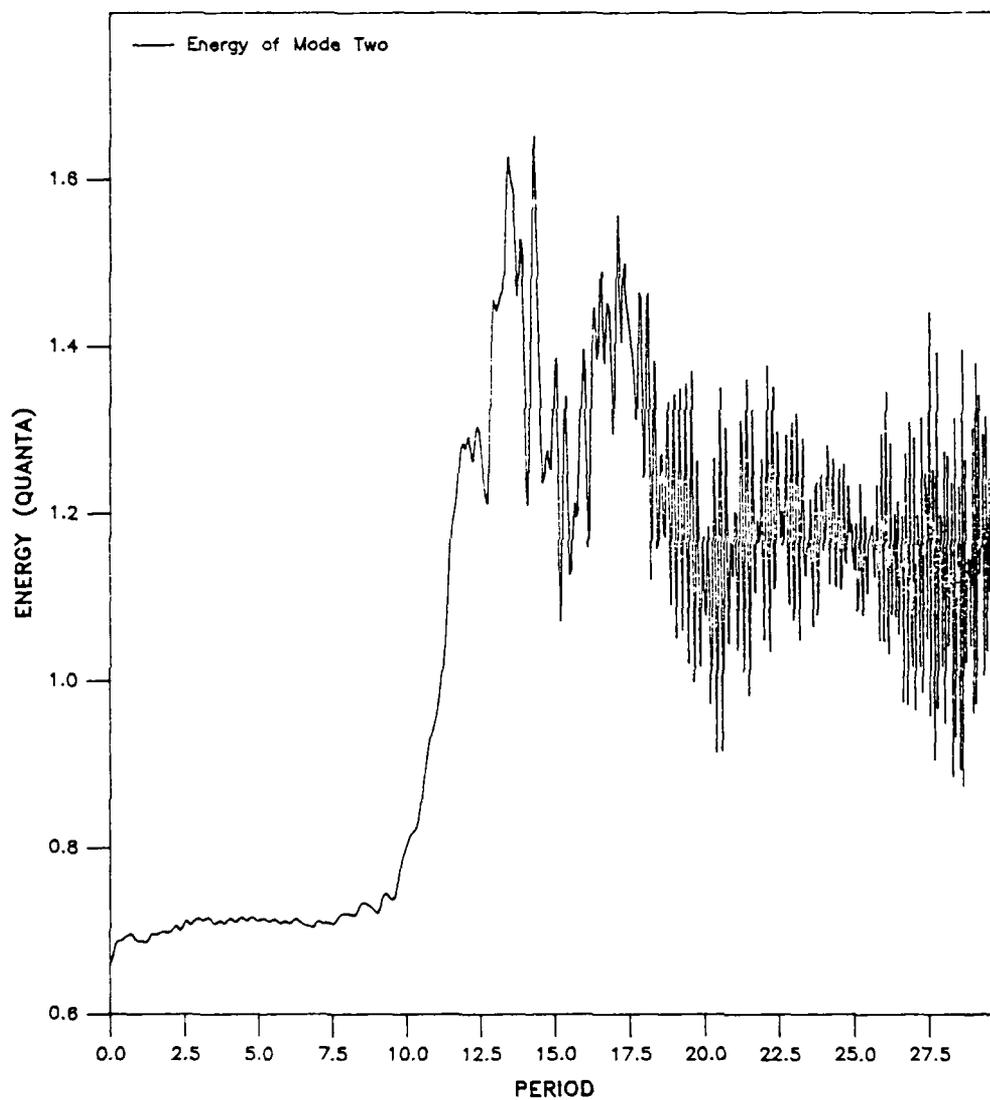
Figure 63

Energy of Mode Three

Harmonic
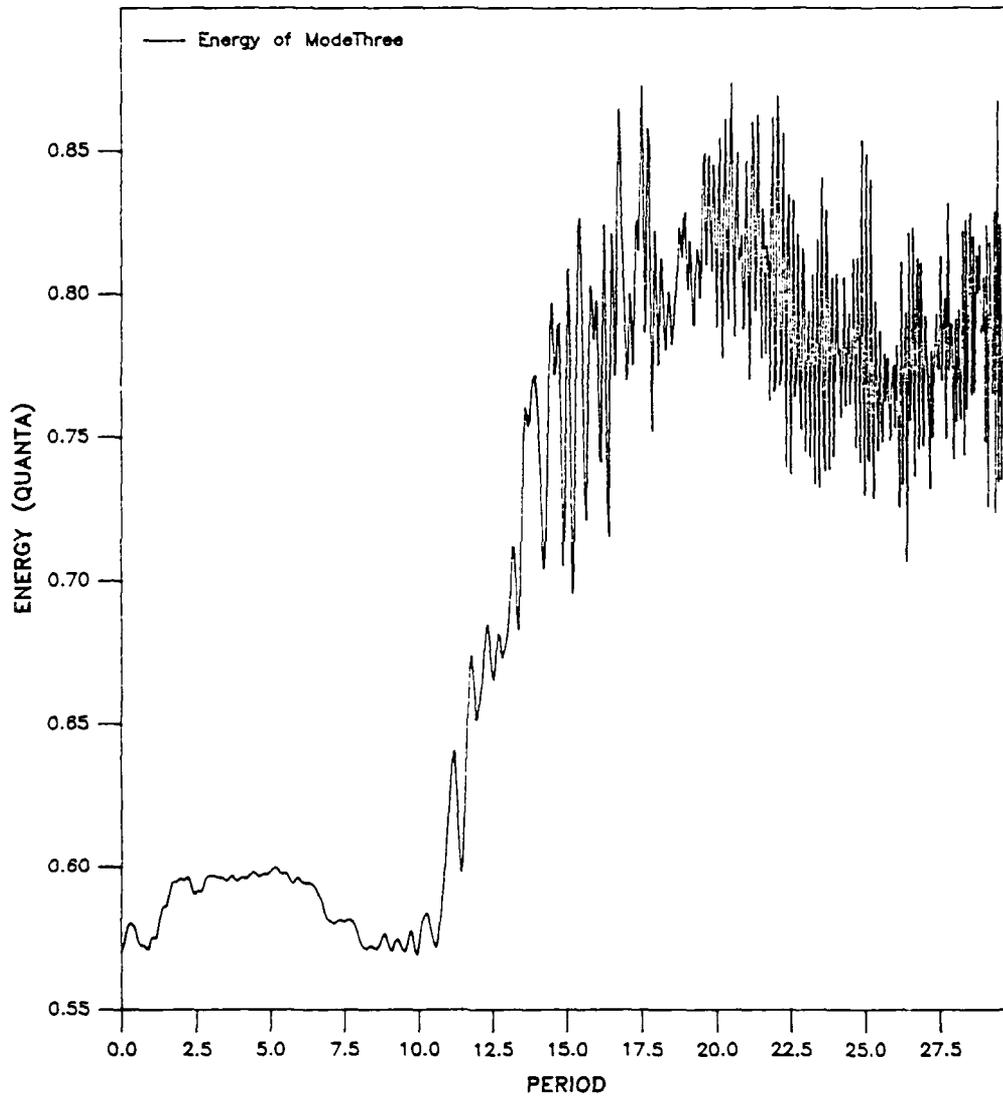
Figure 64

Energy of Mode Four

Harmonic
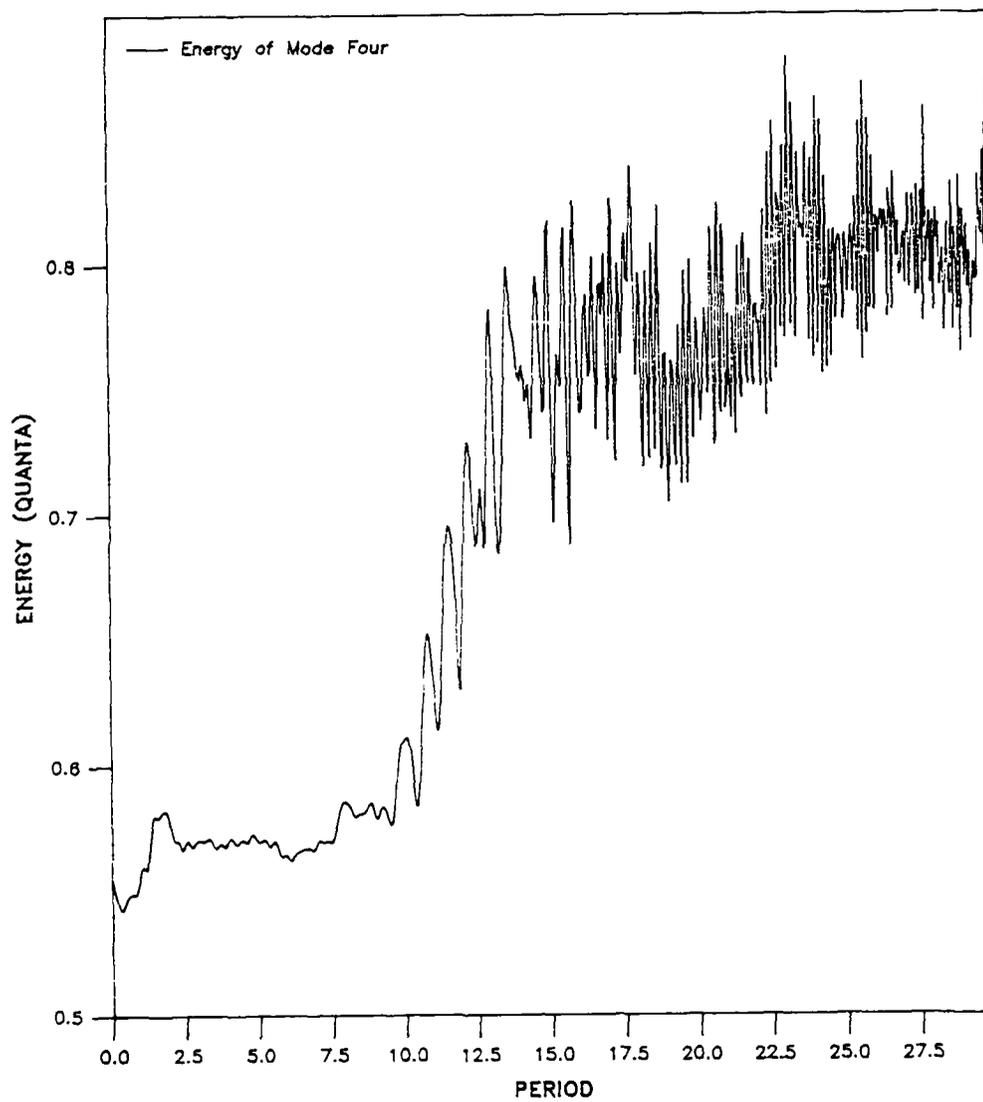
Figure 65

Energy of Mode One

Anharmonic
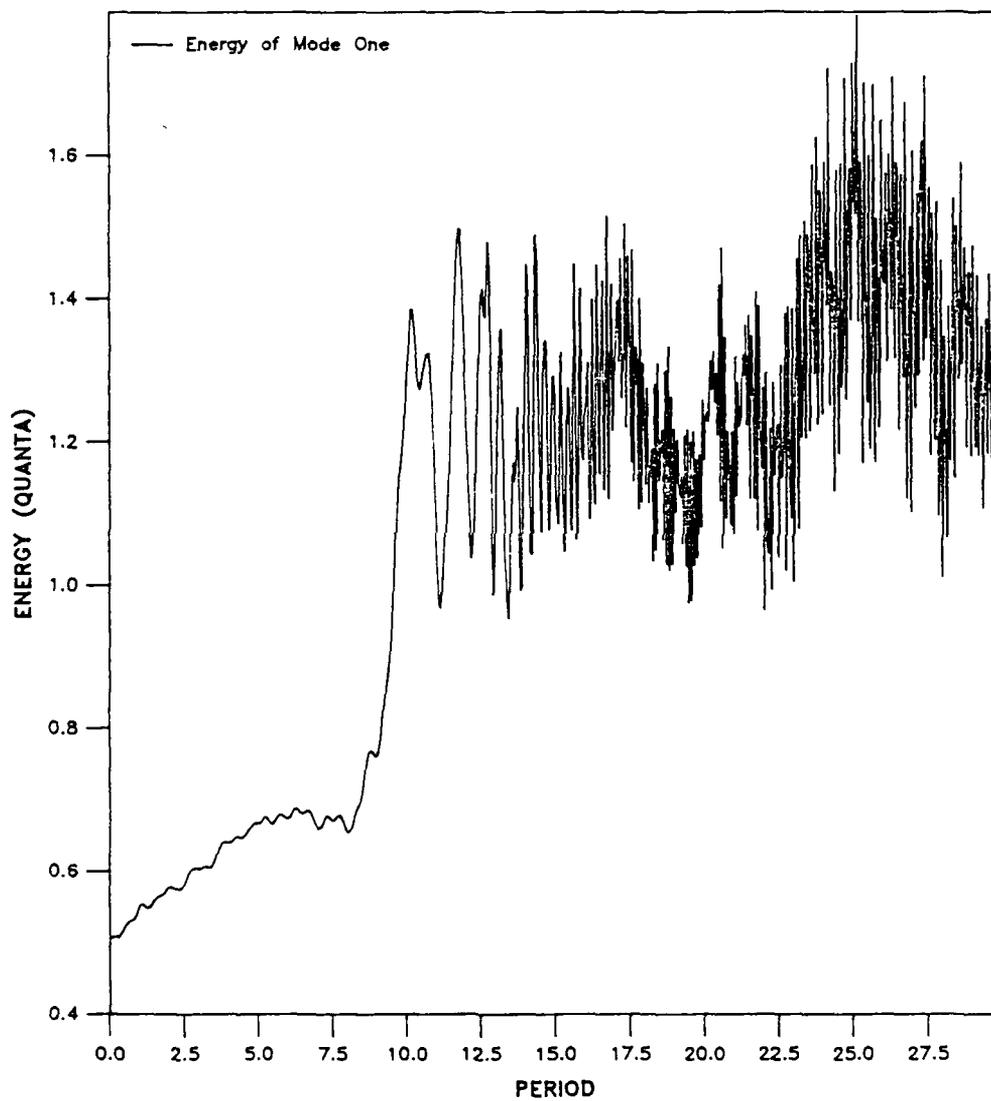
Figure 66

Energy of Mode Two

Anharmonic
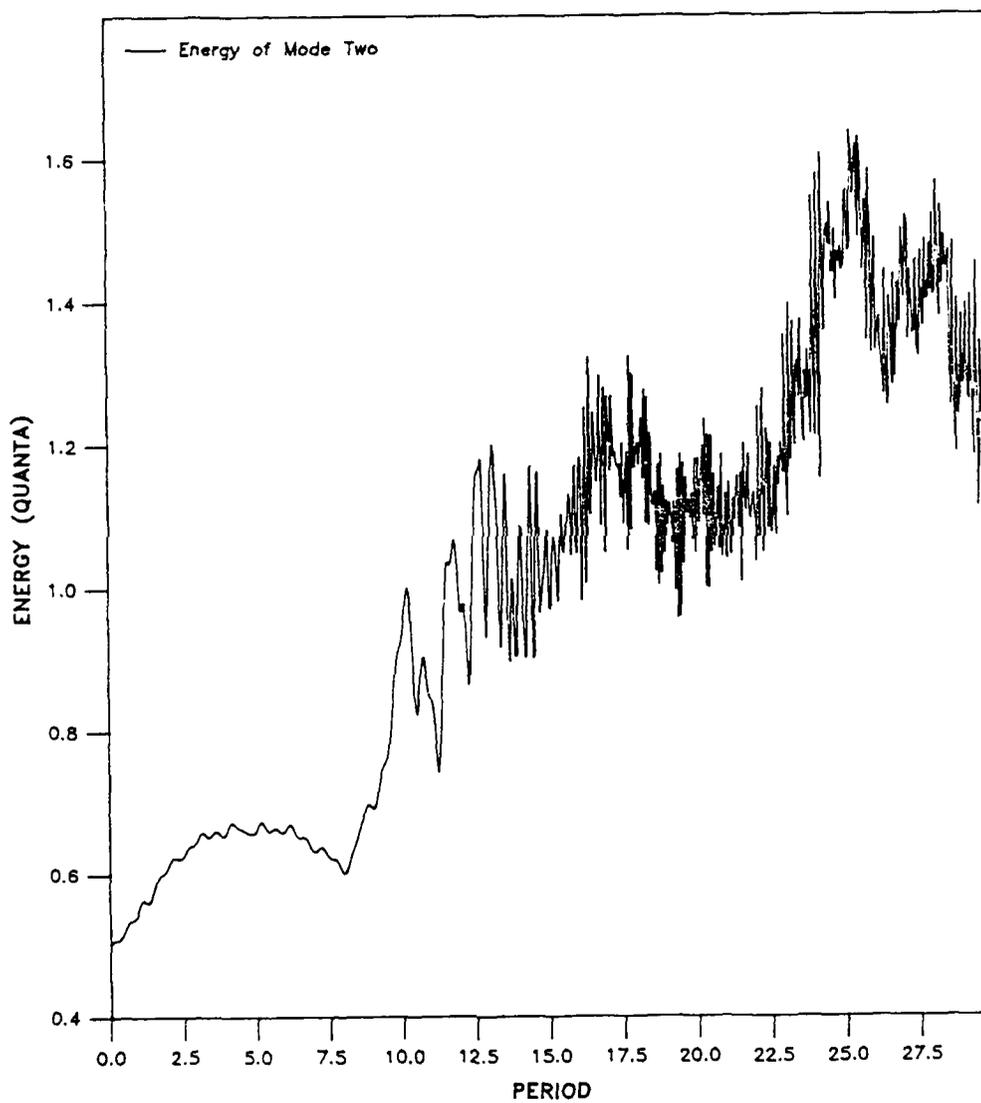
Figure 67

Energy of Mode Three

Anharmonic
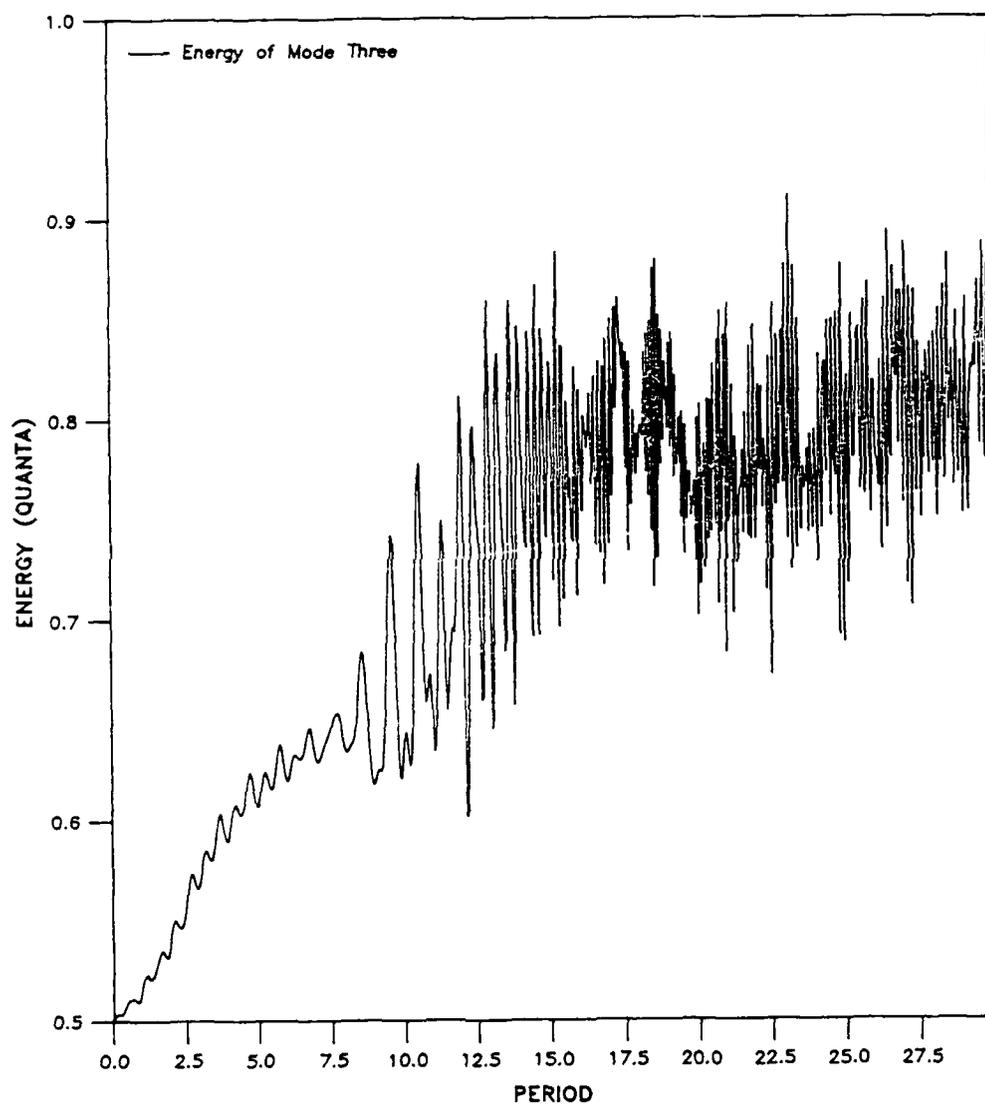
Figure 68

Energy of Mode Four

Anharmonic
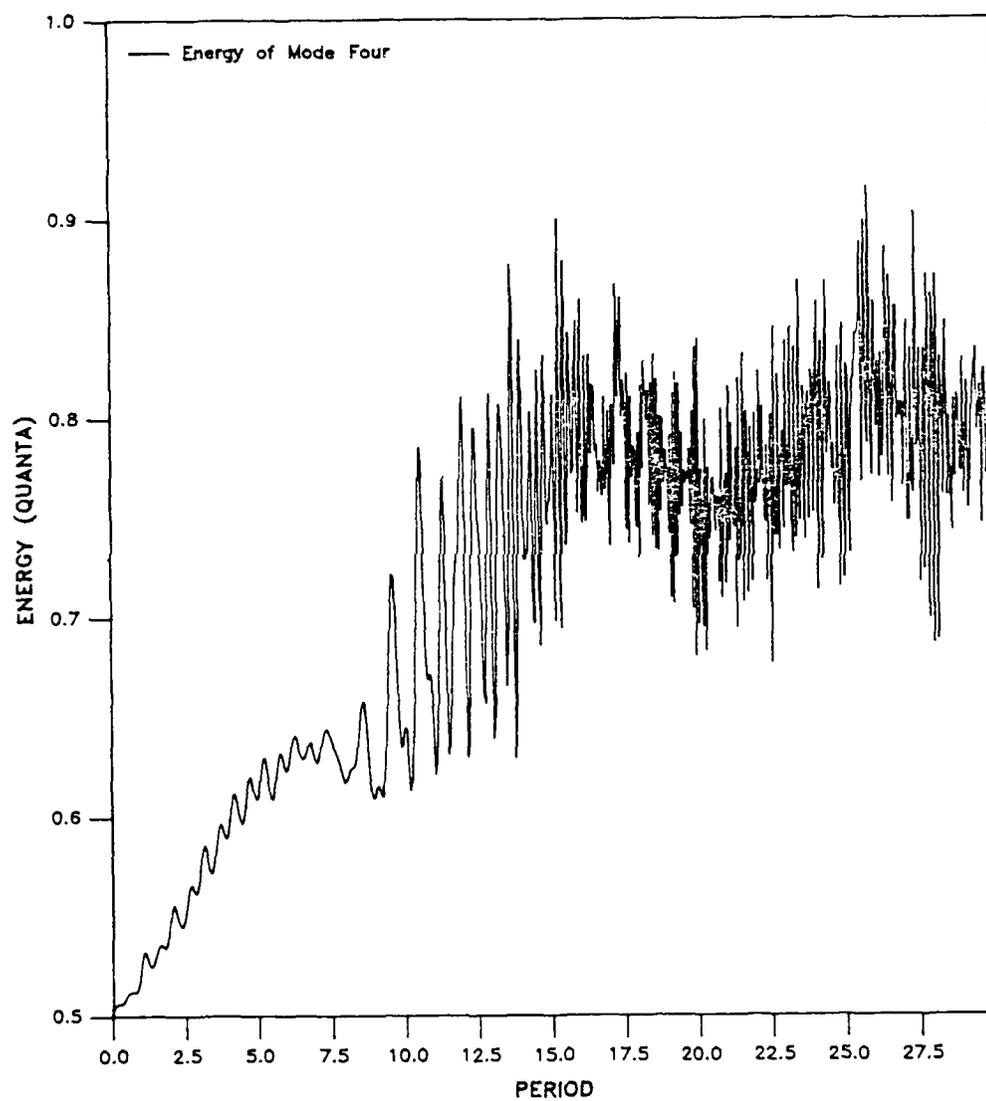
Figure 69

# Energy of Bond R12

Harmonic
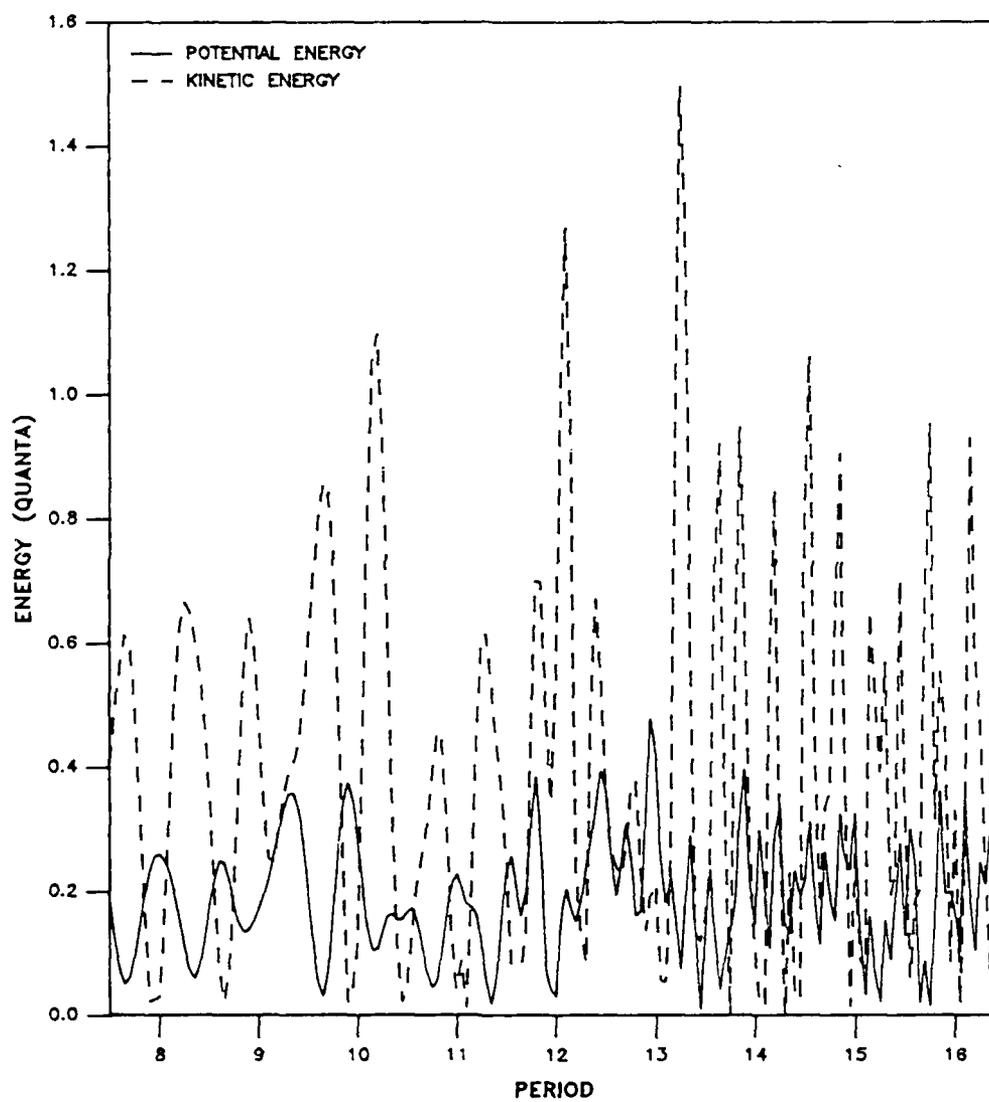
Figure 70

# Energy of Bond R34

Harmonic
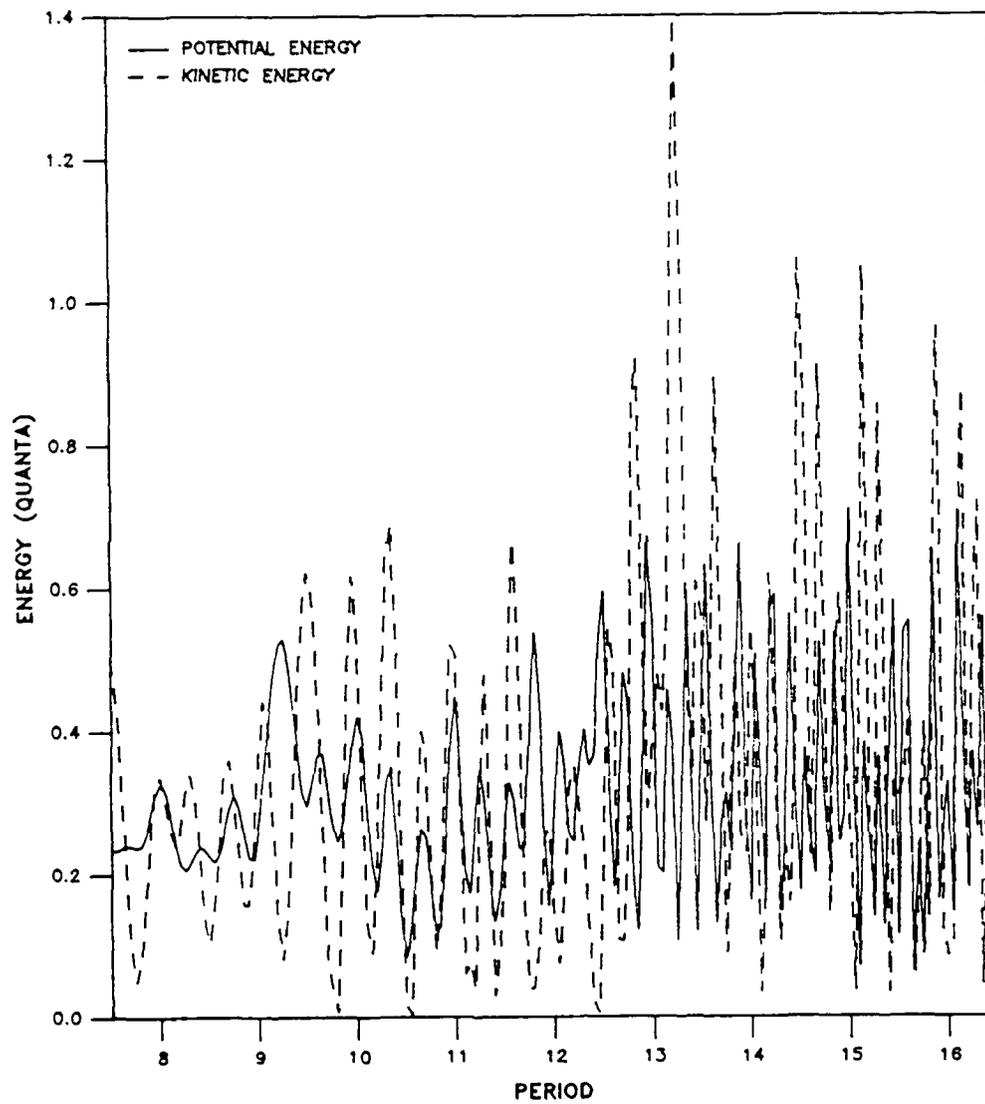

Figure 71

Bond Energy

Harmonic
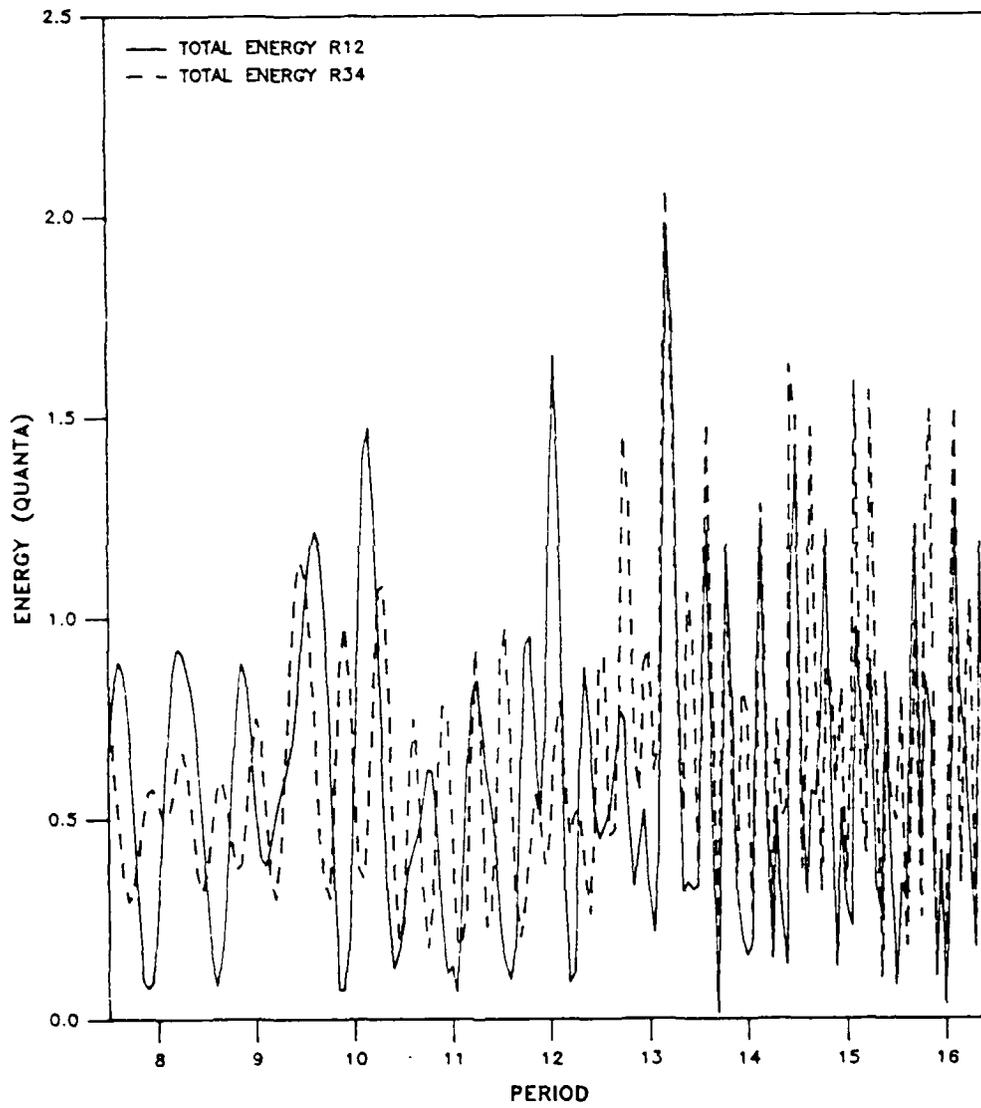
Figure 72

# Energy of Bond R23
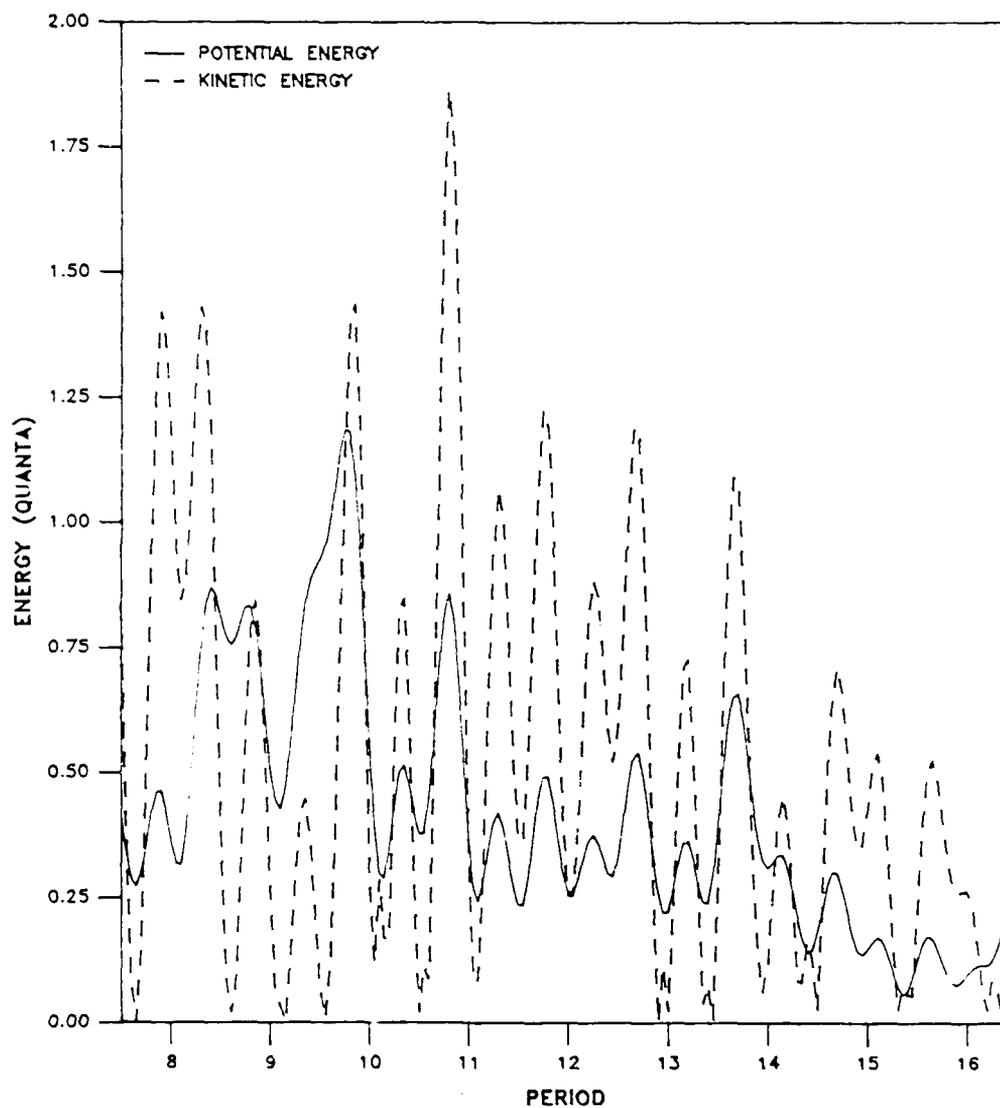
Harmonic

Figure 73

Energy of Bond R23
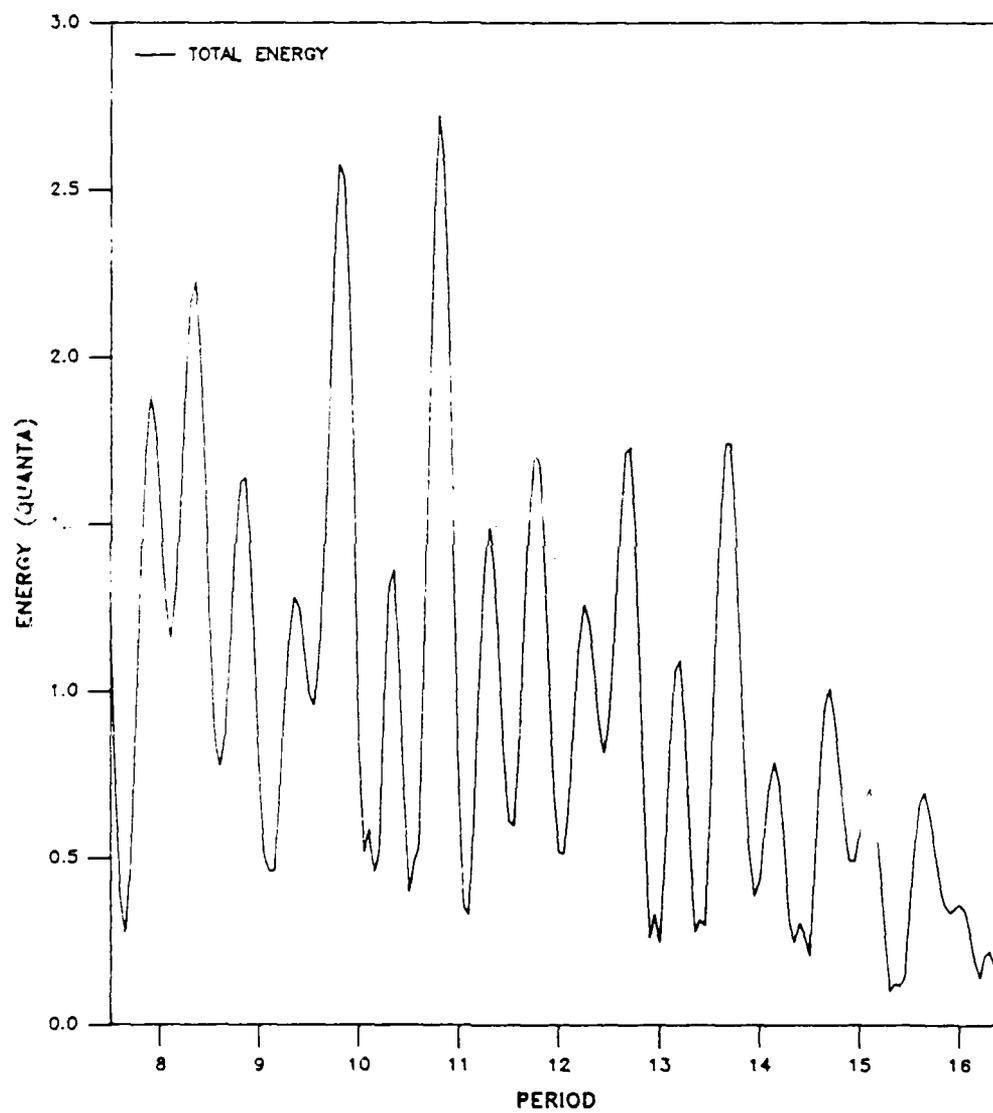
Harmonic

Figure 74

Energy of Bond R12

Anharmonic
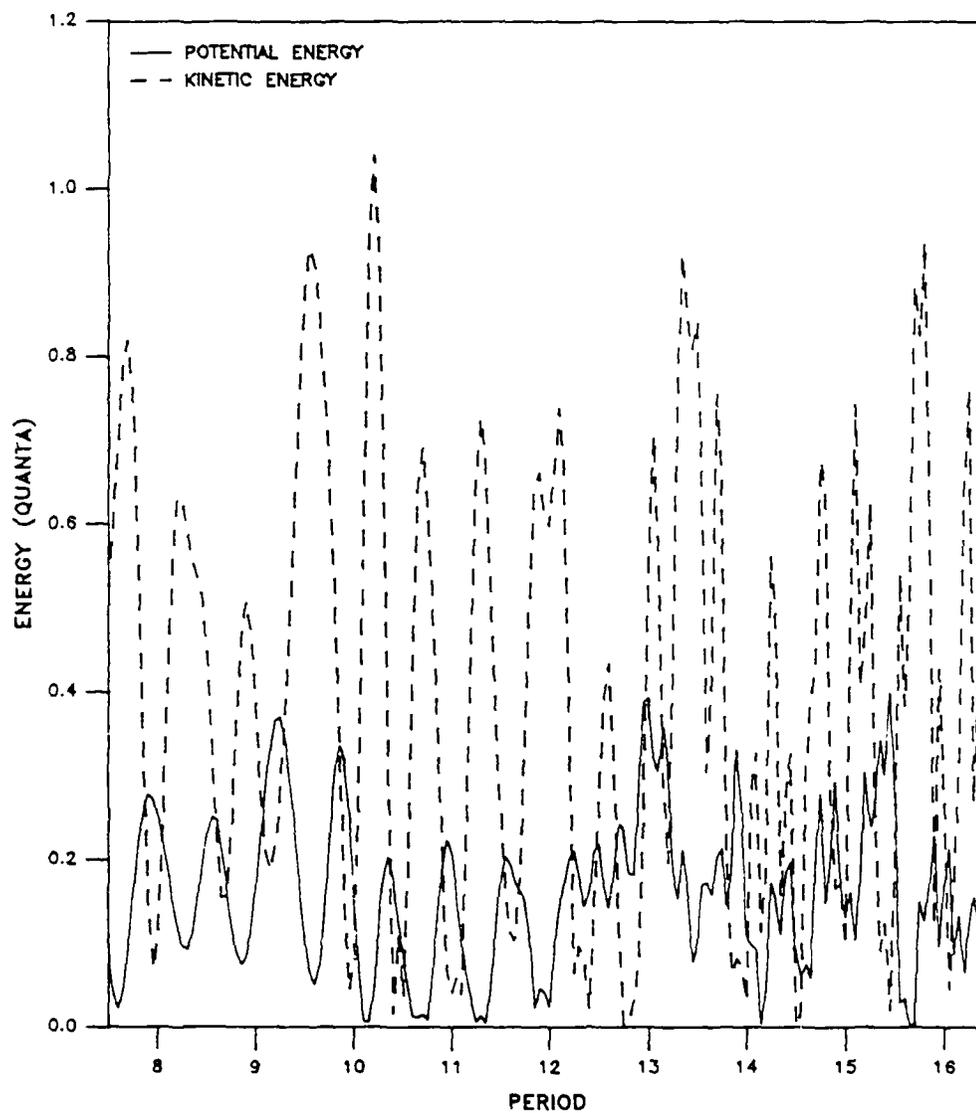
Figure 75

# Energy of Bond R34

Anharmonic
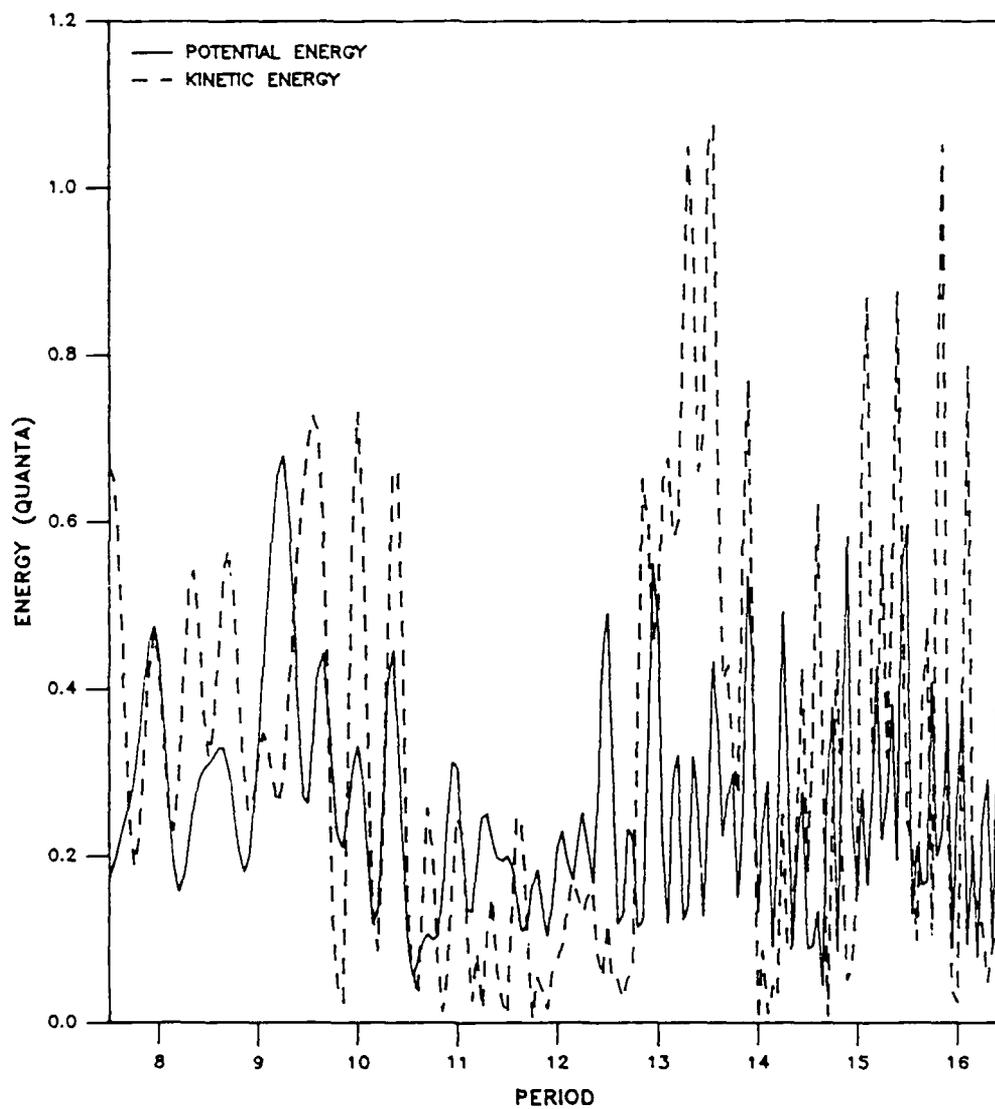
Figure 76

Bond Energy

Anharmonic
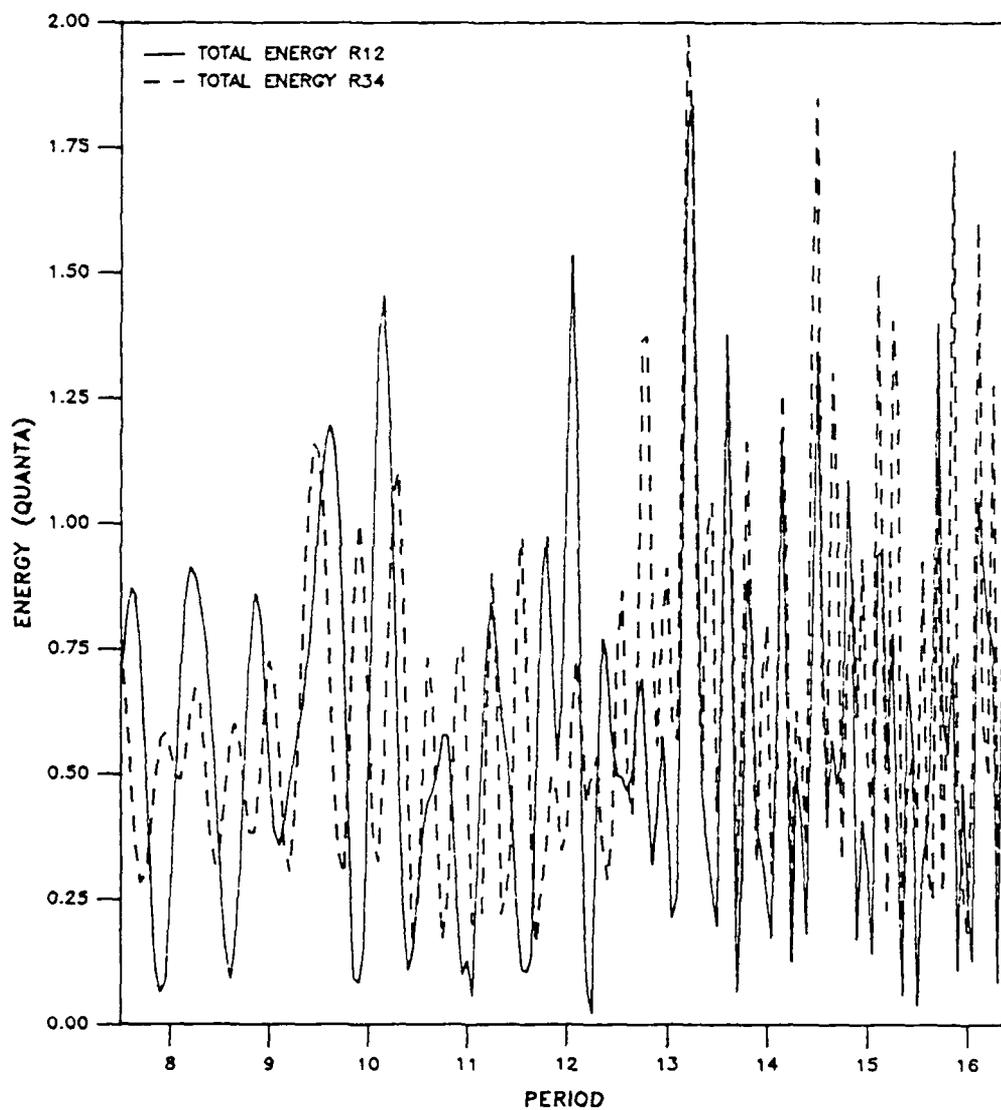
Figure 77

# Energy of Bond R23
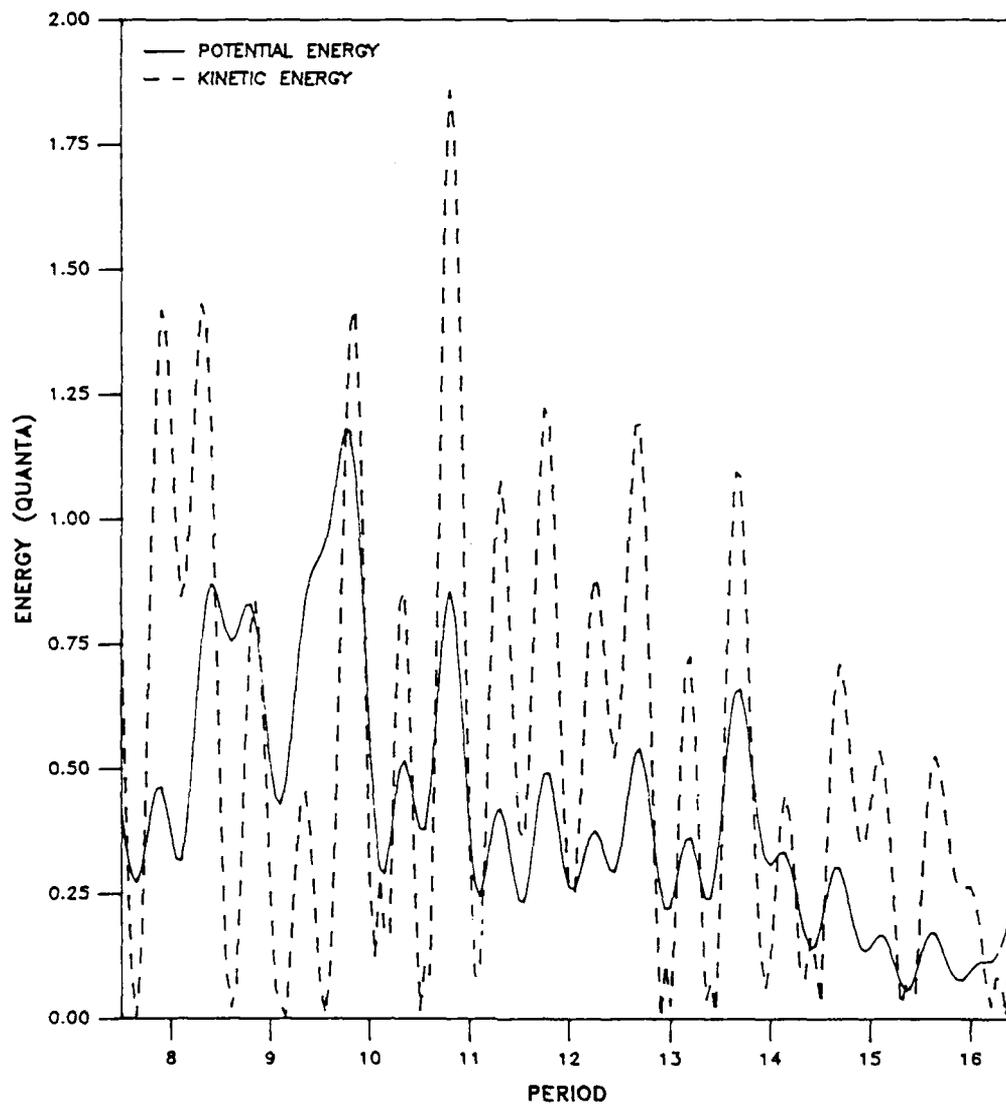
Anharmonic

Figure 78

Energy of Bond R23

Anharmonic
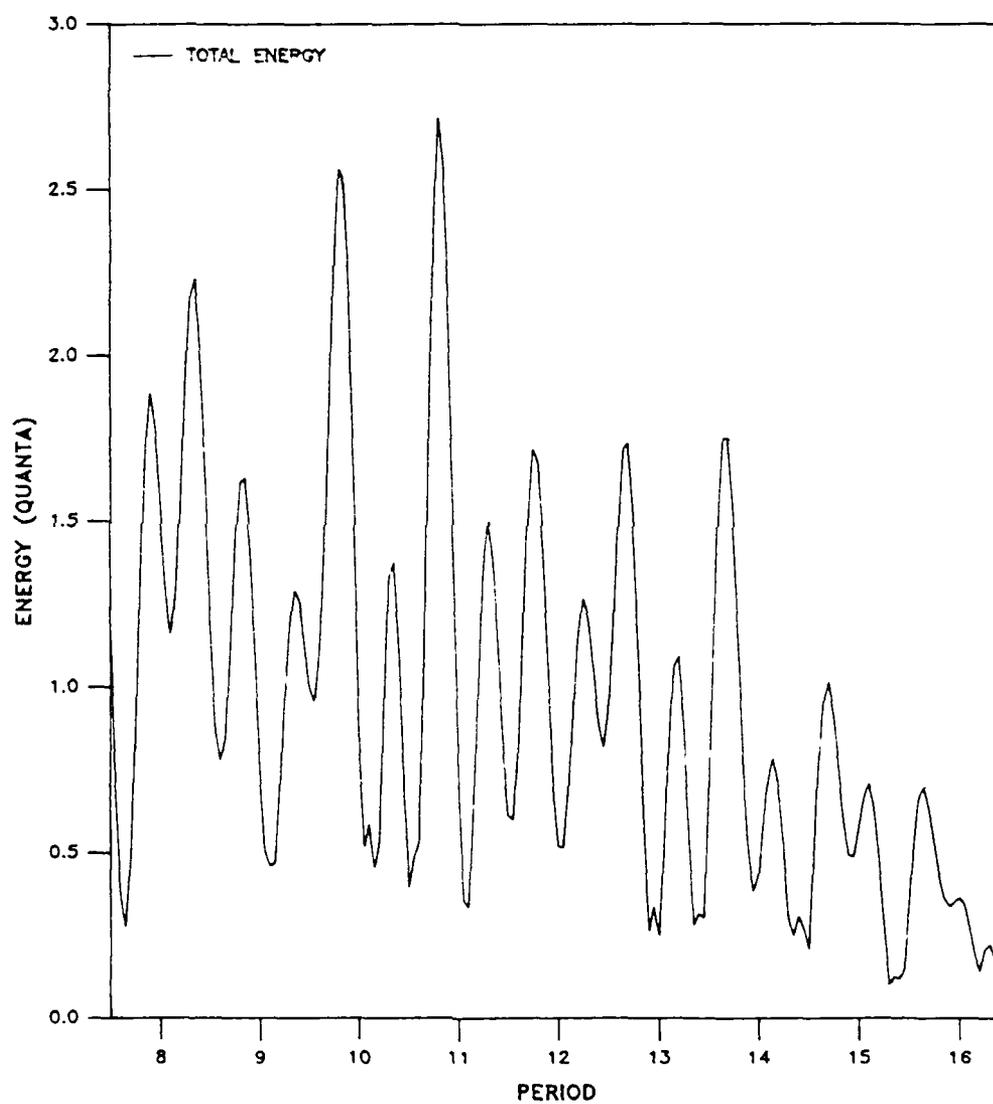
Figure 79

References

1. M. Peynard, S. Odiot, E. Oran, J. Boris, and J. Schnur, "Microscopic Model for Propagation of Shock-induced Detonations in Energetic Solids," Phys. Rev. B **33**, 2350 (1986).

2. R. Rao, Z. Lu, A. Doukas, S. Lee, B. William, P. Harris, and R. R. Alfano, "High Power Picosecond Laser-induced Shock Waves in Condensed Matter," Proceedings of the International Conference on Lasers, 171-177 (1985).

3. George E. Duvall, R. Manvi, and Sherman C. Lowell, "Steady Shock Profile in a One-Dimensional Lattice." J. App. Phys. **40**, 3771 (1969).

4. James Tsai, "Perturbation Solution for Growth of Nonlinear Shock Waves in a Lattice," J. App. Phys. **43**, 4016 (1972).

5. D. H. Tsai and R. A. MacDonald, "Second Sound in a Solid Under Shock Compression," J. Phys. C **6**, L171, (1973).

6. James Tsai, Far-field Analysis of Nonlinear Shock Waves in a Lattice," J. App. Phys. **44**, 4569 (1973).

7. D. H. Tsai and R. A. MacDonald, "Molecular-dynamical Study of Second Sound in a Solid Excited by a Strong Heat Pulse," Phys. Rev. B **14**, 4714 (1976).

8. Arthur Paskin, A. Gohar, and G. J. Dienes, Simulations of Shock Waves in Solids, J. Phys. C **10**, L563 (1977).

9. Jad H. Butteh and John D. Powell, "Shock Propagation in the One-dimensional Lattice at a Nonzero Initial Temperature," J. App. Phys. **49**, 3933 (1978).

10. Jad H. Butteh and John D. Powell, "Solitary-wave Propagation in the Three-dimensional Lattice," Phys. Rev. B **20**, 1398 (1979).

11. F. E. Walker, A. M. Karo, J. R. Hardy, "Comparison of Molecular Dynamics Calculations with Observed Initiation Phenomena," Lawrence Livermore Laboratory, June 5, 1981.

12. A. M. Karo, F. E. Walker, W. G. Cunningham, and J. R. Hardy, "Theoretical Studies of Shock Dynamics in Two-dimensional Structures V. Microscopic Constraints on Shock-induced Signals," Lawrence Livermore Laboratory, reprint, June 18, 1981.

13. Arnold M. Karo, "The Role of Molecular Dynamics on Descriptions of Shock Front Processes, Lawrence Livermore Laboratory, July 22, 1981.

14. Arnold M. Karo, Franklin E. Walker, Warren G. Cunningham, and John R. Hardy, "The Study of Shock-induced Signals and Coherent Effects in Solids by Molecular Dynamics," Lawrence Livermore Laboratory, August 31, 1981.

15. John Dancz and Stuart A. Rice, "Large Amplitude Vibrational Motion in a One Dimensional Chain: Coherent state representation", J. Chem. Phys. **67**, 1418, 1977.

16. Byung Chan Eu, "Quantum Theory of Large Amplitude Vibrational Motions in a One-dimensional Morse Chain", J. Chem. Phys. **73(5)**, 2405, 1980.

17. John S. Hutchinson, James T. Hynes, and William P. Reinhardt, "Quantum Dynamic Analysis of Energy Transfer in Model Hydrocarbons", Chem. Phys. Ltrs. **108(4)**, 353, 1984.

18. Herbert Goldstein, *Classical Mechanics* (Addison-Wesley, 1950).

19. Claude Cohen-Tannoudji, Bernard Diu and Franck LaLoc, *Quantum Mechanics* (John Wiley, 1977).

20. W. H. Flygare, *Molecular Structure and Dynamics* (Prentice-Hall, Inc., Englewood Cliffs, New Jersey, 1978).

21. Chalmers W. Sherwin, *Introduction to Quantum Mechanics* (Henry Holt, New York, 1959).

22. Gordon M. Barrow, *Introduction to Molecular Spectroscopy* (McGraw-Hill Book Company, Inc., 1962).

23. Keith R. Symon, *Mechanics* (Addison-Wesley, 1960).

24. Jerry B. Marion, *Classical Dynamics of Particles and Systems* (Academic Press, 1970).